CHAPTER I

Introduction

1.1 Background

Climate change and global warming is the most significant threat to the living beings in this planet at the twenty-first century. It is distressing that it has already begun when we have just passed the doorstep of the new millennium. Recent seasons have shown the effects of climate change and global warming in the form of extreme temperatures and weather patterns.

Extremities in weather condition causes drought and flood when we look at the phenomenon from a water resources perspective. When increasing populations, growing urban and industrial areas are taken into account, it is obvious that the above water related problems will be of utmost significance throughout the next decades. Extensive care should be given to the operation and management of river basins and dam reservoirs (no matter are they used for water supply or flood control or hydropower) to be able to overcome the water related problems.

Nepal is one of the most water-abundant countries in the world with its 6,000 rivers and rivulets, with total mean annual runoff of 224 billion cubic meters (BCM) and per capita water availability of 9,000 cubic meters (NCVST 2009). Water is the most important resource of a country, and of the entire society as a whole, since no life is possible without water. It has this unique position among other natural resources, like minerals, fuels, forests, live-stock etc. because a country can survive in the absence of any other resources, except this (SK Garg, 2010).

Most of the rivers flow from the north towards the south, generally with high velocity due to high river gradient, most being snow fed originated from the Himalayan range that are covered by perpetual snow. As the topography of the country is steep, rugged and high-angle slope with complex geology, high intensity of rainfall during the monsoon season causes flood, landslide and debris flow. The landslide and flood are the most destructive types of disaster in Nepal. Three quarter of the total land area of Nepal is hilly and many villages are situated on or adjacent to the unstable hill slopes. As a result, landslide and flood with debris flow occurs. Unplanned settlements and physical constructions without due consideration to the natural hazards are considerably aggravating the mountain

environment. On the other hand the landslide add enormous load to the streams and rivers causing flood and debris flow downstream. Each year such types of disasters cause the losses of number of human life and immense damages to agricultural land, crops, human settlements and other physical properties. In July 1993 A.D. Nepal experienced a devastating flood in the terai region of Nepal which took the life of 1336 people and affected 487,534 people. After 1993 A.D. in 1998 A.D. flood and landslide was severe which affected various parts of the country, mainly the terai and the middle Hill region. Similarly, in 2008 A.D. there was also high flood in the Koshi basin which destructed many lives and properties. Also in 2013 A.D. there was high flood in the Mahakali River which destructed many live's and properties (Ministry of Home Affairs).

Nepal has high variability in the distribution of the rainfall same as its topography. It have monsoonal rainfall during June-September, which contributes about 80% of the total rainfall and remaining 20% occur during the winter; mostly from the western disturbances. This rainfall has also its peculiarity in its distribution from low land to high mountainous region in decreasing pattern, of its vast land orientation, sharp physiographic change within short distance, orographic influences the spatial variability of the precipitation pattern.

The changes and shifting in the monsoonal behavioral in recent decades has increased the intensity of the rainfall which has induced floods and destruction to many lives and properties. Nepal is prone to water induced disasters which takes many lives and properties annually. Between 1983 and 2005 floods and landslides accounted for over 60% total deaths due to different types of disasters in the country (Khanal et. al., 2007 cited in Shrestha et. al., 2008).

The effects of the changes in precipitation and temperature are expected to change the balance between 'green water' and 'blue water'. 'Green' water is the water that is used or lost in catchments before it reaches the rivers, while 'blue' water is the runoff that reaches the rivers. Glacial melting and retreat, rapidly thawing permafrost and continually melting frozen soils in higher elevations is already being observed (Eriksson et al. 2009). In the sub-basins dominated by glaciers, this will mean increased downstream flows in the short term, but in the long term, runoff is expected to decrease with the retreating glaciers, causing major reductions in flow and significantly affecting downstream livelihoods and ecosystems (Bates et al. 2008). In the winter months, more precipitation is falling as rain,

which also accelerates deglaciation, and in turn means a shorter winter and earlier snowmelt, ultimately affecting river basins and agricultural systems dependent on surface water diversions for the summer growing season (IWMI 2010). Another particularly significant threat in the Himalayas and directly correlated to rising temperatures are glacial lake outburst floods (GLOFs) that result from rapidly accumulating water into glacial lakes that then burst, sending flash floods of debris and water from high elevations, wreaking havoc on downstream communities and damaging valuable infrastructure like hydropower facilities and roads. There are approximately 9,000 such lakes in the Himalayas, of which 200 are said to be in danger of bursting (Bajracharya et al. 2007). High rates of glacial melt due to increases in temperature are adding to this threat, as the rate of such incidents increased between the 1950s and 1990s from 0.38 to 0.54 events per year (Bates et al. 2008).

Floods are the leading cause of losses among the most devastating natural disasters in the world, claiming more than 20,000 lives per year and adversely affecting about 75 million people worldwide, mostly through homelessness (Smith, 2000). The trends of flood events are increasing more in Asian countries and decreasing in African countries (Bezak et.al. 2014). South Asian countries have a long history of floods (Mishra et al., 2012), among these Nepal is one of the highly affected country. In Nepal flood is a major disaster in terms of fatality and economic loss (Mishra et al., 2012). Due to its geographical and other climatological conditions, rugged and steep topography, extreme weather events and fragile geological conditions, the country is regarded as a disaster hotspot because of vulnerability of the population together with regular and frequent occurrence of different natural hazards. The country's social context characterizes with low level of development as well as low level of institutional capacity consequent to intensify the impact of disasters (NDR, 2009:16).

By global standards, Nepal ranked 23rd in the world in terms of the natural hazard related deaths in two decades from 1988 to 2007 with total deaths reaching above 7000 (IFRC, 2007). It is in 7th position for deaths resulting as a consequence of floods, landslides and avalanches; in 8th position for flood related deaths alone. A UN Report (2008) shows that out of 75 districts in the country, 49 districts are prone to floods and/or landslides, 23 districts to wild fires and one to wind storms. A total of 64 out of 75 districts are prone to disaster of some types (Upreti, 2007).

The research studies on hydrology play an important role to determine the extent of flooding to provide help on these issues to planners. Studies have shown that damage reductions due to forecast improvements can reach up to 35% of annual flood damages (UNISDR, 2004 cited in Shrestha et. al., 2008).

Growing realization about the importance of non-structural measures, including flood forecasting and early warning systems has increased the importance of flood modeling. But the accuracy of hydrological model relies on good rainfall data input in terms of temporal and spatial resolution and accuracy. For real time flood forecasting to be effective real time rainfall information should also be made available, a capability though desirable but not available in most of the Asian countries (Kafle et al., 2007).

Models are not only used for forecasts and predictions, but also as intellectual tools in research and education. Models allow compilation of existing knowledge can serve as a language to communicate hypothesis and can be applied to gain understanding. Development of a model, discussing a model failure or a sensitivity analysis may serve as a way to reflect about theories on the functioning of natural systems. A detailed model may not be operationally applicable at larger scales, but it may allow to study the system and thus to develop reasonable and applicable models for larger scales (Sibert, 1999). Models can be used to examine different hypotheses about the functioning of a catchment (Bathurst & Cooley, 1996 cited in Sibert, 1999). A model may help to investigate which parameter values or input data are most crucial to be estimated accurately.

Reliable estimates of extreme floods are essential for the design and operation of vital infrastructures and for flood risk management and planning. This information is generally obtained through flood frequency estimation techniques (Castellarin et al., 2012). The inaccuracy of flood forecasting using rainfall data has led to the use of statistical methods (GEV, Extreme Value Type I, Log Normal, Log Pearson Type III etc.) to predict flood (Solomon & Prince, 2013). The use of probability model on the sample of annual flood peak of a given period of time, for a particular watershed or region is known as flood frequency analysis (Solomon & Prince, 2013). This involves the fitting of a probability model to the sample of annual flood peaks of a catchment. The model parameters established are then used to predict the extreme events of large recurrence interval (Pegram & Parak, 2004 cited in Mujere, 2011). These analysis techniques are based upon the principle of statistical analysis of series of observed flood events, providing estimates

of the probable magnitude of future extreme events through extrapolation (Castellarin et al., 2012).

To assess the hydrological consequences, the change in precipitation needs to be translated by hydrological models into changes in hydrological quantities, for example, flow or water budget. Hydrological modelling is a commonly used tool to estimate the basin's hydrological response to precipitation. The selection of model depends, on the basin and the objectives of the hydrological prediction in the basin (Hunukumbura et al., 2008). A continuous-simulation hydrologic model can be the appropriate tool which examines the entire spectrum of stream flow, as represented by the flow duration curve. This type of hydrological model generates a continuous record of stream flow from records of precipitation and other climatic variables. Continuous simulation model accounts for hydrologic processes that are neglected in single event flood models. These processes include evapotranspiration, canopy interception, depression storage, percolation, shallow subsurface flow and snowmelt (McEnroe, 2010). The use of such assessment of impacts will allow the various adaptation intervention programs to be targeted to areas where the risk of catastrophic climate induced impacts is the highest (Siddiqui et al., 2012).

The main purpose of this study is to estimate the reliable temporal runoff and flood forecast in the stream by using HEC-HMS model and Regional Climate Model.

1.2 Statement of the problem

Floods occur repeatedly and cause tremendous losses in terms of property and life, particularly in the lowland areas of the country. Hence, they constitute the main hazard. Floods that cause substantial devastation are triggered by different mechanisms: continuous rainfall and cloudbursts, GLOF's, landslide dam outbursts, failure of infrastructure, and sheet flooding or inundation as a result of excessive rain, bank overflow, or obstruction to the flow from infrastructural development. The study will be helpful to understand the hydro-meteorological properties of the basin by establishing the river flow characteristics at the Dam site. The estimation of the high flow, flow duration curve, flood frequency analysis, modeled and projected flow help to provide sustainable water resources planning, management and development. Besides, the study will also provide the scientific review of the basin status.

1.3 Objectives

The main objective of this study is the assessment or estimation of different hydro-meteorological study, perform hydrological modeling, flood frequency analysis, and project the discharge using satellite data of DudhKoshi Basin. Based on this specific objective following objectives were developed.

- Hydrological and meteorological analysis of the study area.
- Develop continuous and event hydrological models for DudhKoshi River Basin.
- Calibrate and validate HEC-HMS model parameters for continuous and event simulations.
- Perform the flood frequency analysis and flood forecast using PMP, PMF
- Projection of future discharge using satellite data.

1.4 Limitations

- Insufficient number of meteorological stations.
- Quality of available data of discharge and rainfall do not have perfect correlation in any event.
- Losses like evaporation, evapotranspiration are not considered in the research.

1.5 Structure of thesis:

The thesis is presented in Five Chapters. Chapter I provide the introduction including the background of the study, statements of the problem and objectives. Chapter II includes the literature review related to this research. Chapter III includes the brief description of the study area, theoretical background and the methodology. Chapter IV gives the result and discussion of the study. At last Chapter V present the Conclusion and Recommendation.

CHAPTER II

LITERATURE REVIEW

2.1 Glacier and Glacier Lakes

Nepal is a Himalayan country and the entire country falls in the Hindu Kush Himalayan Region, which is home to 30% of the world's glaciers (ICIMOD, 2011). Due to rapid melting of glaciers in recent years, glacial hazards have become frequent in highly glaciated regions of Nepal. Since, glacial lake formation and outburst is a phenomenon closely related to glacial retreat, increasing global temperature is of great concern in climate sensitive areas, such as the Nepal Himalayas.

The hydrological responses of the snow-covered and glaciated areas are distinct from the other zones. About 23% of Nepal's total area lies above the permanent snowline of 5000 m (MoPE, 2004). Presently, about 3.6% of Nepal's total area is covered by glaciers (Mool P. et al., 2001). About 10% of the total precipitation in Nepal falls as snow (UNEP, 2001). A study on the glaciers in the Nepal Himalaya (Mool P. et al., 2001) divided the area into four major river basins from east to west. It revealed 3,252 glaciers with a coverage area of 5,323 sq. km and an estimated ice reserve of 481 km^3. According to this study, the Koshi River Basin comprises 779 glaciers with an area of 1,409.84 sq. km and an estimated ice reserve of 152.06 km^3. There are altogether 1,025 glaciers in the Gandaki River Basin which cover an area of 2,030.15 sq. km and the basin has an estimated ice reserve of 191.39 km^3. The Karnali River Basin consists of 1,361 glaciers with an area of 1,740.22 sq. km and an estimated ice reserve of 127.72 km^3. Only 35% of the Mahakali River Basin, comprising 87 glaciers, lies within Nepali territory. The area covered by these glaciers is 143.23 sq. km and the estimated ice reserve is 10.06 km^3. All the lakes at elevations higher than 3,500 m a.s.l. are considered to be glacial lakes (Mool P. et al., 2001). Some of the lakes are isolated and far behind the ice mass. Their inventory of glacial lakes revealed 2,323 lakes with coverage of 75 sq. km in Nepal. The Koshi River Basin contains 1,062 lakes, the Gandaki River Basin 338 lakes, the Karnali River Basin 907 lakes and the Mahakali River Basin (within Nepali territory) contains 16 lakes.

About 25 Glacial Lake Outburst Flood (GLOF) events have been recorded in last 30 years in Nepal among which 10 GLOF events originated from Tibet causing trans-boundary impact (ICIMOD, 2011) (Refer :Table 1). Most of the outburst goes unnoticed due to the remote location of glacial lakes and inadequate stream gauging stations along the rivers

of Nepal (Walder *et al.,* 1997). Though other flood and sediment disasters occur in the Koshi basin, GLOF has gained alarming attention due to huge loss of human lives, infrastructure, cultivable lands and vegetation in low lands caused by a single event. Also, GLOF causes significant impact downstream as the river profile gets shallower and wider, inundating larger areas (Sinha *et al*., 2008).

The incidence of GLOF has led to extensive study and awareness programs about GLOF in countries like Iceland, Norway, and Canada, but in the case of Nepal, only a few GLOF events have been studied in detail (ICIMOD, 2011). The major GLOF events in terms of peak discharge that took place in the Sapta Koshi River basin were outbursts of the Nagma and the Tam glacial lakes on 23 June 1980 and 3 September 1998 with peak discharge of 24,000 m^3/s and 9,800 m^3/s respectively (Refer: Table 2) (Shrestha *et al*., 2010). These peak discharges measured were several orders in magnitude greater than seasonal high floods and the average annual discharge of the Sapta Koshi River (WWF, 2005).

However, in terms of socio-economic effect, outburst of the Dig-Tsho Lake on 4 August 1985 and the Zhangzangbo Lake on 11 July 1981 was catastrophic (Refer: Table 1). Human casualties during the Dig-Tsho event were enormous, along with destruction of the Namche hydro power plant, 14 bridges, and cultivable land. The economic loss during this event was estimated to be more than $500 million (Shrestha *et al.,* 2010). Similarly, the GLOF from the Zhangzangbo Lake in Tibet flooded the Sunkoshi basin and damaged the Araniko Highway, the Nepal-China Friendship Bridge, 10 suspension bridges, and houses with estimated rebuilt cost of $3 million (Shrestha *et al*., 2010). Though outburst of the Tam Lake had higher recorded discharge than the Dig-Tsho and the Zhangzangbo Lake outbursts, its impact on infrastructure and human lives are poorly documented (Osti *et al*., 2009).

GLOF is an extreme event and includes numerous source of uncertainty about physical processes that give rise to such event. Moreover, the rivers in Nepal are poorly gauzed and less documented, thus statistical approach for GLOF data analysis is often desirable. A frequency analysis involves determining relationship between the magnitude and frequency of extreme events by fitting the data sets to a probability distribution and extrapolating peak discharges (Chow *et al.*, 1988). There are various empirical equations established using extensive data sets to estimate the GLOF peak discharge but GLOF in

Nepal Himalayas cannot be accurately analyzed by this method due to the lack of discharge data at site.

Table 2.1: Past Glacial Lake Outburst Flood (GLOF) Events in Nepal

S.N	Date	Name of lake	Location	River Basin
1	450 years ago	Machhapuchare	Nepal	Seti River
2	Aug, 1935	Taraco	Tibet	Bhote koshi
3	1956	Imja	Nepal	Dudh Koshi
4	Jan, 1964	Tiptala	Nepal	Tamur
5	21 Sep, 1964	Chubung	Nepal	Arun
6	21 Sep, 1964	Gelaipco	Tibet	Arun
7	1964	Zhangzangbo	Tibet	Sun koshi
8	1964	Longdo	Tibet	Trishuli
9	1968	Ayaco	Tibet	Arun
10	1969	Ayaco	Tibet	Arun
11	1970	Ayaco	Tibet	Arun
12	3 Sep, 1977	Nare	Tibet	Bhote koshi
13	23 Jun, 1980	Nagma Pokhari	Nepal	Tamur
14	11 July, 1981	Zhangzangbo	Tibet	Bhote koshi
15	27 Aug, 1982	Jinco	Tibet	Arun
16	4 August, 1985	Dig Tsho	Nepal	Dudh Koshi
17	12 July, 1991	Chubung	Nepal	Arun
18	3 Sep, 1998	Tam	Nepal	Dudh Koshi
19	15 Aug, 2003	Kawachi	Nepal	Madi
20	8 Aug, 2004	Kawachi	Nepal	Madi

(Adapted from: Mool *et.al,* 2001)

Table 2.2: Measured GLOF Discharges at Different Gauging Stations of the Sapta Koshi Basin

Glacial lake	Year	Gauging Station	Discharge (m^3/s)	Basin
Nare	1977	Source: GAPHAZ Database	1,200	Dudhkoshi
Nagma	1980	Chatara Kothu (695)	24,000	Tamur
Zhangzangbo	1981	Pachuwarghat (630)	2,316	Bhote Koshi
Jinco	1982	Chatara Kothu (695)	4,160	Arun
Dig Tsho	1985	Rabuwa (670)	4,800	Dudh koshi
Tam pokhari	1998	Rabuwa (670)	9,800	Dudh koshi
Chubung	1991	Turkighat (604.5)	1,810	Arun

(Adapted from Shrestha *et al.,* 2010; DHM Nepal and GAPHAZ Database)

2.2 Rainfall

Globally, Nepal falls within subtropical climate zone. However, due to unique physiographic and topographic feature, it possesses enormous climatic and ecological

diversity within short north-south span of about 130-260 km. The climate types range from sub-tropical in the terai to arctic in the high Himalayas. The remarkable differences in climatic conditions are primarily related to the range of altitude within a short north-south distance. The presence of the east-west extending Himalayan massifs in the north and the monsoonal alternation of wet and dry seasons greatly contribute to local variations in climate.

The annual mean precipitation is found to be 1,857.6 mm in Nepal. But owing to the great topographic variations, it ranges from more than 5,000 mm along the southern slopes of the Annapurna range in western development region of the country to less than 150 mm in the north of the Annapurna range near the Tibetan plateau.

In general, the onset and retreat of easterly monsoon is associated with the change in the direction of seasonal winds and the northward and southward shift of the Inter Tropical Convergence Zone (ITCZ). Nepal receives heavy precipitation when the position of ITCZ is close to the foothills of the Himalaya. Precipitation is also heavy when the monsoon trough formed over Bay of Bengal passes through the country. There is a marked variation of the amount of monsoon precipitation from east to west and from south to north. Generally, eastern Nepal receives first monsoon rainfall and slowly moves towards west. The contribution of the monsoon precipitation is substantially high in eastern part of the country compared to western part. Precipitation also varies significantly from place to place both in local scale as well as in macro scale due to extreme topographic variation. The approaching monsoon winds are first intercepted by foothills of Churia range where intensive rainfall occurs. The rainfall increases with altitude on the windward side, and sharply decreases in the leeward side. Lumle (1,642 m asl) lying south (windward side) of the Annapurna range in Centre of Nepal Himalayas receives over 5,000 mm of annual rainfall, whereas Lomanthang (3,705 m a.s.l.) lying North (leeward side) of the same range receives only about 144 mm of rainfall per year. The monsoon precipitation occurs in the form of snow in the higher altitude, which play a vital role in nourishing the glaciers in the high mountains.

Nepal experiences the monsoon rainfall from June to September when most of the days are cloudy with heavy rainfall and incessant rains are common during these months. About 80 per cent of the annual precipitation in the country fall between June to September under the influence of the monsoon circulation system. The amount of

precipitation varies considerably from place to place because of topographic variations. The amount of monsoon rain generally declines from east to west. Although the success of farming is almost dependent on the timely arrival of the monsoon, it periodically causes problems such as landslides, debris flow and flash floods in the hills and foothills, floods, debris and cutting of land in plains which destroy human lives, livestock, farmlands and properties. Conversely, when prolonged monsoon break takes place severe drought resulting to famine often occurs (Practical Action 2009).

2.3 Water-Induced Disasters

The Himalaya of Nepal is geologically active where the instabilities due to tectonic activity and ongoing erosion are apparent everywhere. These factors, combined with the peculiar meteorological conditions where both the rainfall and river flow vary tremendously in both time and space, make the landscape vulnerable to water-induced disasters such as floods, landslides, slope failures, river bed variation (resulting in subsequent shifting and degradation) and debris flow.

In addition to these natural processes, developmental activities and increasing population have caused further vulnerability and destabilization of land resources. This includes human activities such as deforestation, cultivation of marginal land, road construction in the hill and mountain regions and the encroachment of flood plains. Water- Induced disasters, thus, have been occurring more frequently in recent times.

In Nepal, devastating floods are triggered by different mechanisms which can be classified into five major types:

i) Continuous rainfall and cloudburst (CLOF)

Floods are common throughout the country in the latter stages of the monsoon when the land is saturated and the surface runoff increases. Extremely high intensity precipitation in mountain areas cause landslides on mountain slopes and debris flows and floods along the river valleys. Extreme precipitation events that occurred between 1948 and 1955 caused landslides and debris flows in the mountain areas. They, consequently, led to destructive floods on many rivers in the lowland areas. The highest flood recorded, occurred in the Koshi River in 1954 and was the result of widespread rainfall in its mountain catchment area (Dixit A. 2003). The livelihood options for many families in the mountain areas were threatened. As a response, in 1956, the government began resettlement programs for the severely affected families in the Inner Terai and Terai

regions. At the same time, spontaneous large scale migration from the mountains to the Terai and from the ridges to the river valleys took place immediately after the implementation of a malaria eradication program in the lowland areas (Khanal NR. 2004). Between 1981 and 1998, three events of extreme precipitation with extensive damage have been reported (Chalise SR. and Khanal NR. 2002). Devastating flood associated with high intensity precipitation and consequent landslide and debris flow activities in the mountain terrain occurred in Lele (Lalitpur district) on September 30, 1981; in the Kulekhani-Sindhuli area on July 19-20, 1993; and in Syangja District on August 27, 1998. In the second of these events, the loss of life and property was not confined to the mountain areas where high intensity precipitation had taken place; hundreds of people were also swept away in the downstream areas as far away as Rautahat and Sarlahi districts in the Terai.

ii) Glacial lake outburst flood (GLOF)

Glacial lakes are common in the high mountain areas in Nepal. A recent study shows that there are 3,252 glacial lakes in Nepal (Mool P. et al., 2001a). It also identified 21 GLOF events. Thirteen of these occurred between 1964 and 1998; nine occurred in the Tibetan Autonomous Region (China). The latter affected the areas downstream along trans-boundary Rivers like Sun Koshi, Arun, and Trishuli in Nepal. A GLOF damaged a hydropower plant and many houses along the former in 1981. In 1985, a similar event swept away three persons, one hydropower plant, 14 bridges and 35 houses along the DudhKoshi River. Nearly 26 glacial lakes have been identified as potentially dangerous. This renders much of the infrastructure along the rivers originating from these lakes at immediate risk.

iii) Landslide dam outburst flood (LDOF)

The formation of temporary lakes due to landslide damming is a common phenomenon in the high mountain areas where there are very narrow river channels and steep mountain slopes. Eleven disastrous floods caused by the breaching of landslide dams have been reported in Nepal between 1967 and 1989 (Khanal NR. 1996). The BudhiGandaki River near Lukubesi (1968), the Sun Koshi River near Barhabise (1982), the Balephi Khola in Sindhupalchok (1982) and the Gyangphedi Khola, Nuwakot (1986), the Sunkoshi River in Sindhupalchok Jure (2014), the Kaligandaki River in Myagdi(2015) were dammed by landslides. The resultant outburst floods took a heavy toll of human lives and infrastructure.

iv) Floods triggered by the failure of infrastructure

The floods triggered as a result of poor infrastructural design are also common in Nepal. Eight such floods have been reported. The failure of check dams and embankments in Butwal in 1981 led to loss of 41 lives, 120 houses and one bridge being swept away (ICIMOD, 2007). Similarly, in 1990, 26 people and 880 houses were swept away by a flood triggered by the failure of a check dam on the Rapti River in Chitwan. In 1993, the Bagmati River was dammed for a few hours because of blocking by tree logs at the Bagmati barrage; the ensuing outburst flood swept away 816 people in Rautahat and Sarlahi districts. The Larcha River was dammed by a boulder at the bridge over the highway in 1996; the subsequent outburst flood swept away 54 persons and damaged 22 houses (ICIMOD, 2007).

v) Sheet flooding or inundation in lowland areas due to an obstruction imposed against the flow

Sheet flooding or inundations are common during the monsoon in lowland areas in the Terai. The risk of such hazards has been increasing in recent years as a result of the increasing development of infrastructures such as roads, culverts, check dams etc. and the consequent obstruction in the natural flow of the surface runoff. Moreover, the unilateral construction of roads perpendicular to the natural flow of rivers near the border area between India and Nepal without sufficient drainage and construction of barrages, dams, afflux bunds and dykes have also exacerbated flooding in Nepal.

More than ten cases of such infrastructure induced flood disasters have been reported near the border area. Although the loss of life is comparatively low in the Terai districts, the extent of impact is very high in terms of the number of families affected and the loss estimated. Districts such as Rautahat, Sarlahi, Mahottari and Dhanusa located in the Central Terai are seriously affected by floods. A comparison of the loss and damage incurred between 1970 and 1993-2002 (Khanal NR. 2005) shows that since 1992, the Central and Eastern Terai have been experiencing increasing losses from water-induced disasters. Along with Sindhuli District in the mid-hills, the Central Terai districts of Rautahat, Sarlahi, Mahottari and Dhanusa have been repeatedly and seriously affected by floods (Dixit 2003; Khanal NR 2005).

2.4 Hydrological Modelling

A hydrological system model is an approximation of the actual system. A hydrological system can be defined as a structure of volume in space, surrounded by a boundary that

accepts water and other inputs, operates on them internally and produces an output. The objective of hydrological system analysis is to study the system operation and predict its internal states and output.

A mathematical model is an explicit sequential set of equations and numerical and logical steps that converts numerical inputs to numerical outputs (S. L. Dingman, 2008). The equations represents the qualitative behavior of flows and storage and the parameters-numerical constants that dictate the quantitative behavior.

Hydrologic models are simplified, conceptual representations of a part of the hydrologic cycle. They are primarily used for hydrologic prediction and for understanding hydrologic processes. Hydrological models are widely used for the proper design and management of water resources projects. These are the basis for flood forecasting and early warning system. Simulated series of river flows are used in the design and operation of system of multipurpose reservoirs to optimize the conflicting uses of water resources.

2.5 Modelling Process

There are many different procedures for hydrological modelling. The first step of the modelling is perceptual model and it's not constrained by mathematical theory (K. J. Beven). The mathematical description of the model is the conceptual model. These mathematical equations are coded in suitable computer program to run and the model parameters are estimated. Once the model parameters have been specified, the next stage is validation of those predictions. The flow chart here describes the modelling process in the hydrological system.

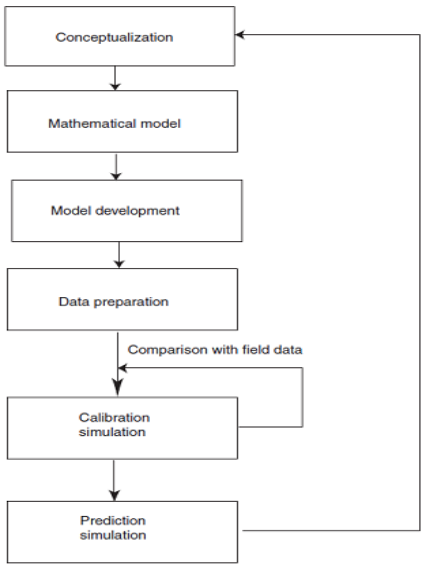

Figure 2.1 Schematic outline of different steps in modelling process

2.6 Classification of Hydrological Model

The hydrological models can be mainly classified into two main categories: physical model and abstract model. The physical models are scaled model and abstract models refer the system in mathematical and logical form. The operation of system is described

by forming set of equations and logical statements. The models are classified according to three main criteria:

- Randomness (deterministic or stochastic)
- Spatial variation (lumped or distributed)
- Time variability (time-dependent, time-independent)

There are several systems of classification of hydrological models and one of these is shown
in figure.

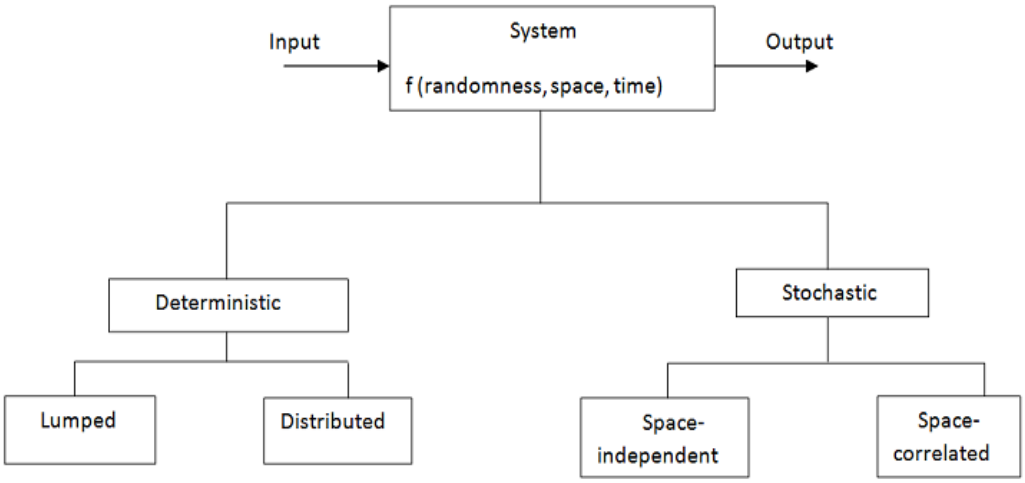

Figure 2.2 Classification of hydrological models

2.7 Lumped and Distributed Models

The models that have been typically used are the lumped models. Lumped models are systems where all of the parameters which impact the hydrologic response of a watershed are spatially averaged together to create uniformity across the basin (HEC 2000) (Johnson 1997) (Shah 1996a). Lumped models consider a watershed catchment as one complete unit, characterized by a relative small number of parameters and variables (Refsgaard 1997). The spatial variability of parameters within the basin are ignored or averaged (Feldman, 2000; Lastoria, 2008; Tessema, 2011) and response of smaller sub-basins is not accounted and the basin response is evaluated only at the outlet (Cunderlik, 2003). This type of model are not usually applied to simulated event level processes but if the primary purpose is to predict discharge, then these models are equally good (Bevan, 2001 cited in Cunderlik, 2003).

These type of model fully allow spatial variation of model parameters at a chosen resolution and hence generally require large and often unavailable data for parameterization in each grid, but can provide accuracy of the highest degree if governing physical processes are properly applied (Cunderlik, 2003). Although the use of distributed model has been encouraged in hydrological application, the problem of uncertainty in parameter estimation and uncertainty in model identification become common, as with increasing degree of spatial discretization, these models can easily become over-parameterized and ill-represented (Pechlivanidis et al., 2011). Additionally, there is not a clear trend in the literature supporting the superiority of distributed against lumped model spatial resolution in terms of accuracy of flow forecasts at the catchment outlet (Pechlivanidis et al., 2011). Several sources of uncertainty like parameter estimation, data uncertainty and model structure identifiability could contribute to this result (Beven, 2009, cited in Pechlivanidis et al., 2011).

2.8 Event Based and Continuous Based

On the temporal basis, models can be classified as event based models or continuous models (Cunderlik, 2003). Event based models take into account a single storm event (Pechlivanidis et al., 2011). Since their objective is the evaluation of direct runoff, the emphasis is placed on infiltration and surface runoff, and also these models are not suitable for the simulation of dry-weather flows (drought analysis) as there is no provision for moisture recovery between storm events (Cunderlik, 2003).

Continuous models simulate a longer period, predicting watershed response both during and between precipitation events (Feldman, 2000). These take account of all runoff components, including direct and indirect runoff and the rate of moisture recovery during dry periods; and are suitable for simulation of daily, monthly or seasonal streamflow, usually for long-term runoff volume forecasting and for estimates of water yield (Cunderlik, 2003).

2.9 HEC-HMS

The Hydrologic Modeling System (HEC-HMS) is designed to simulate the precipitation-runoff processes of dendritic drainage basins. It is designed to be applicable in a wide range of geographic areas for solving the widest possible range of problems. This includes large river basin water supply and flood hydrology, and small urban or natural watershed runoff. Hydrographs produced by the program are used for studies of water availability,

urban drainage, flow forecasting, future urbanization impact, reservoir spillway design, flood damage reduction, floodplain regulation, and systems operation.

The program is a generalized modeling system capable of representing many different watersheds. A model of the watershed is constructed by separating the water cycle into manageable pieces and constructing boundaries around the watershed of interest. Any mass or energy flux in the cycle can then be represented with a mathematical model. In most cases, several model choices are available for representing each flux. Each mathematical model included in the program is suitable in different environments and under different conditions. Making the correct choice requires knowledge of the watershed, the goals of the hydrologic study, and engineering judgment.

HEC-HMS is a product of the Hydrologic Engineering Center within the U.S. Army Corps of Engineers. The program was developed beginning in 1992 as a replacement for HEC-1 which has long been considered a standard for hydrologic simulation. The new HEC-HMS provides almost all of the same simulation capabilities, but has modernized them with advances in numerical analysis that take advantage of the significantly faster desktop computers available today. The software includes many traditional hydrologic analysis procedures such as event infiltration, unit hydrographs, and hydrologic routing. HEC-HMS also includes procedures necessary for continuous simulation including evapo-transpiration, snowmelt, and soil moisture accounting. Advanced capabilities are also provided for gridded runoff simulation using the linear quasi-distributed runoff transform (ModClark). Supplemental analysis tools are provided for parameter estimation, depth-area analysis, flow forecasting, erosion and sediment transport, and nutrient water quality. It also includes a number of features that were not included in HEC-1, such as continuous simulation and grid cell surface hydrology. It also provides a graphical user interface to make it easier to use the software. The program is now widely used and accepted for many official purposes, such as floodway determinations.

2.10 History

The first version as HEC-I was completed in 1968 and was enhanced throughout the 1970's and 1980's where it was connected to the Data Storage System (DSS) for storing and retrieving time-series data (Scharffenberg & Pak, 2009). The success of HEC-1 led to the development of several products for specialized application likeHEC-1F, which

helped start an era of system operation based o near real-time simulation; HEC-1C, that experiment with that experimented with continuous simulation and demonstrated almost foremost part in researches happening at that time in academia; and HEC-1FH, designed for interior flood simulation. These all variants were designed to run on mainframe or mini computers before the invention of personal computers and as the computer memory was scarce at that time, HEC-1 could only compute hydrographs with up to 2000 ordinates (Scharffenberg & Pak, 2009).

In 1991 a new R & D project called "NexGen" (Next Generation Software Project) was started and development of new pieces of software was initiated (Scharffenberg & Pak, 2009) including the development of HEC-HMS (Scharffenberg & Fleming, 2010; Scharffenberg & Pak, 2009) which replaced HEC-1 (Scharffenberg & Pak, 2009).

This initial program release was called Version 1.0 and included most of the event-simulation capabilities of the HEC-1 program; the second major release called Version 2.0 focused on continuous simulation where the addition of the soil moisture accounting method extended the program from an event-simulation package to one that could work equally well with event or continuous simulation applications (Scharffenberg & Fleming, 2010).

The present computational engine draws on over 30 years' experience with hydrologic simulation software and many algorithms from previous programs HEC-1, HEC-1F, PRECIP and HEC-1FH have been modernized and combined with new algorithms to form a comprehensive library of simulation routines (Scharffenberg & Fleming, 2010). HEC-HMS has once been considered to be the state of art product of its kind available in public domain (Cunderlik, 2003).

2.11 Studies on Hydrological Model in Nepal

Nepal et al., (2014) analyzed upstream-downstream linkages of hydrological dynamics in the Koshi river basin using J2000 hydrological model. In his study, the spatial distribution of precipitation & trend analysis was used to analyze the past climatic trend in the region. The process-oriented and distributed J2000 hydrological model adapted and implemented to simulate the hydrological processes of the region. He concluded that the DudhKoshi river might shift from a melt dominate river to a rain dominated river under assumed warming scenarios.

IWMI Nepal did the study on hydrology and impact of climate change on the Koshi Basin using SWAT (Soil and Water Assessment Tool). The model was used to simulate the hydrology and to calculate sub-basin wise water balances in the Koshi Basin (Bharati et.al).

Kafle et al., 2007 have studied about developing flood forecasting models for the Bagmati Basin. They used SCS-CN method of HEC-HMS to estimate direct runoff. The rainfall-runoff model predicted the peak discharge, based on point gauge data, fairly accurately. But they concluded that the model needed further refinement for smaller discharges and the methodology could be applied for peak flow computation for flood forecasting.

Chang, 2009 simulated the rainfall runoff hydrologic model in ShihMen watershed, Taiwan using the SCS-CN method in HEC-HMS. He used Clark's Unit Hydrograph to be the transform method in simulation. In the simulation, he found that when the retention time was longer, there was much inaccuracy in the peak flood time. However, when the retention time was shorter, the Clark's Unit Hydrograph was more effective in commanding peak fold time.

Ezee 2009 studied various hydrological parameters influencing basin runoff calibrating for West Rapti Basin, Nepal using semi distributed model, HEC-HMS 3.1.1. The study compared various options provided for sub-basin loss and reaches routing and assessed the sensitivity of parameters. It was observed that SCS CN method overestimated the flow. Initial abstraction and suction head seemed less sensitive parameter while saturated hydraulic conductivity and curve number were highly sensitive.

S. DHAKAL 2014 used a partially distributed hydrological model to examine the potential effect of forest fire on runoff in a Mediterranean Catchment in SE France. The Hydrological Engineering Center's Hydrological Modeling System (HEC-HMS) was used for this purpose. Daily discharge and rainfall data from 1975 to 1991 were available. Different short events were selected and two representative storms were modelled with and without a fire scar. The model was calibrated and validated with the observed data and was employed to simulate the after fire scenario. The model revealed that, after forest fire, the peak discharge in the stream can rise from 10% to 50 % while the general pattern of discharge does not change much. A better result was obtained when the antecedent rainfall before the storm event was fed in the system.

Ramdas et al. 2012 assessed the impacts of climate change on catchment scale by incorporating the future rainfall and temperature data downscaled using SDSM 4.2 into the HEC-HMS 3.4 model in Tunga-Bhadra river Basin. The change in simulated stream flows, evapotranspiration and water balance in the study area between current and future scenarios were investigated. As a result, hydrology of the basin was modeled quite well by HEC-HMS except for the high flows.

Reshma et al., 2013 used HEC-HMS to simulate runoff processes in Walnut Gulch Experimental Watershed in Arizona. They used Green-Ampt, CUH and kinematic wave methods for the simulation. In the result, it was observed that simulation of peal flow showed less variation than volume of runoff and time to peak when compared to the observed hydrographs.

Hydrological analysis or Grand Goudine Bayou, Louisiana was performed by Mason, (2011) involving selecting an appropriate transform method. Three transformed methods were tested viz. the Synder method, the SCS method and the Clark's Unit Hydrograph (CUH) method. Upon calibrating and comparing the transform methods, the results showed that the Synder method and the SCS method overestimated peak flow while the CUH method gave reasonable outflows owing to the reason that the CUH method accounts for storage within the watershed.

Arekhi, 2012 compared different methods for estimation of rainfall losses for prioritizing these methods to simulate runoff of Kan Watershed (197 km2) located in Tehran province of Iran. Arekhi compared initial and constant loss method, Green and Ampt method, deficit and constant loss method by considering two objective functions, PEPF and PEV. Finally, the initial and constant loss method was selected as optimum method for the purpose set because it gave better results than the other two methods in 70% of the events.

2.12 Flow Duration Curve

The flow-duration curve is a cumulative curve that shows the percent of time that flow in a stream is likely to equal or exceed during a given period (Searcy 2002). It combines in one curve the flow characteristics of a stream throughout the range of discharge, without regard to the sequence of occurrence. In addition, it shows the percentage of time river flow can be expected to exceed a design flow of some specified values and to show the discharge of the stream that occurs or is exceeded some percent of time (e.g. 60 percent of the time). Flow-duration analysis can be used for many purposes in the field of water

resources engineering and have been used to solve problems in water management, flood control, hydropower and scientific comparison of streamflow (Vogel and Fennessey 1995, Searcy 2002). The flow-duration curve of gauging stations in the Dudhkoshi river basin is provided in Figure 5.18. The period of the analysis is from 1978 to 2008. The discharge of higher than 500 m^3/s occurs more than 50 percent of the time and the lowest flow is higher than 200 m^3/sec.

2.13 Flood Frequency Analysis

Flood frequency analysis is one of the important studies of river hydrology. Flood frequency analysis involves fitting of a probability model to the sample of annual flood peaks recorded over a period of observation, for a catchment of a given region. It is essential to interpret the past record of flood events in order to evaluate future possibilities of such occurrences. The estimation of the frequencies of flood is essential for the quantitative assessment of the flood problem. The knowledge of magnitude and probable frequency of such recurrence is also required for proper design and location of hydraulic structures and for other allied studies. After a detailed study of the gauge data and its descriptive parameters such as mean, standard deviation, etc. and applying probability theory, one can reasonably predict the probability of occurrence of any major flood events in terms of discharge or water level for a specified return period (Singh, 2004). However, for reliable estimates for extreme floods, long data series is required; the use of historical data in the estimation of large flood events has increased in recent years (Archer, 1999; Black & Burns, 2002; Williams & Archer, 2002). Actually, there is no methodology available that can determine the exact amount of flood. Various methods available are either based on probability or empirical.

Methods based on Probability Theory are Gumbel, Log Normal and Log Pearson III distribution type, etc. (Sharma et al. 2003), studied flood risk zoning of Khando river and Osti (2008) conducted feasibility study on Integrated Community Based Flood Disaster Management of Banke, District using these formulas. Various empirical approaches such as Creager's formula, WECS/DHM Method, Modified Dicken's Method, B.D. Richard's Method, Synder's Method, etc. are also used for determining discharge for un-gauged basin. In WECS/DHM Method, the most significant independent variable is the area of the basin below 3000 m elevations. In most of the flood analysis cases, WECS/DHM Method seems to be reasonable (Ranjit, 2006). Gautam and Kharbujha (2006) studied about the flood hazard of Bagmati River using WECS/DHM Method.

In recent years, Satellite Rainfall Estimation is used in hydrological models to predict runoff and river discharge, and subsequent likelihood of floods and flash floods; area at risk of drought; and other rainfall related events. Satellite based rainfall estimates and products derived from them are accessible through the internet, and are being used for many diverse meteorological, hydrological, agricultural, and other applications throughout the world (Shrestha, 2008).

Flood frequency analysis uses historical records of peak flows to produce guidance about the expected behavior of future flooding. Two primary applications of flood frequency analyses are:

- To predict the possible flood magnitude over a certain time period.
- To estimate the frequency with which floods of a certain magnitude may occur.

2.14 Projected Discharge using RCM Data

Also called as future climate data. The outputs of the regional climate model (RCM) PRECIS developed by the Hadley Centre of the UK Meteorological Office was used for generating the future gridded climatic dataset. The PRECIS RCM is based on the atmospheric components of the ECHAM05 GCM from the Max Plank Institute for Meteorology, Germany. It generally runs with 50 km horizontal resolution with the option of fining to 25 km.

For more specific analytical tasks such as forecasting of absolute changes in agriculture yields at farm level, estimating surface runoff, river discharges at basin level etc., GCMs are not the appropriate tool. To satisfy this demand of detail, climate information derived from GCMs need to be downscaled for a country like Nepal, as it has a complex topography towards the northern parts of the country. Regional Climate Model (RCM) is the most reliable option for downscaling coarse resolution of GCMs outputs to fine resolution (12, 20 and 25 km) grids, incorporating local topography in Nepal and its surroundings and used PRECIS, RegCM4 and WRF models for downscaling of GCMs climate information over Nepal. By choosing three different models, the assimilated results are not model dependent, but representative for the natural climate variability. Lateral Boundary Conditions (LBCs) from several GCMs were used with different emission scenarios (SRES) to project future climate changes over Nepal due to continued anthropogenic inputs of greenhouse gases. A1B is regarded as “medium” and A2 is regarded as “high” emission trajectory as proposed under the SRES (IPCC, 2007). The

future climate projections were run for the period 2030 to 2060 (representative for mid-21st century) for Nepal with A1B and A2 scenarios.

Nepal region has varying topography and simulating reasonable regional climate over such a region is a challenge to RCMs. Due to availability of gridded observations from DHM Nepal at high resolution (25km, 20km and 12km) an assessment of the RCM (precipitation) performance has been carried out and presented in this dissertation (www.dhm.gov.np).

2.15 Impact of climate change on Himalayan hydrology

Glacier fed rivers provide much of the water supply for agriculture in various regions such as Canadian prairies and central Asia for hydroelectric power production in France, Switzerland, Norway and even Nepal. In comparison with other types of stream flow, glacier run-off has unusual features such as large diurnal fluctuations and maximum flow during summer. Glaciers act as reservoirs that store water in solid form in cool summers and winters and release large amounts in hot dry summers when water from other sources is in short supply. There is also long-term storage; the mean annual flow of a glacier-fed river, measured during a period of glacier retreat, overestimates the amount of water available should the glaciers start to advance. On the other hand, long continued retreat, a likely consequence of "green-house warming", will eventually reduce or even eliminate this source of water. To forecast the flow of glacier fed streams requires an understanding of accumulation and ablation processes and of glacier hydraulics (W.B.Paterson).

The Himalayan Rivers are expected to be very vulnerable to climate change because snow and glacier melt water make a substantial contribution to their runoff (Singh, 1998). However, the degree of sensitivity may vary among the river systems. The magnitudes of snowmelt floods are determined by the volume of snow, the rate at which the snow melts and the amount of rain that falls during the melt period (IPCC, 1996b). Gurung (1997) has revealed that there will be decrease in runoff in dry seasons and increase in runoff in monsoon season under the doubled CO_2 scenario using the Canadian Climate Centre Model (CCCM) and Geophysical Fluid Dynamics Laboratory (GFDL) models.

Based upon the results from high resolution general circulation models (GCMs), the IPCC (1990) reports for the Indian subcontinent stated that by 2030, on 'business-as-usual' scenarios, the warming will vary from 1 to 2 ˚C throughout the year. Precipitation will change little in winter and will generally increase throughout the region by 5 to 15 % in

summer. The model results obtained from the greenhouse warming experiment suggested an increase of more than 2˚C over the monsoon region in the next 100 years.

The precipitation fluctuation in Nepal is not the same as the all-India precipitation trend but it is well related with rainfall variations over northern India (Shrestha et al., 2000). Precipitation over land generally increased over the 20th century between 30˚ N and 85˚ N, but notable decreases have occurred in the past 30 to 40 years from 10˚ S to 30˚ N (IPCC, 2008). But in Nepal there is an increase in precipitation (analysis from 1978 to 2001) i.e. 0.6 % annually (Chaulagain, 2003) though it lies between 26˚ to 30˚ N.

According to ICIMOD (2011), by the 2050s access to fresh water in Asia, particularly in the larger basin is projected to decrease as the rates of warming in the HKH region is higher than the global average. With the region the rates in the western Himalayas, eastern Himalayas, and the plains of the Ganges basin over the last 25 years are lower (0.01-0.03 °C per year, respectively), and those in the central Himalayas (Nepal) and the Tibetan Plateau appear to be considerably higher (0.004-0.09 °C per year and 0.03-0.07 °C per year) respectively. Warming will affect the amount, timing and distribution of precipitation and result in increased snowmelt and runoff, affecting river water supplies; and reduce permafrost coverage, altering vegetation composition.

CHAPTER III

Study Area

River Basins in Nepal

3.1 Background

Depending on the source and discharge, the rivers in Nepal can be classified into three types. The Mahakali, Karnali, Gandaki and the Koshi are the four main river systems. They originate in the Himalaya and carry snow fed flows with significant discharge even in the dry season. These rivers are perennial and have tremendous potential as a source of irrigation and hydropower development. The Babai, West Rapti, Bagmati, Kamala, Kankai and the Mechi are medium rivers. These rivers originate in the Midlands or the Mahabharat Range and are fed by precipitation as well as groundwater regeneration (including springs). These rivers too are perennial but are commonly characterized by a wide seasonal fluctuation in discharge. In addition to these large and medium river systems, there are a large number of small rivers in the Terai which mostly originate in the Siwalik Range. These rivers are seasonal with little flow during the dry season which renders them unsuitable for year round irrigation or hydropower generation without surface storage. The rivers in Nepal are characterized by wide, seasonal fluctuation of flow. The monthly flows generally reach their maximum in July-August and decline to their minimum in February-March. About 80% of the total flow occurs during five months (June - October) and the rest during the remaining months. It can be generalized that the smaller the size of the river catchment area, the wider is the range of flow fluctuation (WECS, 2011).

Among these river basins, the DudhKoshi basin is study area for this task and other basins are only briefly explained here.

3.2 Koshi River Basin

The Koshi also called Saptakoshi for its seven Himalayan tributaries— Tamor, Arun, Dudh Koshi, Likhu, Tama Koshi, Sun Koshi and Indrawati. Some of the rivers of Koshi system, such as the Arun, the Sun Koshi and the Tama Koshi originate in Tibet. It is one of the largest tributaries of the Ganges.

Nepal has a total estimated potential of 83,290 MW out of which economically exploitable potential is 42,140 MW. The Koshi river basin contributes 22,350 MW of this

potential (360 MW from small schemes and 1875 MW from major schemes) and the economically exploitable potential is assessed as 10,860 MW (Yogacharya K S, 2000).

It is the largest river basin of Nepal and lies between latitudes 26°52'0" to 29°6'41"N and longitude 85°44'51" to 89°14'53"E. The location of the confluence of three major tributaries Arun, Tamor and Sun Koshi rivers is at 26°54′47″N, 87°09′25″E, Tribenighat, Nepal. According to DHM Nepal, it comprises an area of about 54, 100 sq.km at the Chatara-Kohtu gauge station and drains eastern part of the country. Out of a total catchment area, 29,400 sq.km. lies in Tibet (China) and the remaining in Nepal. The highest elevation in this basin is 8,848 m a.s.l. (Mt. Everest) to 140 m a.s.l.

The major rivers which are responsible for flow in the Saptakoshi are Tamor, Arun and Sun Koshi River. But there are other many small rivers which join to the Saptakoshi. The sub-catchments of the Saptakoshi are shown in figure 3.1 and their areas at the gauge stations are shown Table 3.1.

Table 3.1 Description of the rivers and gauge stations in the Saptakoshi basin

S. No	Staion Index	Name of River	Location	Latitude(N)	Longitude (E)	Elevation (m)	Catchment Area (Sqkm)		Discrepancy	Local CA (Sqkm)
							From DHM	From GIS		
1	600.1	Arun	Uwa Gaon	27 35 21	87 20 22	1294	26750	29616	11%	29616
2	647	Tamakosi	Busti	27 38 05	86 05 12	849	2753	2898	5%	2898
3	695	Saptakosi	Chatara- Kothu	26 52 00	87 09 30	140	54100	58053	7%	200
4	681	Sunkosi	Hampuachuwar	26 55 15	87 08 45	150	18700	17936	-4%	4315
5	627.5	Melamchi	Helambu	28 02 21	85 32 07	2134	84	117	39%	117
6	602.5	Hinwakhola	Pipletar	27 17 45	87 13 30	300	110	112	2%	112
7	620	Balephi	Jalbire	27 48 20	85 46 10	793	629	659	5%	659
8	652	Sunkosi	Khurkot	27 20 11	86 00 01	455	10000	10201	2%	1974
9	684	Tamur	Majhitar	27 09 30	87 42 45	533	4050	4530	12%	4530
10	690	Tamur	Mulghat	26 55 50	87 19 45	276	5640	6008	7%	1477
11	630	Sunkosi	Pachuwar Ghat	27 33 30	85 45 10	602	4920	5004	2%	4227
12	670	Dudhakosi	Rabuwa Bazar	27 16 14	86 40 02	460	4100	3419	-17%	3419
13	650	Khimtikhola	Rasnalu Village	27 34 30	86 11 50	1120	313	326	4%	326
14	602	Sabayakhola	Tumlingtar	27 18 36	87 12 45	305	375	406	8%	406
15	606	Arun	Simle	26 55 42	87 09 16	152	30380	33503	10%	1721
16	604.5	Arun	Turkeghat	27 20 00	87 11 30	414	28200	31670	12%	2053

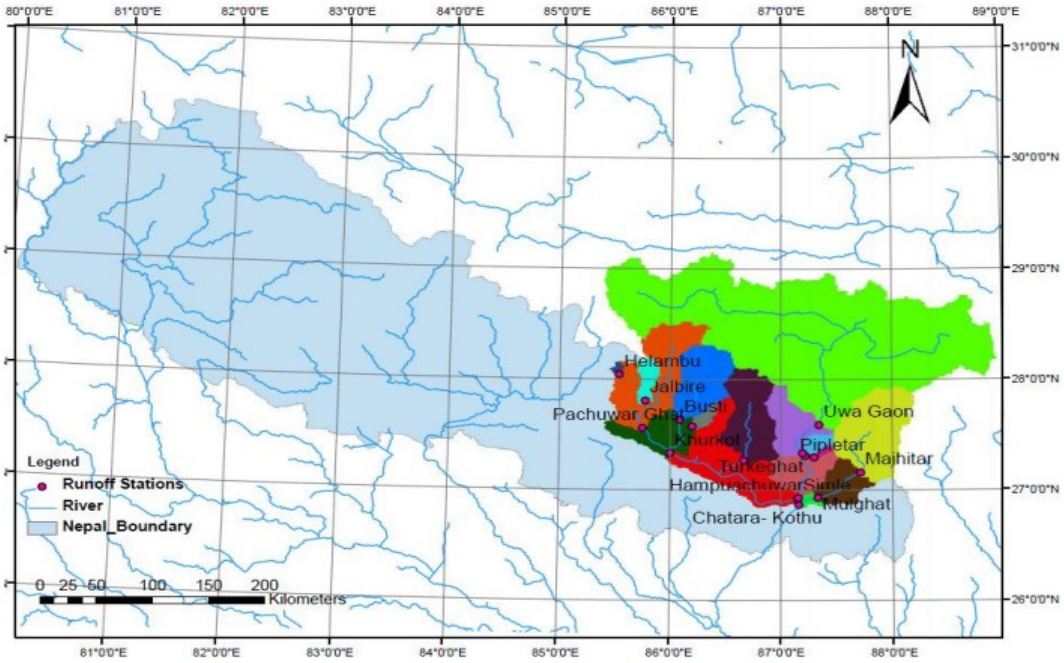

Figure 3.1 Sub-catchments at different gauge stations of the Saptakoshi basin (ICIMOD, 2011)

3.3 Gandaki or Narayani River Basin

The river network of central Nepal is occupied by the Gandaki River system. This basin comprises Trishuli, BudhiGandaki, Marsyangdi, Daraudi, Madi, Seti and Kali Gandaki River. It has a total catchment area of 46,300 square kilometers. The West-Rapti River drains Rapti Zone in Mid-Western Region, Nepal, then Awadh and Purvanchal regions of Uttar Pradesh state, India before joining the Ghaghara a major left bank tributary of the Ganges.

3.4 Karnali River Basin

The Karnali River is a perennial, turbulent and undisturbed river of the Himalayas, which is the longest river of Nepal. It originates from Mansarover and Rakes Lake and receives many snow fed river which are as Mugu Karnali, Humla Karnali, Tila, West Seti, Thuli Bheri and Sani Bheri at Himalayan belt. The Karnali basin lies between the mountain ranges of Dhaulagiri and Nanda Devi, in the western part of Nepal. The area around these features is the hydrographic nexus of South Asia since it holds the sources of the Indus and its major tributary the *Sutlej*, the Karnali—a Ganges tributary—and the Yarlung Tsangpo/Brahmaputra.

3.5 Mahakali River Basin

The Mahakali River flows between the countries of India and Nepal acts as the west boundary of Nepal. It originates from Kalapani at an altitude of 3600 m and finally joins with the Ganges River System. There are two important tributaries of the Mahakali River in Nepal. These two rivers are the Chamelia River and the Limpiyadhura River. The snowcapped mountain peaks are the major origin of the Mahakali River in Nepal. The *Mahakali* or *Kali* along the Nepal-India border on the west joins the Karnali in India, where the river is known as *Goghra* or *Ghaghara*.

3.6 Dudhkoshi River

3.6.1 Location and Drainage System

Dudhkoshi River is a major tributary of the Sapta-Koshi basin, located in the Solukhumbu region of Nepal with high contribution of flow, approximately 150 km east of Kathmandu and is a part of the larger Sapta-Koshi river basin (figure 3.2). The world's highest peak lies in the basin area which form the backbone of the mountain chain. The study area is located in the northeast of Nepal Himalayas (CIWEC). Geographically, Dudhkoshi river basin has the length of 120 km which extends from 27.65 – 28.10 N to 86.52 –87.00 E (ICIMOD 2011). This region is one of the most glaciated region.

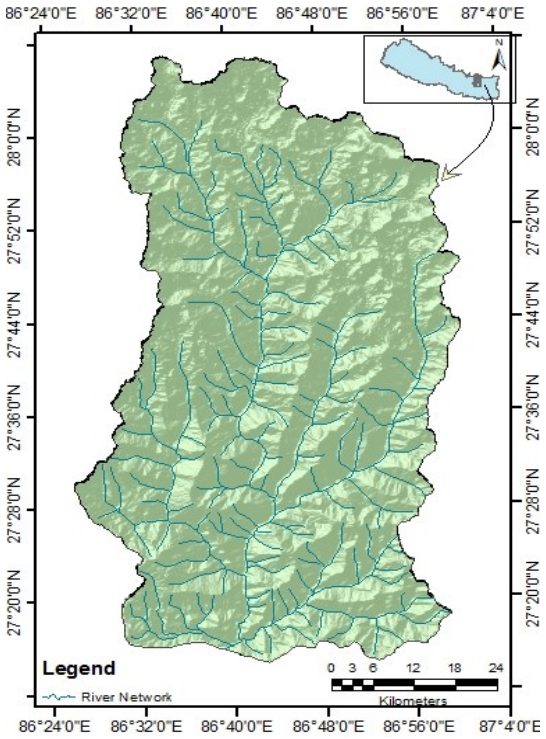

Figure 3.2 Location and drainage network of Nepal Himalayas.

It has an elongated shape with its main axis oriented north-south. The study area is situated in the monsoon dominated eastern Himalaya situated at Rabuwa Bazar, which contain high Himalayan range, high mountainous, middle mountains ranging from 8848 m to 430 m above sea level and is one of the country's largest and most important basins in terms of glaciers and glacier lakes.

Dudhkoshi River is a major tributary of the Sapta Koshi River system to which it contributes approximately 12% of the flow. The river rises in the High Himalayas from

two main sources 12-15 km north-west and north-east of Namche Bazar respectively. The river flows in a mainly southerly direction until reaching the dam site, when it takes an abrupt change in direction to the south-west, towards the Sun Koshi River, a distance of 27 km. Some of the tributaries of Dudhkoshi are Imja khola, Bhote Koshi, Hunga Khola, Dudu Khola, Kaku Khola, Solu Khola & source of inflow being from small tributaries situated upstream of the damsite is Thotne Khola on the right bank and Rawa Khola on the left bank.

Since 1964, DHM has maintained a gauging station in Dudhkoshi River at Rabuwa Bazar, Station No. 670 ($27^0$16'14" N, $86^0$40'02" E, elevation 460 m above sea level). The river gradient at the gauging site is around 0.8% and increases in the range of 9%-20% as the higher mountains are approached (CIWEC). The average daily and monthly flow and instantaneous maximum and minimum, annual discharges and water levels are available at Rabuwa Bazar; the long-term mean annual flow of Dudhkoshi River at Rabuwa is about 202 m^3/s (DHM, 2009).

3.6.2 Hydro-meteorology

The rainfall probabilities, space and time distribution of rainfall, recurrence interval of major storms, snow melt and runoff, around the study area determines by the hydro-meteorological study of area. For this study the reference data *i.e*. precipitation and runoff are taken from Department of Hydrology and Meteorology (DHM). Out of the five meteorological stations, 1202 (86.72, 27.70), 1203 (86.57, 27.43), 1204 (86.75, 27.35), 1219 (86.58, 27.50) & 1220 (86.37, 27.29); four stations 1202, 1203, 1204, and 1219 are only used in the calculation of the rainfall analysis.

3.6.3 Climatic Condition

The climate of the Himalayan region in general is greatly influenced by the Indian monsoon system. The summer monsoon dominates the climate from May to September and westerly circulation dominates from November to March (winter monsoon). Within Nepal, the onset of summer monsoon starts from the eastern part (the Koshi river basin) from mid-June to September (Ueno et al. 2008). During the summer season, the Tibetan Plateau warms rapidly relative to the Indian Ocean. The resulting low pressure over Asia/Himalaya and higher pressure over the Indian Ocean gives rise to the strong low-level atmospheric pressure gradient that in turn generates the southwest monsoon (Overpeck et al. 1996) which brings moist air currents flow from the Bay of Bengal to

the Indian sub-continent. When the moist flow approaches the land, maximum precipitation occurs upstream and over the lower windward slopes of the west-and south-facing Mountain barriers (Medina et al. 2010). The latitude of the basin and its physiography are the principal factors which influence the annual cycle of climate experienced throughout the basin. Temperature and precipitation vary substantially from south to north.

There are primarily four seasons in the region. They are: the winter (December - February), the pre-monsoon period (March - May), the monsoon period (June - September) and the post-monsoon period (October - November) (Shrestha et al. 1999). The temperature starts to rise after February and reaches its maximum level during the monsoon season. The rainy season coincides with the summer monsoon. The basin has tropical to sub-tropical climate at the lower altitude (Terai and Siwalik) characterized by a hot and wet summers and mild and dry winters. The Middle Mountain (the Lesser Himalaya) exhibits a warm temperate monsoon climate. The higher altitude area has sub-alpine to alpine climate up to 4,800 m associated with low temperatures. Higher than snowline exhibit very cold climatic conditions where the temperature remains below zero degree Celsius throughout the year which provides conditions for the development of glaciers in the region. (MoFSC 2002, Mool et al. 2001b).

About 80% of the total annual precipitation occurs during the months of June through September, however, this varies annually (Ueno et al. 2008). During this period, the region receives intense rainfall which brings floods and widespread damage to property and lives. The Koshi river basin experiences floods every year which impact eastern Nepal and the plain areas of India.

3.6.4 Topography and Physiographic condition

The Dudhkoshi basin is bordered in the north by the vast Tibetan Plateau, in the east by Arun River Basin, in the west by Likhu River basin. The basin has high gradient and steep topography ranging from 430 m – 8848 m a.s.l. It has wide range of climatic condition sub-tropical to alpine climate in the highs, with basin area of 3849 km^2.

In general, the lower-elevation basin area, the Terai and Siwalik region, is covered by tropical evergreen and deciduous riverine forest with mixed vegetation such as grassland and shrub land. In the middle mountain areas, the natural vegetation includes broad leaved forests.

Between 2,000-4,000 m, the vegetation type in the basin area is dominated by coniferous forest along with grass land. Higher than 4,000 m, the area is dominated by essentially bareland with few patches of grasslands and shrubland. Higher than 5,500 m, there are rocky mountain peaks covered by glaciers and permanent snow cover (MoFSC 2002, Sharma et al. 2000a). In short, Dudhkoshi basin consists 14% of the glacierized region, 41% forest areas, 11% agriculture land, bareland 25% and rest 9% (S.Nepal, 2012).

The Himalaya of Nepal is geologically active where the instabilities due to tectonic activity and ongoing erosion are apparent everywhere. These factors, combined with the peculiar meteorological conditions where both the rainfall and river flow vary tremendously in both time and space, make the landscape vulnerable to water-induced disasters such as floods, landslides, slope failures.

3.6.5 Glacier and glacier lakes

The DudhKoshi basin is the one that contains the highest number of glacial lakes as well as lakes associated with glaciers. Altogether 98 major glacial lakes are associated with the glaciers. This includes also the blocked lakes within the range of 1.65 km. The areas of the major glacial lakes range from 0.021 sq.km to 0.529 sq.km and their elevations are between 4,349 m asl and 5,636 m asl. There are 267 supra glacial lakes, out of which only 31 lakes are larger than 0.02 sq.km in area. The sub-basin consists of 10 blocked lakes and 33 moraine-dammed lakes which are susceptible to Lake Outburst. Thirteen lakes are identified as potentially dangerous in the Dudh Koshi basin. The potentially dangerous lakes of the DudhKoshi basin are Kdu gl 28 (Lumding Tsho), Kdu gl 55 (Dig Tsho), Kdu gl 349 (Chokarma Cho), Kdu gl 350 (Imja Tsho), Kdu gl 399 (Tam Pokhari), Kdu gl 449 **(Hungu Lake**), Kdu gl 459 (East Hungu 1), Kdu gl 462 (East Hungu 2), Kdu gl 464 and Kdu gl 466 (West Chamjang). Among these, Dig Tsho and Tam Pokhari already had outburst events in 1985 and 1998 respectively. The glacial lake Kdu gl 349 (Chokarma Cho) has also drained out in the past but this is not recorded.

3.7 Research Design

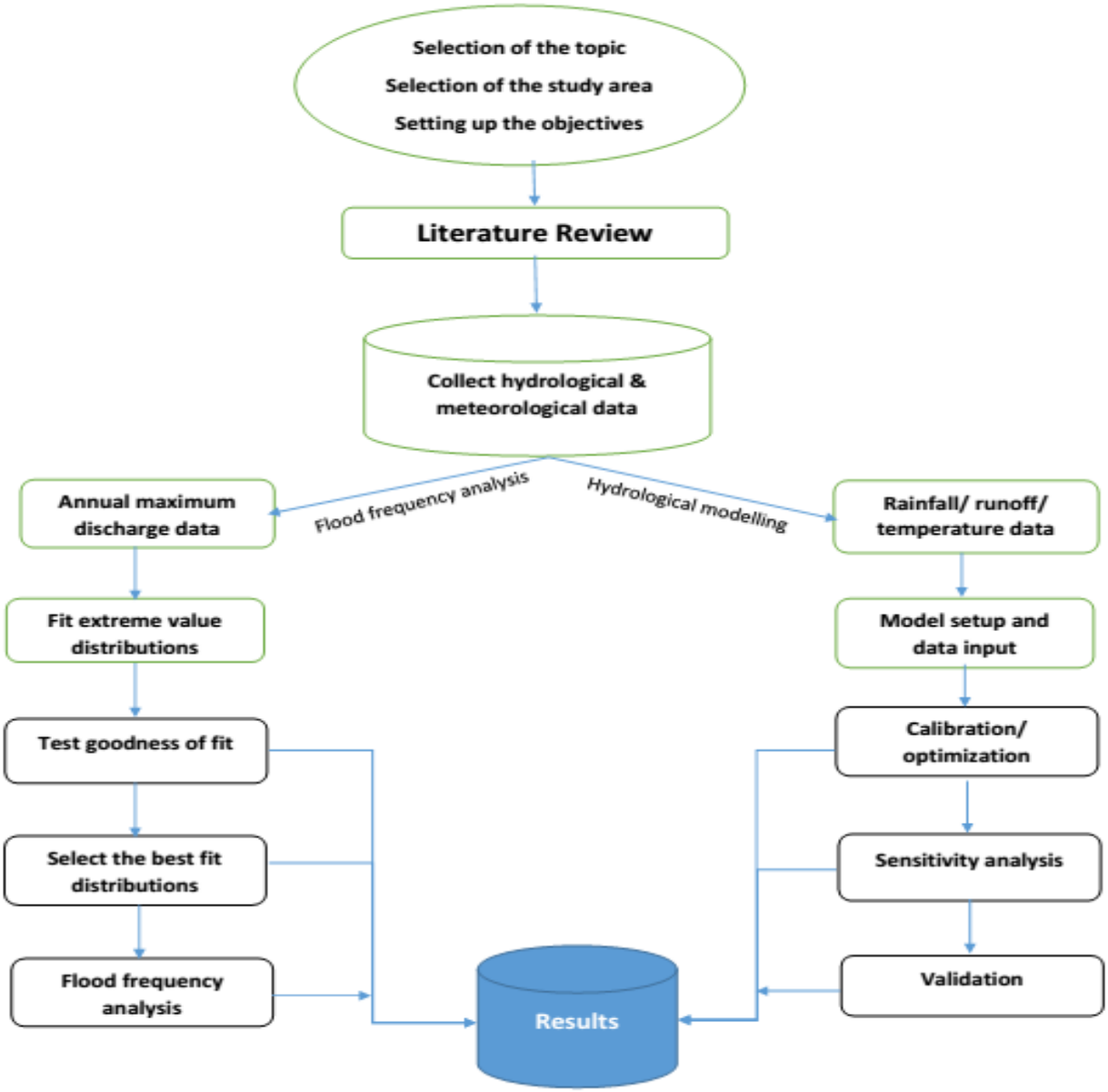

Figure 3.3 Research Design

3.8 Methodology

In this study, different methods and different tools are adopted. 4 monthly rainfall stations were used in basin analysis. GIS and HEC-HMS are the tool for analysis of the study of the basin. Total 31 years (1978 to 2008) of daily discharge data are used for long term mean monthly and annul discharge. And for flood frequency analysis, maximum instantaneous data and maximum discharges of these years are used. 20 hydrological stations lie in Koshi basin which is used for regional analysis.

3.9 Method of Data Collection

Generally, secondary data is carried out for this study. The meteorological and hydrological data were collected from Department of Hydrology and Meteorology (DHM). For literature review, journals, book reports and past study of related subject matter were collected from NAST, Recham, SOHAM, TU- library, and NEA library and from different websites. The detailed methods for the calculation and estimation of these parameters are further described in the subsequent sections.

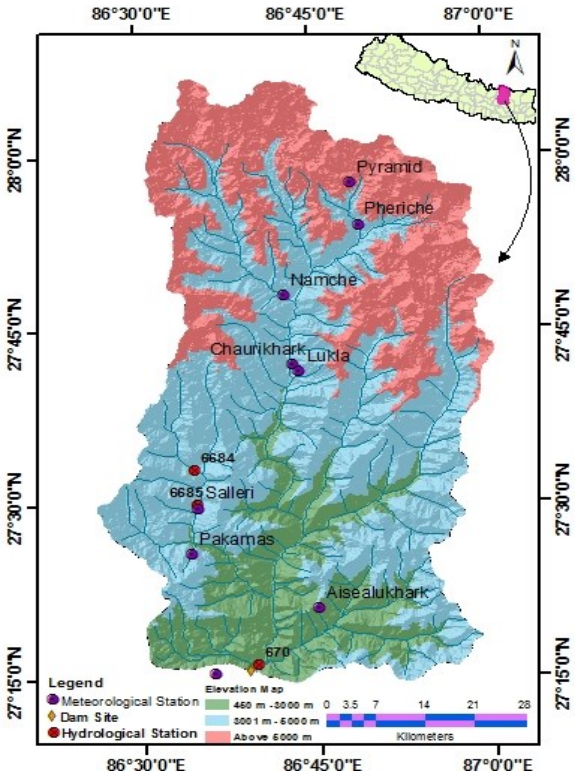

Figure 3.4 Hydro-meteorological Stations

3.10 Flow Analysis

For the proper assessment of the hydrological discharge, long term flow data are essential. The hydrological analyses were carried out using long term flow data of Rabuwa bazar gauging station. Mean monthly and annual flows at gauging site were estimated by the following approaches:

i) WECS – DHM Method 1990;
ii) WECS – DHM Method 2004;
iii) Regional Analysis
iv) Transformation Method

3.10.1 WECS – DHM Method 1990

In July 1990, a report on "Methodologies for Estimating Hydrologic Characteristics of Ungauged Locations in Nepal" was published by Water and Energy Commission Secretariat and Department of Hydrology and Meteorology (WECS/DHM, 1990).

WECS in collaboration with DHM has developed a regression equation for estimating the hydrologic characteristics of the ungauged basin. The method consists of the regression equation for estimating the long term average monthly flow in which the flood flow in any river of catchment area below 3000 m of elevation is given by

$$Q_2 = 1.8767(A+1)^{0.8783} \quad \text{..... 3.1}$$

$$Q_{100} = 14.63(A+1)^{0.7342}$$

..... 3.2

Where, suffix 2 and 100 stand for the return periods in numbers of years. The flood flows for any other return period **T** is then given by:

$$Q_T = exp(lnQ_2 + S\alpha) \quad \text{..... 3.3}$$

Where ***S*** stands for a standardized normal variat for particular return period **T (Table 6.1)**. α is calculated as,

$$\alpha = \ln(Q100/Q2)/2.326$$

..... 3.4

Table 3.2 Values for Standard Normal Variate for Various Return Periods

Return Period (T) years	Standard Normal Variate (S)
2	0
5	0.842
10	1.282
20	1.645
50	2.054
100	2.326

The equation is as follows:

Q (mean month) = C x (Area of the basin)^{A1} x (Area below 5000m+1)^{A2} x (monsoon wetness index) ^{A3}

…… 3.5

The basin characteristics like area of the basin, area below 5000 and monsoon wetness index remain same, whereas the coefficients C, A1 and A2 are different for each month resulting unique equations for estimating the flow.

3.10.2 WECS – DHM Method 2004

DHM has revised the DHM-WECS method using long range and larger number of hydro-meteorological data. In Modified DHM 2004 flood estimation method, the flood with two years and hundred years return periods flood values (Q_2 and Q_{100}) were computed based on the drainage area below 3 km elevation as given in the equations below.

$$Q_2 = 2.29 \times A_{<3km}^{0.86}$$ ……

3.6

$$Q_{100} = 20.7 \times A_{<3km}^{0.72}$$ …….

3.7

Where, Q is the flood discharge in m^3/s and A is the basin area in km^2. The subscript 2 and 100 indicate 2 year and 100 year flood respectively. Similarly the subscript <3km indicates area below 3000 m elevation.

The regression equation, thus, developed is of the form:

$$Y = a + bX_1 + cX_2 + dX_3$$ …….. 3.8

Where **Y** is the discharge for a given for a given month after an appropriate transformation, **a, b, c** and d are coefficients. **X_1, X_2** are average elevation of the catchment (m) and annual precipitation (mm) respectively. **X_3** represents catchment area below 3000 m or 5000 m as required. It is noted here that **X_1 = 4874 m, X_2 = 1973 mm, X_3 = 736.69 km^2** (< 3,000m) or **2029.65 km^2** (< 5,000m).

Limitation of WECS/DHM 1990 and WECS/DHM 2004 method is: it only considers the area below 5000 m a.s.l.

3.10.3 Regional Analysis

The stream flow records of 17 gauging stations within the Koshi basin were collected and used for the Regional Analysis. The mean monthly flow of these stations are given in Table 3.2.

Table 3.3 Data used for Regression Analysis

SN	Station No.	Location	River Name	Used Data From	Used Data To	Area (km^2)	Jan	Feb	Mar	Apr	May	Jun	Jul	Aug	Sep	Oct	Nov	Dec	Annual
1	600.1	Uwa Gaon	Arun	1985	2010	26750	67.5	69.4	82.5	96.4	151	358	635	725	523	245	115	80.3	262.3
2	602.5	Pipaltar	Hinwa Khola	1974	2008	110	2.1	1.66	1.46	2.23	4.99	10.2	15.6	16.8	14.3	8.99	5.01	3.13	7.2
3	604.5	Turkeghat	Arun	1975	2008	28200	107	106	123	157	257	620	1140	1230	917	422	200	138	451.4
4	606	Simle	Arun	1986	2008	30380	197	184	206	238	346	664	1280	1500	1070	554	324	258	568.4
5	610	Barabise	Bhote Koshi	1970	2008	2410	24.3	21.7	20.9	25.6	39.2	88.4	180	262	169	82.8	43.1	29.6	82.2
6	620	Jalbire	Balephi Khola	1970	2008	629	13	11.3	10.8	12.2	17.7	54.1	136	169	118	52.3	25.6	17.3	53.1
7	630	Pachaur Ghat	Sunkoshi	1970	2008	4950	57.6	49.8	47.6	53.2	80.1	212	561	702	467	206	110	74.1	218.4
8	602	Tumlintar	Sabhaya Khola	1974	2008	375	6.31	5.32	4.92	6.67	16.1	33.7	52.7	55.3	50	26.4	13.2	8.46	23.3
9	647	Busti	Tamakoshi	1971	2008	2753	29.2	25.6	24.8	28.2	52.1	165	425	496	312	122	57.6	37.9	148.0
10	650	Rasnalu	Khimti Khola	1970	2008	313	5.92	5	4.65	5.21	8.61	36	86.7	90.4	54.5	24.2	11.9	7.88	28.4
11	652	Khurkot	Sunkoshi	1970	2008	10000	110	92	84.4	95.3	155	497	1330	1760	1080	457	220	141	501.8
12	660	Saghutar	Likhu	1970	2008	823	14.9	12.4	11.5	12.8	18.5	52.7	146	162	122	60.4	32	20.2	55.5
13	670	Rabuwa Bazar	Dudh Koshi	1964	2008	3720	44.5	36.6	34.9	41.7	72.2	246	570	604	445	189	89.5	58.2	202.6
14	680	Kampughat	Sunkoshi	1970	2008	17600	195	168	153	167	242	828	2470	2810	2010	902	391	248	882.0
15	684	Majhitar	Tamor	1986	2008	4076	52.5	46.3	48.9	71.5	133	320	643	786	501	222	108	70.4	250.2
16	690	Mulghat	Tamor	1965	2008	5640	68.2	56.2	55.3	81.9	180	479	947	1050	749	346	155	94.7	355.2
17	695	Chatara	Tamor	1977	2008	54100	387	335	337	425	759	1890	3980	4530	3420	1610	813	523	1584.1

Source: Stream Flow Summary, DHM, 2012

Based on the monthly flow data, regression equation for each month has been derived with regression parameters shown in Table 3.3 (Fitting equation to the data for the annual average flow is shown in Figure 3.5. The generated long term mean monthly flow by this method for the Dudhkoshi at gauging site is shown in Table 3.5. The average annual mean flow came to be 217.9 m^3/s. The error even for Rabuwa Station is more than 22.2%, in some months. As the coefficient of determination is very good (> 0.9), it can be said that the regression equations, thus, derived are quite capable to estimate the flow at ungauged sites for Dudhkoshi Basin.

Table 3.4 Regression Parameters for regression equation

Used Formula		$Q = mA^n$
where	Q	Flow (m^3/s)
	A	Catchment Area (km^2)
	m	constant
	n	constant

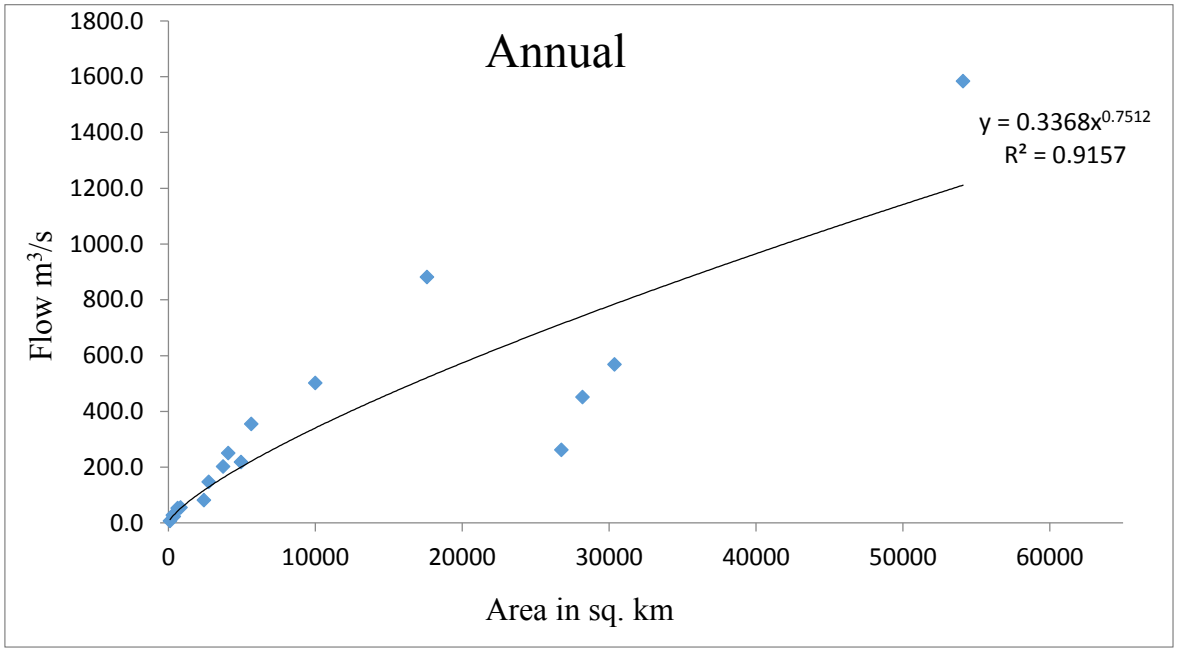

Figure 3.5 Relation between Annual Average Flow and Area

Table 3.5 Coefficient values of long term monthly and annual average flows of regression equation

Coefficient	Jan	Feb	Mar	Apr	May	Jun	Jul	Aug	Sep	Oct	Nov	Dec	Annual
m	0.0847	0.0614	0.0466	0.0638	0.1442	0.431	0.8373	0.8977	0.7003	0.3902	0.211	0.1471	0.3368
n	0.7472	0.7698	0.801	0.7879	0.7537	0.7406	0.7543	0.7637	0.7519	0.7303	0.7197	0.7103	0.7512
R^2	0.9408	0.9562	0.9695	0.9669	0.9473	0.9305	0.8904	0.8893	0.9038	0.9166	0.9212	0.9231	0.9157

Table 3.6 Long term monthly and annual average at gauging site

Months	Jan	Feb	Mar	Apr	May	Jun	Jul	Aug	Sep	Oct	Nov	Dec	Annual
Regional Method	75.5	67.2	63.9	76.4	117.1	242.4	442.9	503.9	379.7	208.9	124.2	90.2	217.9
Damsite Transposed	43.9	36.1	34.3	41.2	74.6	247.9	597.0	616.3	474.7	178.8	86.3	58.8	207.5
WECS-DHM 2004	49.2	42.8	20.1	23.7	37.5	215.4	436.0	590.8	368.4	179.8	89.2	61.6	176.2
WECS-DHM 1990	33.0	28.0	26.5	31.2	47.6	46.6	358.1	414.5	308.4	137.1	71.8	46.5	129.1

3.10.4 Transformation Method

Transformation method is based on the principle that for a hydrological similar catchment, the gauged basin can be transformed to ungauged basin using Catchment Area Ratio (CAR) method.

$$\frac{Q_{damsite}}{Q_{Rabuwa}} = \left(\frac{A_{damsite}}{A_{Rabuwa}}\right)^{q} \times \left(\frac{P_{damsite}}{P_{Rabuwa}}\right)^{n} \quad \text{..... 3.9}$$

For average flow q is close to 1 and for maximum flow it is close to 0. Actually it is a function of WECS/DHM method. It is noted here that when n=0, it is only area transformation. If q=1 and n=1, the equation 3.9 becomes;

$$\frac{Q_{damsite}}{Q_{Rabuwa}} = \frac{A_{damsite}}{A_{Rabuwa}} \times \frac{P_{damsite}}{P_{Rabuwa}} \quad \text{..... 3.10}$$

In case of Dudhkoshi 670, it has the measured flow data. It has to be transformed to the dam site. A relation fairly accurate for instantaneous peaks takes the following form, which is also suggested by DHM for the instantaneous flood flows (DHM, 2004). For the instantaneous flood flows, the transposition factor will be taken as:

$$\frac{Q_{damsite}}{Q_{Rabuwa}} = \left(\frac{A_{damsite}}{A_{Rabuwa}}\right)^{0.5} \quad \text{..... 3.11}$$

3.11 Flood Frequency Analysis

A statistical method rather than the usual design storm unit hydrograph approach was used to derive the design flood for the dam site. The analysis of the flood flows for the Dudhkoshi at Rabuwa have been carried out by taking the yearly maximum discharge from DHM (1978 to 2008).

Similarly, the peak discharge data of 31 years is used for the flood frequency analysis of Dudhkoshi River. Thus, Gumbel or EV1 (Extreme Value Type I), LPT-III, and Log Normal distribution was used for analysis of observed discharges and estimate the flood peak discharge in the DudhKoshi Region. The result is then compared with the results obtained by analyzing the peak flow data simulated by the model.

3.11.1 Gumbel Distribution (EV1)

This Extreme Value Distribution was introduced by Gumbel (1914) and is commonly known as Gumbel's Distribution. It is one of the most widely used probability distribution functions for extreme values in Hydrological and Meteorological studies for the prediction of flood peaks, maximum rainfall, maximum wind speed, etc.

According to his theory of extreme events, the probability of occurrence of an event equal to or larger than a value of x_0

$$P(X \geq x_0) = 1 - e^{-e^{-y}} \qquad \ldots\ldots\ldots\ldots\ldots$$

3.12

In which y is a dimensionless variable given by

$$y = \alpha(x - a)$$
$$a = \bar{x} - 0.45005\sigma_x$$

Thus

$$y = \frac{1.2825(x - \bar{x})}{\sigma_x} + 0.577 \qquad \ldots\ldots\ldots\ldots\ldots$$

3.13

Where $\bar{x}$ = mean and σ_x = standard deviation of the variate X. In practice it is the value of X for a given P that is required and the eqn. is transposed as

$$Y_p = -\ln[-\ln(1 - P)] \qquad \ldots\ldots\ldots\ldots\ldots$$

3.14

Noting that return period T = 1/P and designating Y_T = the value of y, commonly called the reduced variant, for a given T,

$$Y_T = -\left[\ln \ln \frac{T}{T-1}\right]$$
$$Y_T = -\left[0.834 + 2.303 \log \log \frac{T}{T-1}\right] \qquad \ldots\ldots\ldots\ldots\ldots$$

3.15

So, the value of variate X with a return period T is

$$x_T = \bar{x} + K\sigma_x$$
$$where,\ K = \frac{(y_T - \overline{y_n})}{\sigma_n} \qquad \ldots\ldots\ldots\ldots\ldots$$

3.16

$\overline{y_n}$ = mean of reduced variate (it is table value)

σ_n = standard deviation of reduced variate (it is table value)

3.11.2 Log-Pearson Type III Distribution

The procedure to be adopted in using this distribution to arrive at the flood discharge of any given return period is as follows. If X is the variate of a random hydrologic series, then the series of Y variates where

$y = \log x$ …..……

3.17

are first obtained. For this Y series, for any recurrence interval T, gives

$y_T = \bar{y} + k_T \sigma_y$ …...……..

3.18

Where k_T = a frequency factor which is a function of recurrence interval T and the coefficient of skew C_s,

σ_y = standard deviation of the Y variate sample

$= \sqrt{\sum(y - \bar{y})^2/(N-1)}$ and

C_s = coefficient of skew of variate Y

$= \frac{N\sum(y - \overline{y})^3}{(N-1)(N-2)\sigma_y^3}$ ……...

3.19

$\bar{y}$ = mean of the y value

N = sample size (number of years of record).

The design flood is now given by

x_T = antilog (y_T) ……

3.20

When the skew is zero, i.e. $C_s = 0$, the log-Pearson Type III distribution reduces to **Log Normal Distribution.**

3.12 Probable Maximum Precipitation (PMP)

Probable maximum precipitation is defined as the depth of rainfall that approaches the upper limit of what the atmosphere can produce. Probable maximum precipitation is necessary for estimating the probable maximum flood, basis of which main hydraulic structures are to be designed. Chow's equation is used for statistical approach of PMP in this study. This approach is recommended by WMO manual.

$PMP = P + K*\sigma$ …… 3.21

Where, P is mean annual maximum values

K is frequency factor which depends upon the statistical distribution of the series, number of year of recorded and the return period. (This factor is heavily depends on rainfall duration and Chow's limits is 6 to 30), σ is standard deviation.

3.13 Probable Maximum Flood

The Probable Maximum Flood (PMF) is the flood that may be expected from the most severe combination of critical meteorological and hydrologic conditions that are reasonably possible in a particular drainage area. Generally, Probable Maximum Flood (PMF) is considered to be equivalent to approximately twice the 10,000 year flood.

3.14 Model Setup

Since this study was based on a lumped approach, the rainfall data of all the stations were arithmetically averaged to generate a single time-series. A hydrological system in HEC-HMS is generally by completing following steps (Feldman, 2000):

a) Creating a new project
b) Creating gauge data
c) Entering basin model data
    i) Adding basin elements like sub-basin, junction, reservoir diversions reach, sources and sinks
    ii) Selecting model components for basin elements (e.g. for sub-basin: loss method, transform method, base flow method)
    iii) Entering initial values (those of before calibration) of selected model parameters.
d) Entering precipitation model data
e) Entering control specification
f) Creating and executing a "run"
g) Viewing the results

3.14.1 Model selection

Simulation Type Method	Loss Method	Transform Method	Baseflow
Continuous Monthly	Deficit and Constant loss Method	Clark's Unit Hydrograph	Constant
	SCS Curve Number	Clark's Unit Hydrograph	None

Description of the chosen methods

Curve number method

SCS-CN method, developed by Soil Conservation Services (SCS) of USA in 1969, is a simple, predictable, and stable conceptual method for estimation of direct runoff depth based on storm rainfall depth. It relies on only one parameter, Curve Number. Currently it is a well-established method, having being widely accepted for use in USA and many other countries (Subramanya, 2008).

This method estimates precipitation excess as a function of cumulative precipitation, soil cover, land use, and antecedent moisture, using the following equation:

$$Q = \frac{(P-Ia)^2}{P-Ia+S} \quad \text{…….....} \quad 3.22$$

Where, Q= accumulated precipitation excess at time t

P= accumulated rainfall depth at time t

I_a = the initial abstraction (initial loss)

S= potential maximum retention

Until the accumulated rainfall exceeds the initial abstraction; the precipitation excess, and hence the runoff, will be zero (Feldman, 2000)

From analysis of results from experimental watersheds, it has been found that:

$I_a = 0.2S$

Therefore, the cumulative excess at time t is:

$$Q = \frac{(P-0.2S)^2}{P+0.8S} \quad \text{..... 3.23}$$

The potential maximum retention, S, and watershed characteristics are relates through an intermediate parameter, the curve number, CN, as:

$$S = \begin{cases} \frac{1000 - 10CN}{CN} & \text{(foot pound system)} \\ \frac{25400 - 254CN}{CN} & \text{(SI)} \end{cases} \quad \text{..... 3.24}$$

Deficit and Constant Loss Method:

This method is a quasi-continuous variation on the initial and constant loss method. Both the methods are described below.

In the initial and constant rate method, the maximum potential rate of rainfall loss, f_c, is constant throughout an event. And initial loss, I_a, represents interception and depression storage. The rainfall excess, pe, at time t is given by (Feldman, 2000):

$$pe_t = \begin{cases} 0 & if\ \sum p_i < I_a \\ p_t - f_c & if\ \sum p_i > I_a\ and\ p_t > f_c \\ 0 & if\ \sum p_i > I_a\ and\ p_t < f_c \end{cases} \quad \text{..... 3.25}$$

Where, pt is the rainfall depth during the time interval Δt. The initial and constant includes three parameters, which represent a) basin initial condition, b) physical properties of the basin soils, and c) physical properties of basin land use:

- Initial abstraction (loss) I_a (mm)
- Constant loss rate fc, (mm/hr),
- Impervious area of the basin (%)

The initial abstraction parameter defines basin initial condition. If the basin is in a saturated condition, I_a will nearly zero. If the basin is dry, then I_a will represent the maximum rainfall depth that can fall on the basin with no runoff. The constant loss rate is the ultimate infiltration capacity of the soils (Feldman, 2000).

Unlike in the initial and constant loss model, the initial loss can recover after a prolonged dry period in the deficit and constant loss model. To use this model, the initial loss and constant rate plus the recovery rate must be specified. The moisture deficit is tracked

continuously, calculated as the initial abstraction volume less precipitation volume plus recovery volume during dry periods 9feldman, 2000).

Clark's Unit Hydrograph Method:

Clark's model derives a watershed UH by explicitly representing two critical processes in the transformation of excess precipitation to run off.

- Translation or movement of the excess from its origin throughout the drainage to the watershed outlet.
- Attenuation or reduction of the magnitude of the discharge as the excess is stored throughout the watershed.

Based on the continuity equation and the linear reservoir model, the outflow O from storage at time t is given by:

$O_t = C_aI_t+C_bO_{t-1}$ …….. 3.26

In which I_t = average inflow to storage at time t;

C_b = routing coefficients, and are calculated as:

$$C_a = \frac{\Delta t}{R+0.5\Delta t} \quad \text{…….. 3.27}$$

$Cb = 1-C_a$

Where R = a constant linear reservoir parameter. It is an index of the temporary storage of precipitation excess in the watershed as it drains to the outlet point. It, too, can be estimated via calibration if gauged precipitation and stream flow data are available (Feldman, 2000).

Time of Concentration:

Time of concentration (Tc) is the time required for runoff to travel from the hydraulically most distant point in the watershed to the outlet. The hydraulically most distant point is the point with the longest travel time to the watershed outlet, and not necessarily the point with the longest flow distance to the outlet. Time of concentration is generally applied only to surface runoff and may be computed using many different methods. Time of concentration will vary depending upon slope and character of the watershed and the flow path.

In hydrograph analysis, time of concentration is the time from the end of excess rainfall to the point on the falling limb of the dimensionless unit hydrograph (point of inflection) where the recession curve begins figure 3.6.

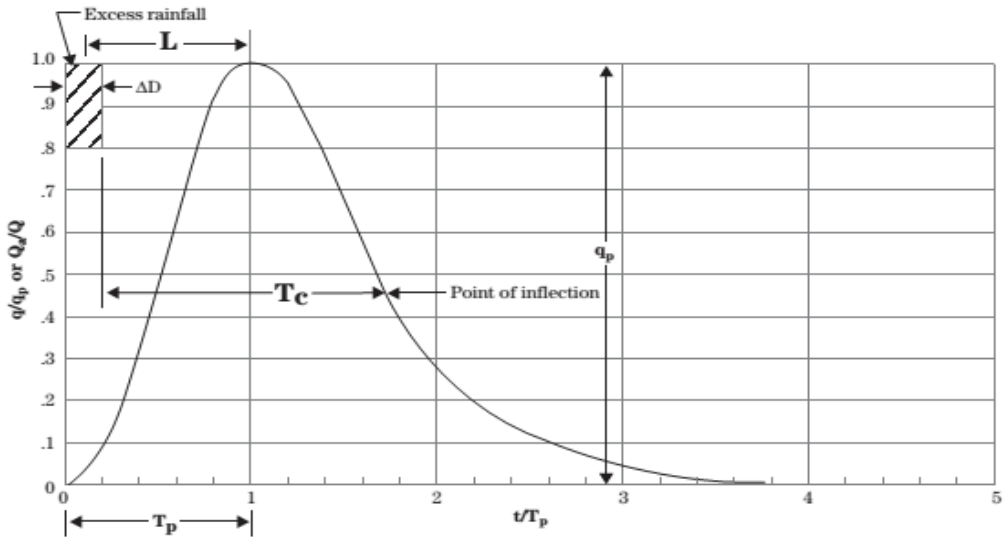

where:
L = Lag, h
T_c = time of concentration, h
T_p = time to peak, h
ΔD = duration of excess rainfall, h
t/T_p = dimensionless ratio of any time to time to peak
q = discharge rate at time t, ft^3/s
q_p = peak discharge rate at time T_p, ft^3/s
Q_a = runoff volume up to t, in
Q = total runoff volume, in

Figure 3.6 The time of concentration (Tc) to the dimensionless unit hydrograph

Storage Coefficient

The basin storage coefficient, R, is an index of temporary storage of precipitation excess in the watershed as it drains to the outlet point. It can be estimated via calibration if gaged precipitation and streamflow data are available. Though R has units of time, there is only a qualitative meaning for it in the physical sense. Clark (1945) indicated that R can be computed as the flow at the inflection point on the falling limb of hydrograph divided by the time derivative of flow.

For estimating Storage Coefficient (R or Sc) value

Sc = c*Tc (Russel, Kenning, Sumcell, 1979) ……. 3.28

with

T_c = time of concentration

c is a calibration parameter that, depending on the use of the soil, takes the following values:

densely forested area 8-12

predominantly agricultural area 1.5-2.8

towns 1.1- 2.1

Constant Monthly Method:

The parameter of this model is the monthly baseflow. These are best estimated empirically, with measurements of channel flow when storm runoff is not occurring. In the absence of such records, field inspection may help establish the average flow. For large watersheds with contribution from groundwater flow and for watersheds with year-round precipitation, the contribution may be significant and should not be ignored. On the other hand, for most urban channels and for smaller streams in the western and southwestern US, the base flow contribution may be negligible.

3.15 Model calibration and validation

Model calibration figure 3.7 is a systematic process of adjusting model parameter values until model results match acceptably the observed data. The quantitative measure of the match is described by the objective function, which in the rainfall-runoff models measures the degree of variation between computed and observed hydrographs. The calibration process finds the optimal parameter values that minimize the objective function and thus increases the fit between real and simulated data. Further, the calibration estimates some model parameters that have no direct physical meaning. Calibration can either be manual or automated (optimization). Manual calibration relies on user's knowledge of basin physical properties and expertise in hydrologic modelling. In the automated calibration model parameters are iteratively adjusted until the value of the selected objective function is minimized (Cunderlik & Simonovic 2004).

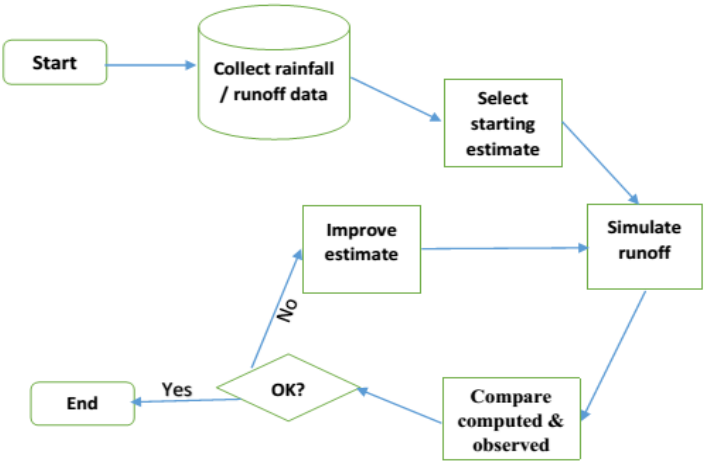

Figure 3.7 Schematic of model calibration procedure, (Redrawn from Feldman, 2000)

In runoff modelling validation usually means the test of a model with independent data. It is the process of showing whether a site specific model is capable of making accurate predictions for periods that are not included in the calibration process (Sibert, 1999). Generally in the validation process the parameters obtained from the calibration process are kept constant but the parameters that represent the basin initial conditions can be changed (Cunderlik & Simonovic, 2004).

3.16 Process of event and continuous simulations

Event Simulation

The hydro-meteorological data of any year or of any event during the period of 31 years from 1978 – 2008 did not correlate inspite of hard work. So continuous simulation is used instead.

Continuous Simulation:

A 10 year long time period from Jan 1990 to Dec 1999 was selected for the calibration of the continuous model which was validated by a ten year long time duration form Jan 2000. The calibration method used was manual.

3.17 Glacier and Glacier Lakes

The largest glacier in the Koshi basin is Ngojumba Glacier with an area of 82.61 km^2; however, the largest glacier in Nepal is Kanchenjunga Glacier with an area of 94.52 km^2. Changes in mountain glaciers are among the best natural indicators of climate change (Oerlemans, 1994; Houghton and others, 2001) and there has been a significant impact on this high mountain glacial environment. The glaciers are melting rapidly (Fujita and others, 2001), leading to the formation of new glacial lakes, the expansion of existing moraine dammed lakes and the potential for glacial lake outburst floods (GLOFs) (Watanabe and others, 1994). Most of the lakes, above 3500 m a.s.l., formed in response to warming temperatures during the second half of the 20th century (Yamada and Sharma, 1993; Mool and others, 2001). The largest of the lakes in Dudhkoshi basin is Imja-Tsho with an area of about 0.95 km^2, recorded as one of the fastest-growing lakes in the entire Himalaya (Bajracharya and others, 2007). Understanding the response of glaciers and glacial lakes to rising temperatures is an essential aspect of planning water resources as well as managing the potential for GLOF disasters.

A form of flash flood in which water from a lake associated with a glacier is released suddenly, resulting in the outflow of a huge volume of water and sediment downstream. Such catastrophic flooding often results in serious loss of life and damage to property in downstream areas. Nepal, like many other mountainous countries, is highly vulnerable to GLOFs. At least 14 GLOF events have been identified as originating in the Nepal Himalayas, although the exact dates of some remain unknown, and a further 10 events originating in Tibet Autonomous Region, China, are known to have had an impact in Nepal (ICIMOD, 2011). The Dig Tsho outburst in 1985 and the Tampokhari outburst in 1998 both led to considerable loss of life, property and infrastructure and severely affected the livelihoods of the people living in downstream areas (Dwivedi, Acharya, & Simard, 2000; Vuichard & Zimmermann, 1987).

The Himalaya of Nepal is geologically active where the instabilities due to tectonic activity and ongoing erosion are apparent everywhere. These factors, combined with the peculiar meteorological conditions where both the rainfall and river flow vary tremendously in both time and space, make the landscape vulnerable to water-induced disasters such as floods, landslides, slope failures.

In addition, the rapid melting of glaciers certainly increases the river runoff with the decrease of glacier reserve. The surface run off will decreases after reaching at certain

threshold resulting scarcity of fresh water resources. Still nobody knows the time of threshold, but the immediate impact of global warming has already been faced due to GLOFs in the HKH region. Due to rapid melting of glaciers, the number and area of moraine dammed lakes are increasing. The dammed moraines are characterized by loose and unstable debris of silt to boulder in size. The ultimate result of continuous increasing lake area is the out breaching of dammed moraine with catastrophic CLOF, LDOF & GLOFs.

Status of Glaciers, Glacial Lakes and GLOF in Nepal	
Glaciers	3252
Glacier area	5323 sq km
Glacial lakes	2323
Glacial lake area	75 sq km
Glacial lakes larger than 0.02 sq km in area	411
Glacial Lakes attached with Glacier	347
Potentially dangerous glacial lakes	20
GLOF in Tibet/China damage inside Nepal	10
GLOF in Nepal	12

Figure 3.8 ICIMOD, APN, UNEP 2004

3.18 Factors related to terrestrial/hydrological systems

The characteristics of terrestrial/hydrological systems play a pivotal part in driving flood risk. The most pertinent are catchment size, geology, landscape, topography and soils; the latter are often strongly modified by human intervention. River discharge is an integrated result of processes in the drainage basin—from precipitation to runoff. Land-use and land-cover changes also affect floods, as do engineering developments such as dikes and reservoirs that regulate flow processes. Alterations in catchment surface characteristics (e.g. land cover), flood-plain storage and the river network can all modify the physical characteristics of river floods. Increased urbanization has led to soil sealing and growth of impermeable surfaces, reducing the accommodation space for flood waters. The reduction of forest and wetland coverage is also reducing the role of these ecosystems in buffering flood events (Bradshaw et al. 2007). In urban areas, the value of the runoff coefficient (portion of precipitation that enters a stream) is high, while the water-storage capacity (as in flood plains and wetlands) is low, in contrast to rural (and especially

forested) areas. Hence, urban and rural catchments of the same size and topography will react differently to the same amount of precipitation. The peak discharge in the urban area is usually much higher, and the time-to peak is shorter, than in the rural areas (Kundzewicz et al. 2012). Assessment of the multiple drivers of flood risk in Shanghai (Wu et al. 2012) showed that rapid urban expansion, infilling of natural drainage networks, changes in precipitation intensities and runoff coefficients have largely influenced flood risk. Processes of urbanization also lead to increased occupation of flood plains and, often, inadequate drainage planning. These urbanization issues are universal, but often at their worst in informal settlements, where there will be no investment in drainage solutions, and flooding regularly disrupts livelihoods and undermines local food security. A further concern for low- and middle-income cities, particularly in developing countries, is that floods become contaminated with human waste (Hardoy et al. 2001), leading to higher rates of infectious disease, such as cholera, cryptosporidiosis and typhoid fever (Kovats and Akhtar 2008) occurring after floods. However, the river stage and thus the risk of flooding also depend on engineered alterations to river courses and depths and artificial flood containment, such as dikes built to protect settlements. Reservoirs, whether developed specifically for flood protection, or intended also to provide water storage, can substantially reduce short-duration flood waves, but during major flood events, their positive effects decrease and may even turn negative. Costly elements of road infrastructure, such as bridges, culverts and embankments (for roads and railways), are vulnerable to erosional damage in heavy precipitation and floods. Even the structures used to control flood events may aggravate the risk and the resulting damage when an extreme flood occurs. Along the Indus, during the 2010 Pakistan flooding, close to 2000 fatalities occurred and approximately 20 million people were displaced, with the devastating impacts attributed in part to anthropogenically reduced river water and sediment conveyance capacity of the river channel to dam/ barrage-related backwater effects and to multiple failures of irrigation system levees. The numerous failures extended from upstream areas on Indus tributaries, where some record discharges did occur, to downstream Indus reaches and the delta, where peak discharges were by no means extreme (Syvitski and Brakenridge 2013). Where levees hold, downstream flood peaks are higher than would otherwise have been the case; where they fail, local flood damage can be catastrophic. In coastal areas and behind levees along inland rivers, levee structures meant to protect against flooding have sometimes instead worsened flood damage by not allowing the free discharge of flood water to the sea (e.g. in Thailand in

2011) or overbank water return to the main channel (e.g. in the Pakistan 2010 event). Seneviratne et al. (2012) assessed that there is limited to medium evidence available to assess climate-driven observed changes in the magnitude and frequency of floods at regional scales. However, the available instrumental records of floods at gauge stations are limited in space and time and because of the confounding effects of changes in land use and engineering. Furthermore, there is low agreement in this evidence and thus overall low confidence at the global scale regarding even the sign of these changes. Changing flood risk is especially problematic in semi-arid regions where spate occurrence and magnitudes can be highly erratic.

CHAPTER IV

RESULTS AND DISCUSSIONS

4.1 Meteorology

4.1.1 Rainfall Data and Analysis

Department of Hydrology and Meteorology (DHM) is the sole authority for the establishment of meteorological, climatological and hydro-metric stations and collection, processing and publishing of hydrological and meteorological data. A fully equipped climatological station has rain gauge (manual or automatic), maximum-minimum thermometer, pan-evapometer, sunshine recorder, wind vane, where as there are number of stations, which have only manual rain gauge recording 24-hour rainfall, every morning at 8:45 am NST.

The catchment lies in monsoon driven area occurring high amount of precipitation. There are five rainfall stations lying in the study area, Station No. 1202, 1203, 1204, 1219, 1220, out of which 1220 is not in operation from some years, so identified the relevant stations and obtained secondary data (monthly rainfall data). The average rainfall of the station along with other stations lying nearby is given in Table 4.1.

Table 4.1 Precipitation station and their normal and annual values used in the study

S.N.	Index No.	lon	lat	Station	Jan	Feb	Mar	Apr	May	Jun	Jul	Aug	Sep	Oct	Nov	Dec	Annual
1	1102	86.05	27.67	Charikot	14.45	25.04	42.16	77.68	154.01	312.76	549.78	526.97	267.96	62.77	11.31	14.31	2059.22
2	1109	85.67	27.08	Pattharkot(East)	11.68	12.21	15.02	53.39	134.44	269.73	589.87	395.29	325.13	108.02	6.60	13.45	1934.83
3	1202	86.72	27.7	Chaurikhark	16.80	32.72	27.94	59.90	105.44	313.77	587.45	549.38	301.45	56.01	12.57	12.77	2076.20
4	1203	86.57	27.43	Pakarnas	13.65	17.26	34.64	47.37	99.97	279.59	515.80	500.13	255.06	60.66	12.41	11.30	1847.86
5	1204	86.75	27.35	Aisealukhark	19.80	19.48	38.11	67.50	181.43	395.07	605.18	527.35	321.27	90.71	17.99	15.18	2299.06
6	1206	86.5	27.32	Okhaldhunga	11.86	14.80	25.77	57.12	147.56	312.33	473.77	391.05	242.40	61.57	11.39	13.78	1763.40
7	1207	86.42	27.48	Mane Bhanjyang	11.38	12.91	18.73	48.66	103.60	188.89	304.07	221.56	147.42	35.08	7.83	9.81	1109.93
8	1210	86.43	27.13	Kurule Ghat	10.58	12.41	18.50	47.12	83.31	135.14	286.19	185.49	131.75	44.46	11.48	14.17	980.60
9	1211	86.83	27.03	Khotang Bazar	19.84	13.18	28.30	47.35	115.62	202.09	336.38	221.23	166.48	48.62	8.52	13.77	1221.38
10	1212	86.93	26.73	Phatepur	13.32	10.89	13.21	50.68	119.24	248.99	485.00	423.74	263.95	75.73	7.85	7.77	1720.35
11	1219	86.58	27.5	Salleri	12.25	15.44	28.07	50.27	98.50	248.39	461.58	428.60	243.37	54.58	12.04	7.64	1660.72
12	1222	86.8	27.22	Diktel	11.24	15.42	22.43	63.60	161.59	282.98	344.00	288.27	191.22	38.22	11.68	13.72	1444.37
13	1224	86.38	27.55	Sirwa	12.36	19.13	36.61	67.68	131.54	291.84	493.56	451.02	264.20	60.03	16.44	10.30	1854.71
14	1301	87.28	27.55	Num	27.88	66.08	108.67	285.93	528.73	887.71	897.92	728.57	598.04	224.07	34.76	18.57	4406.95
15	1303	87.33	27.28	Chainpur (East)	12.54	18.81	38.71	95.75	199.80	235.75	300.60	281.22	210.35	57.59	15.16	10.00	1476.28
16	1304	87.28	27.05	Pakhribas	13.78	16.40	28.20	64.67	148.63	270.80	386.81	338.78	203.75	59.81	12.01	11.26	1554.90
17	1305	87.28	27.13	Leguwa Ghat	4.95	12.58	24.41	77.19	130.99	159.09	206.66	185.82	118.02	35.64	10.73	4.19	970.28
18	1307	87.35	26.98	Dhankuta	11.66	17.25	27.00	50.69	104.88	154.39	259.67	171.81	132.67	43.81	13.42	10.19	997.44
19	1308	87.33	26.93	Mulghat	11.58	16.64	25.53	50.91	119.25	178.08	301.26	196.95	153.81	46.06	13.97	8.95	1122.99
20	1309	87.15	26.93	Tribeni	11.23	18.28	22.78	63.10	136.05	281.63	483.80	331.78	281.90	59.36	13.45	8.82	1712.19
21	1311	87.28	26.82	Dharan Bazar	12.45	20.22	27.95	74.00	170.62	326.77	570.07	471.11	393.99	141.04	14.06	10.08	2232.36
22	1320	87.27	26.7	Tarahara	15.32	13.56	21.37	66.36	173.37	295.97	535.38	377.73	309.44	90.80	10.56	11.61	1921.48
23	1321	87.22	27.28	Tumlingtar	8.08	10.42	25.64	85.18	176.69	220.62	281.64	228.10	216.38	62.50	11.79	8.68	1335.73
24	1322	87.17	26.97	Machuwaghat	12.03	11.87	21.21	51.21	139.76	243.45	361.81	234.44	191.94	44.34	9.63	10.82	1332.52
25	1325	87.15	27.37	Dingla	14.53	20.36	39.82	87.74	196.80	317.11	425.71	386.39	350.03	99.55	12.74	12.56	1963.35
26	AWSN	86.42	27.48	Namche	7.35	8.53	8.80	18.08	30.28	116.98	263.05	204.85	113.03	24.65	4.05	3.58	803.20
27	AWS3	86.43	27.41	Lukla	3.20	19.28	29.96	46.64	111.84	313.80	559.60	448.48	227.56	43.60	17.60	1.88	1823.44
28	AWS2	86.82	27.9	Pheriche	1.68	1.80	4.32	8.68	11.86	37.00	131.08	124.21	65.42	12.38	0.78	0.56	399.77
29	AWS1	86.81	27.96	Pyramid	1.02	1.47	4.09	5.56	8.48	37.94	88.40	111.37	43.52	4.96	2.22	0.77	309.81

The Satellite rainfall using Tropical Rainfall Measuring Mission (TRMM) 3B42 (0.25*0.25) spatial resolution, the annual rainfall is found to be 1620 mm. But from the observed data of station rainfall, the long term average rainfall of the basin is 1971 mm, which excludes the upper regime of the basin area. The study area receives 82.9% of annual rainfall in monsoon season (June – September). Among monsoon months, July is the wettest month which receives 542.5 mm (i.e. 27.5% of the total annual rainfall). Likewise, December is the driest month which receives 11.7 mm (i.e. < 1% of the total annual rainfall). Figure 4.1 shows the monthly rainfall distribution of the study area.

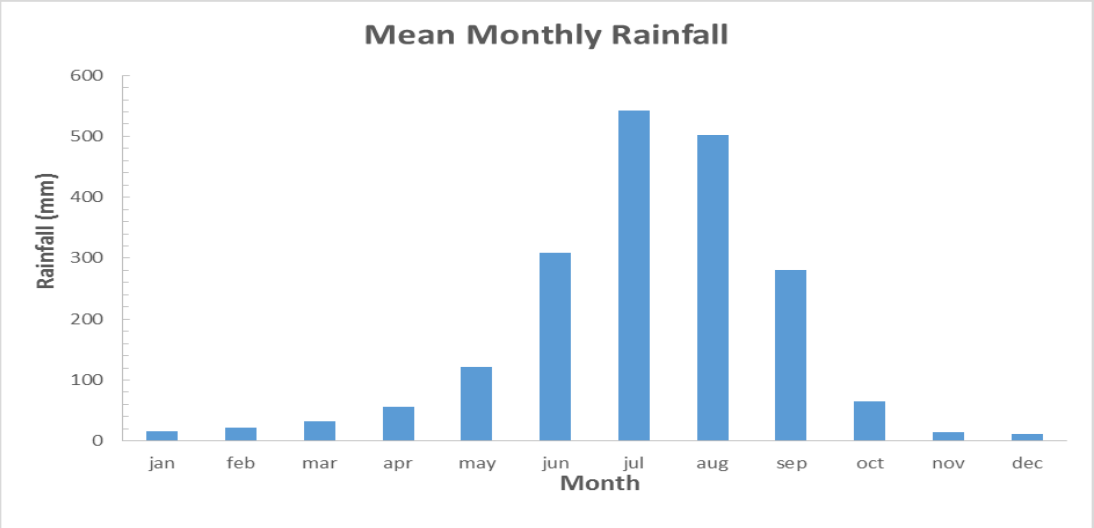

Figure 4.1 Average Rainfall of Dudhkoshi Basin

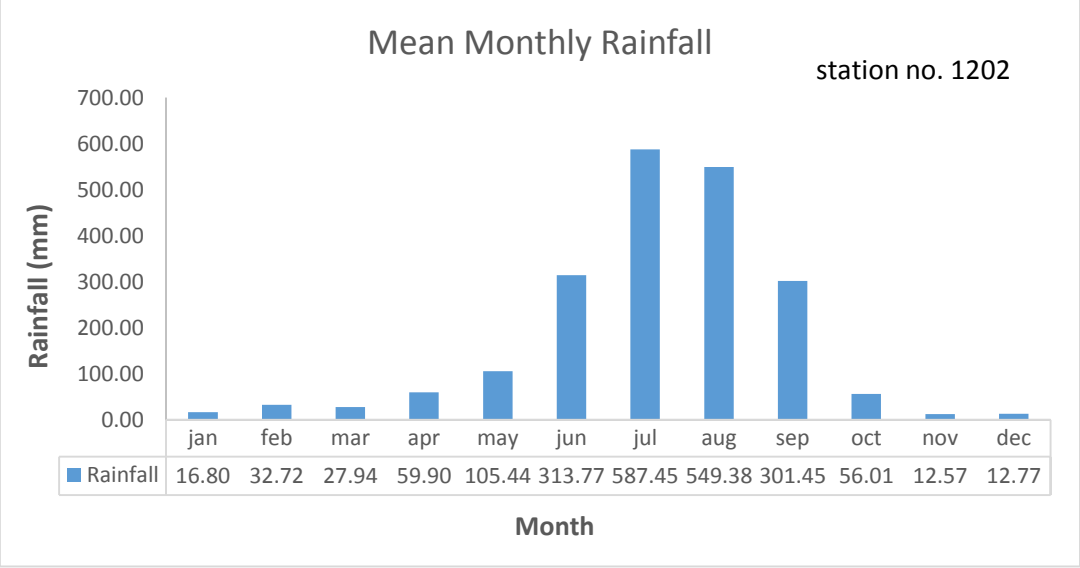

Figure 4.2 Mean Monthly rainfall of Chaurikharka (Station N0. 1202)

As shown in figure, the rainfall station of Chaurikharka receives lowest rainfall in November and highest in july.

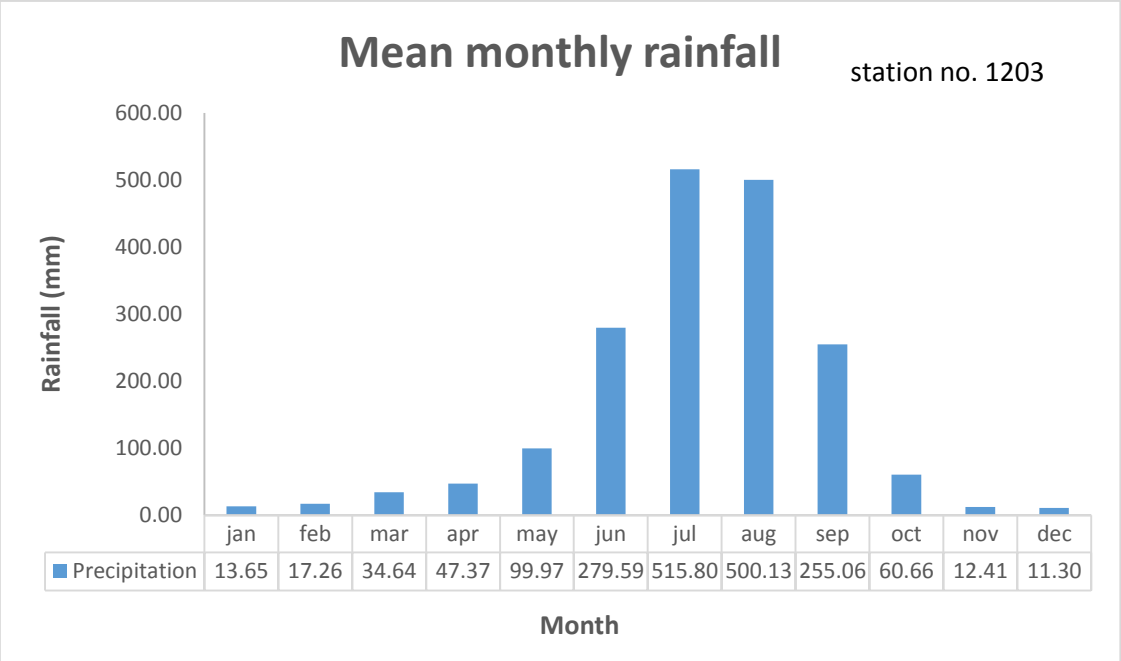

Figure 4.3 Mean monthly rainfall of the Pakarnas Station

As shown in figure rainfall station in Pakarnas receives lowest rainfall in December and highest in July months respectively.

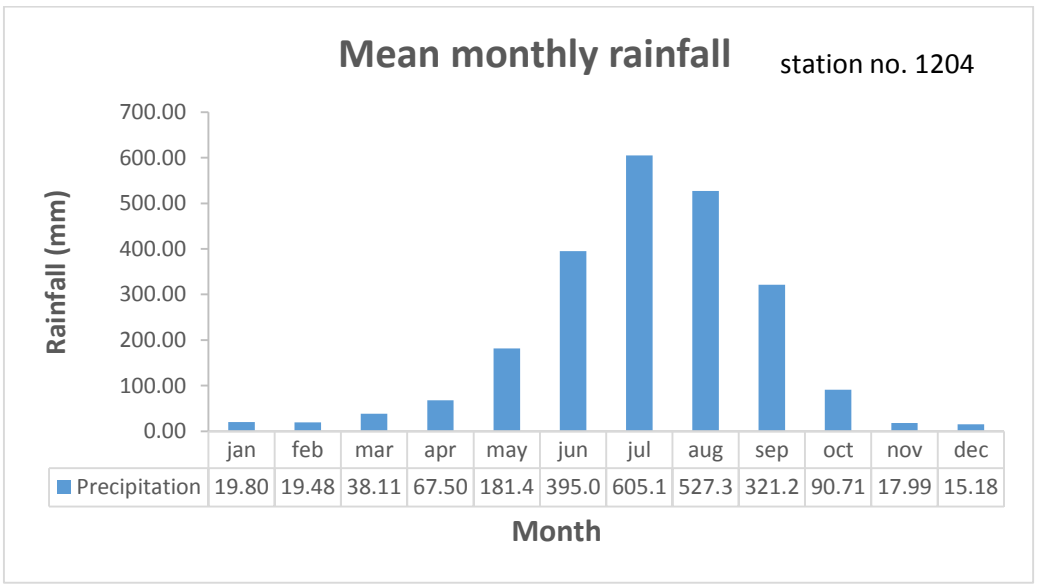

Figure 4.4 Mean monthly rainfall of the Aisealukharka Station

As shown in figure rainfall station in Aisealukharka receives lowest rainfall in December and highest in July months respectively.

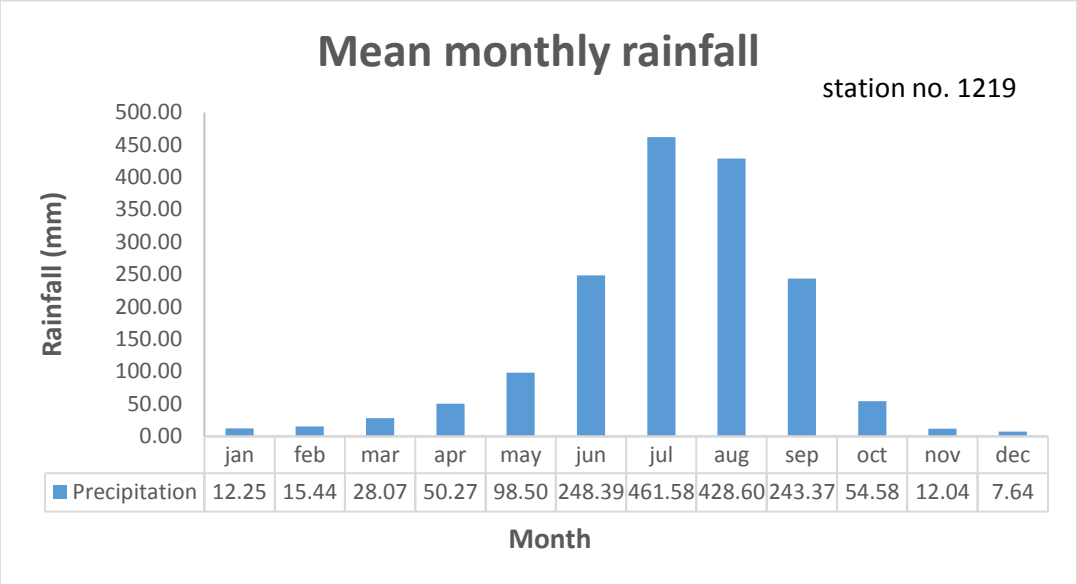

Figure 4.5 Mean monthly rainfall of the Salleri Station

As in figure the rainfall station of Salleri receives lowest rainfall in December and highest in July Month respectively.

4.1.2 Precipitation Pattern of Various Station in Dudhkoshi Basin

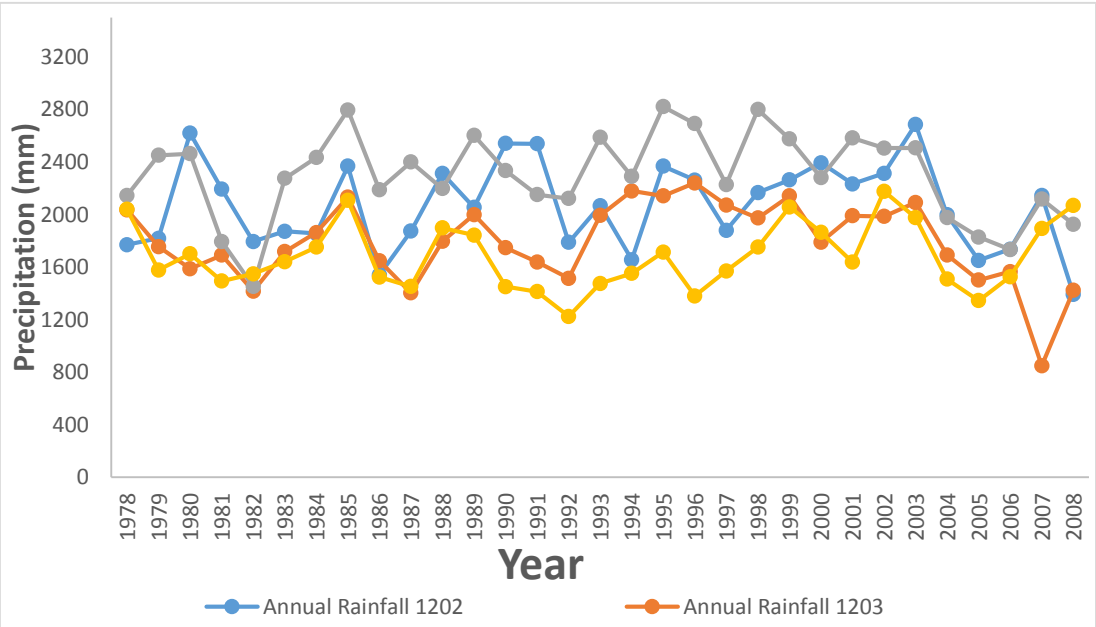

Figure 4.6 Precipitation pattern of various rainfall station in Dudhkoshi Basin

The annual rainfall of different stations in Dudhkoshi Basin shows the similarity in rainfall distribution in spite of being different in amount.

There are various method of estimating average rainfall: Arithmetic Average, Theissen Polygon and Isohyetal Method.

4.1.3 Arithmetic Average Method

As there are five rainfall stations in the study area with long term data and recently some projects have established stations which are in operation since few years and have less data. Here, we have used only four rainfall stations (station no. 1202, 1203, 1204, and 1219). The arithmetic average rainfall is therefore 1971 mm.

4.1.4 Isohyetal Method

In this method, contour line was drawn using GIS from point data measured over the eastern and central regions and clip by the study area. Since DHM has less data of higher elevation, the point data of higher elevation was taken from the NAST/EvK2. By this method, the average rainfall came to be 1444.2 mm. The Isohyetal map of the DudhKoshi Basin is depicted in Figure 4.7.

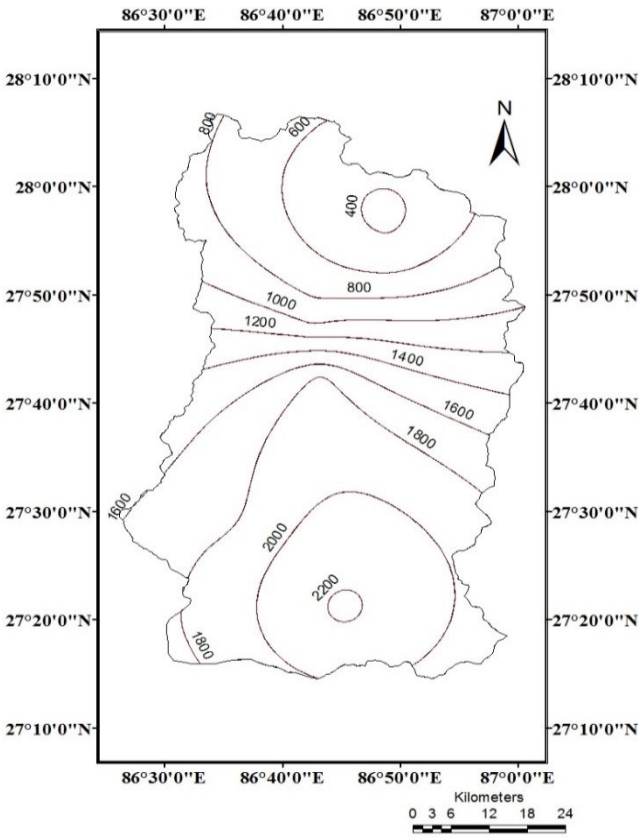

Figure 4.7 The Isohyetal Map of DudhKoshi Basin

4.1.5 Frequency Analysis of 24 hour Rainfall of Different Stations

The 24-hr rainfall for various return period was estimated by fitting Gumbel distribution to the 24-hr annual maximum rainfall data. The monthly rainfall values (1978-2008)

shows annual rainfall value as high as 152 mm (station no.1202) in 2000 BS, 172 mm (station no. 1203) in 2007 BS, 193 mm (station no. 1204) in 1983 BS, and 86.5 mm (station no. 1219) in 1987 BS respectively.

Table 4.2 The 24-hr rainfall for various return periods of station no. 1202 (Chaurikharka)

Return Period	Correction Factor	Gumbel Coefficient	Rainfall (mm)
2	0.37	-0.15	75.70
5	1.50	0.86	104.02
10	2.25	1.54	122.78
15	2.67	1.91	133.36
20	2.97	2.18	140.77
25	3.20	2.39	146.47
50	3.90	3.02	164.05
100	4.60	3.64	181.50

The above figure represents the highest intensive rainfall expected once in 100 year return period is equal to or exceeding 181.5 mm.

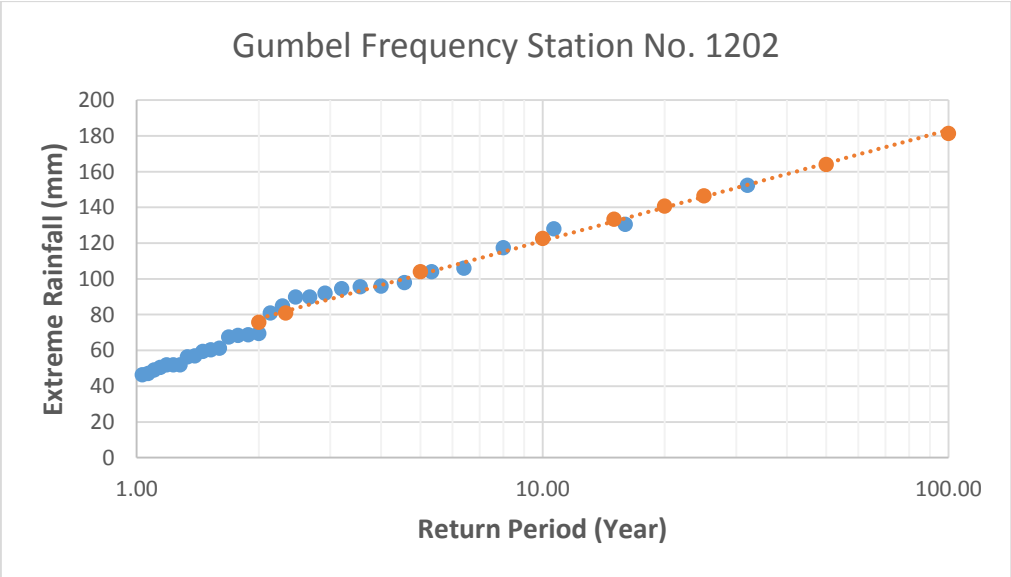

Figure 4.8 The 24 Hours Maximum Rainfall for different Return Periods

Table 4.3 The 24-hr rainfall for various return periods of station no. 1203 (Pakarnas)

Return Period	Correction Factor	Gumbel Coefficient	Rainfall (mm)
2	0.37	-0.15	80.55
5	1.50	0.86	107.27
10	2.25	1.54	124.96
15	2.67	1.91	134.94
20	2.97	2.18	141.93
25	3.20	2.39	147.31
50	3.90	3.02	163.90
100	4.60	3.64	180.36

The above figure represents the highest intensive rainfall expected once in 100 year return period is equal to or exceeding 180.36 mm.

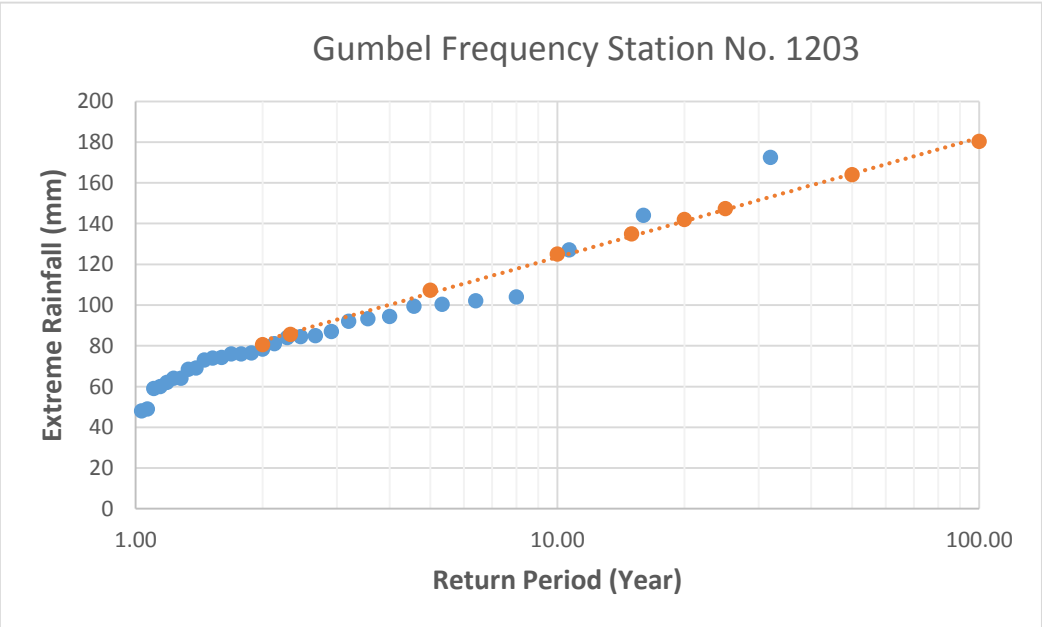

Figure 4.9 The 24 Hours Maximum Rainfall for different Return Periods

Table 4.4 The 24-hr rainfall for various return periods of station no. 1204 (Aisealukharka)

Return Period	Correction Factor	Gumbel Coefficient	Rainfall (mm)
2	0.37	-0.15	105.86
5	1.50	0.86	148.61
10	2.25	1.54	176.92
15	2.67	1.91	192.89
20	2.97	2.18	204.07
25	3.20	2.39	212.69
50	3.90	3.02	239.22
100	4.60	3.64	265.56

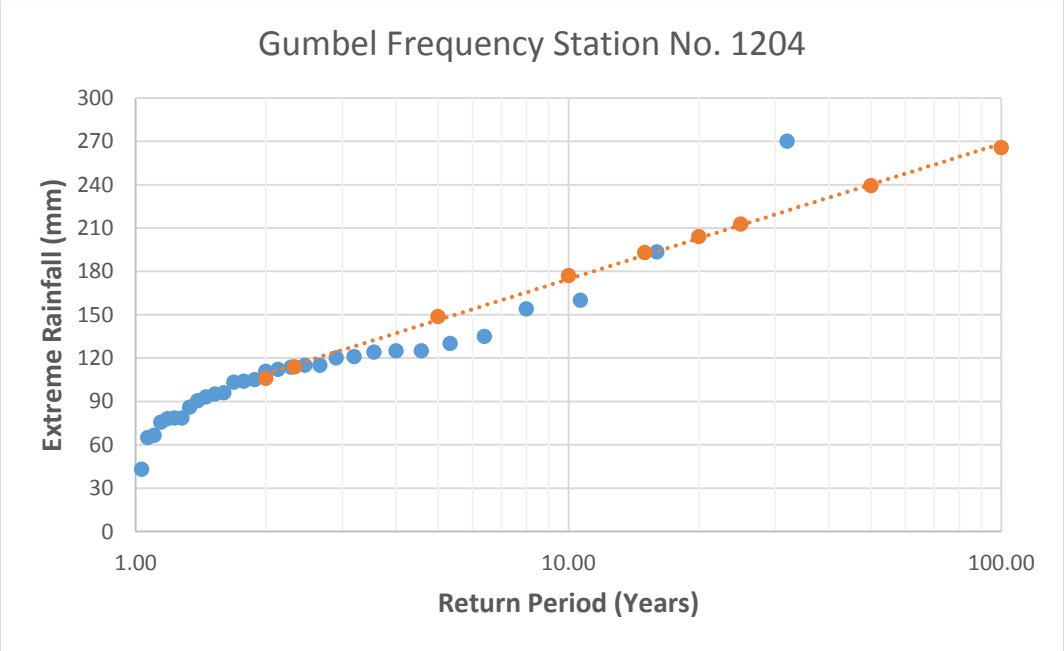

Figure 4.10: The 24 Hours Maximum Rainfall for different Return Periods

The above figure represents the highest intensive rainfall expected once in 100 year return period is equal to or exceeding 265.56 mm.

Table 4.5 The 24-hr rainfall for various return periods of station no. 1219 (Salleri)

Return Period	Correction Factor	Gumbel Coefficient	Rainfall (mm)
2	0.37	-0.15	61.40
5	1.50	0.86	75.11
10	2.25	1.54	84.19
15	2.67	1.91	89.31
20	2.97	2.18	92.90
25	3.20	2.39	95.66
50	3.90	3.02	104.17
100	4.60	3.64	112.62

The above figure represents the highest intensive rainfall expected once in 100 year return period is equal to or exceeding 112.62 mm.

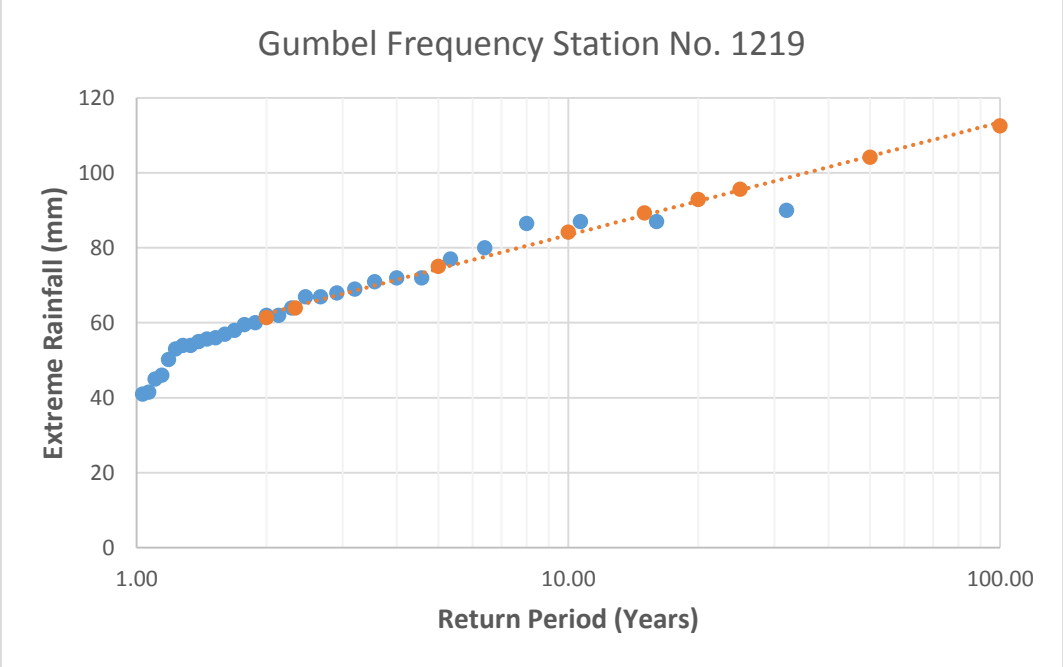

Figure 4.11 The 24 hr maximum rainfall for different return periods

4.1.6 Probable Maximum Precipitation (PMP)

From the result of 31 years data, the mean of annual maximum values is 80.0 mm and standard deviation is 27.9. Thus, the PMP is found to be 596 mm.

4.2 Hydrology

4.2.1 Reference Hydrology

Dudhkoshi is a major tributary of Sapta Koshi Ri ver. So, DHM has established the hydrometric station at Rabuwa Bazar (index no. 670), which is about 2 km upstream of the damsite. Similarly, other gauging station available is on the Solu Khola, the tributary of Dudhkoshi River. The details of these gauging stations are shown in the table below.

Table 4.6 DHM Hydrological Gauging Station in Dudhkoshi River Basin

S.No.	Gauge Station	Type of Station	River	Location	Operator	Comments
1	670	Cable Way, Water Level (manual) and AWS, Real time gauging station	Dudhkoshi	Rabuwa Bazar, Approx.2 km u/s of damsite	DHM	Estd in 1964
2	668.5	Water level	Solu Khola	Salme	DHM	Estd in 1987

The total catchment area of Dudhkoshi River at Gauging Site and proposed dam site is 3722 km^2 and 3849 km^2 respectively. The hydrological parameters established at the gauging station in Rabuwa are transposed to the dam site using catchment area ratio method is as explained in the following section.

Table 4.7 Observed and Transformed Flow of Dudhkoshi

Station	670	Damsite
River	Dudhkoshi	Dudhkoshi
Location	Rabuwa Bazar	2 km downstream of damsite
Area (km^2)	3722	3849
PPT (mm)		1444.2
Month	**Observed Flow (m^3/s)**	**Transposed Flow (m^3/s)**
Jan	42.9	44.1
Feb	35.3	36.2

Mar	33.7	34.6
Apr	40.5	41.6
May	74.2	76.2
Jun	248.6	255.4
Jul	586.5	602.5
Aug	601.5	617.9
Sept	464.6	477.3
Oct	176.8	181.6
Nov	85.5	87.8
Dec	56.9	58.4
Annual	204	207.5

4.2.2 Assessment of Long Term Average Flows

The routine procedure for the collection of hydrological data consists of taking discharge measurements 6 to 7 times in a year to include the entire flow regime of low, medium and high flows. These discharge measurement data are used to construct the rating curve at the station, which is reviewed every year. The water levels (gauge height) are recorded there times a day at 8:00, 12:00 and 16:00 hours daily. The station rating curve is then used to convert the validated water level data into the corresponding discharge data. The monthly mean and the annual extreme high and low flow for each gauging stations are published on the regular basis for public use of the data.

Flow Analysis

The latest available processed digital daily stream flow data and the annual maximum flood and low flow data at Rabuwa bazar of Dudhkoshi River (index no. 670) from 1964 to 2008 are collected from DHM.

4.2.3 Long Term Hydrology

For the proper assessment, long term flow data are essential. Hence, the long term flow data need to be generated for the damsite. This should be based on long term recorded data of the available gauged hydrological stations. The hydrological analysis was, therefore, carried out using long term flow data of Rabuwa. For Dudhkoshi Basin upstream of dam site area below 3000 m asl is 865.69 km^2, area between 3000 and 5000

m asl is 2029.65 km^2 and area above 5000 m asl is 1083 km^2 respectively. Mean monthly and annual flows at damsite were estimated by the following methods.

i. WECS/DHM 1990-Method

Table 4.8 Monthly Average Flow estimated by WECS/DHM 1990 Method

Months	Jan	Feb	Mar	Apr	May	Jun	Jul	Aug	Sep	Oct	Nov	Dec	average
Q (m^3/s)	33.0	28.0	26.5	31.2	47.6	46.6	358.1	414.5	308.4	137.1	71.8	46.5	129.1

ii. WECS/DHM 2004 Method

It is noted here that X1(average elevation of catchment) = 4199 m, X2 (annual precipitation) = 1971 mm, X3 (catchment area) = is 865.69 km^2 (<3,000 m) or 2029.65 km^2 (<5,000 m). This gives runoff coefficient (runoff discharge ratio).

Table 4.9 Monthly Average Flow estimate by WECS/DHM 2004 Method

Month	Constant	Coefficient of Avg. Elevation	Coefficient of Annual Precipitation	Coefficient of A<3,000 m	Coefficient of A<5,000 m	Transformation	Monthly Average
Jan	-16.7	1.36	0.47	0.82	-	Ln	37.54
Feb	-17.2	1.42	0.456	0.814	-	Ln	32.46
Mar	0.384	-	-	-	0.091	Squar Root	20.10
Apr	0.181	-	-	-	0.104	Squar Root	23.68
May	0.0001	-	-	-	0.136	Squar Root	37.54
Jun	-19.5	1.61	0.709	0.872	-	Ln	158.76
Jul	-16.3	1.26	0.759	0.884	-	Ln	332.28
Aug	-14.7	1.24	0.622	0.871	-	Ln	452.14
Sep	-13.7	1.09	0.594	0.872	-	Ln	286.23
Oct	-15.3	1.21	0.6	0.846	-	Ln	138.62
Nov	-16.7	1.36	0.543	0.826	-	Ln	67.94
Dec	-17	1.39	0.504	0.822	-	Ln	46.84
						Average	136.18

The methods such as WECS/DHM 1990 and 2004 methods only considers the area below 5,000 m asl. So these methods can only be in pre-feasibility study of any project.

iii. Regional Monthly Flow Regression Analysis

Based on the monthly flow data, regression equation for each month has been derived with regression parameters shown in table **3.5** (Example of fitting equation to the data for the annual average flow is shown in Figure 3.5). The estimated and generated long term mean monthly flow by this method for Dudhkoshi at Dam Site are shown in Table 4.9. The average annual mean flow came to be 217.9 m^3/s, which is very near to the observed value.

Table 4.10 Long Term Mean Flow Estimated by Regional Method

Months	Jan	Feb	Mar	Apr	May	Jun	Jul	Aug	Sep	Oct	Nov	Dec	Annual
Regional Method	75.5	67.2	63.9	76.4	117.1	242.4	442.9	503.9	379.7	208.9	124.2	90.2	217.9
Damsite Transposed	43.9	36.1	34.3	41.2	74.6	247.9	597.0	616.3	474.7	178.8	86.3	58.8	207.5

iv. Transformation Method

Long term stream flow series for the Dam Site of DudhKoshi River has been generated by transforming the observed stream flow records at Rabuwa Gauge site using Equation (3.11) and presented in Table 4.9. From this method, the long term mean annual flow at the Dam site came to be 207.5 m^3/s.

It gives the runoff coefficient of 0.86 (i.e., runoff volume is less than rainfall volume) which is possible. But the value is little high which denotes that the imperviousness of the drainage area, as the basin covers 14 % glaciated area with steep slope and barren mountainous region. About 2500 km^2 of the basin area is above altitude of 3200m asl and which is partially or fully barren. It shows that equation (3.11) have produced satisfactory estimates in this case. The runoff coefficient value obtained with annual average runoff of 207.5 m^3/s (1704.2 mm) and rainfall 1442 mm (isohyetal method). Here, result obtained from Equation (3.11) method is taken as the representative flow.

4.2.4 Selection of Appropriate Flow Hydrograph

All the flow data estimated from the above-mentioned methods were plotted in Figure 4.11 to compare their values and are given in Table 4.10. It shows that the Regional Method has projected higher values than other method. During the monsoon season, the projected discharge is high. Regional method has incorporated high flows resulting from

high rainfall that occur in other basins of the region. Further the Regional Method is based on the average of the large and small area, spatial heterogeneity; various monsoon patterns as well as snowmelt behavior are not similar in different areas. WECS-DHM (1990) method has produced quite low value of flows in dry season or wet and erratic in characteristic. It is also not a suitable hydrograph for the basin. WECS-DHM (2004) method has also produced quite low value of flows in dry seasons and peak is sharper that mean peak discharge occurs for very short duration, which is not good for reservoir project. The hydrograph produced from model seems the best fit for the basin.

Table 4.11 Comparison of Long Term Monthly Flow. Unit: m^3/s

Months	Jan	Feb	Mar	Apr	May	Jun	Jul	Aug	Sep	Oct	Nov	Dec	Annual
Regional Method	75.5	67.2	63.9	76.4	117.1	242.4	442.9	503.9	379.7	208.9	124.2	90.2	217.9
Damsite Transposed	43.9	36.1	34.3	41.2	74.6	247.9	597.0	616.3	474.7	178.8	86.3	58.8	207.5
WECS-DHM 2004	49.2	42.8	20.1	23.7	37.5	215.4	436.0	590.8	368.4	179.8	89.2	61.6	176.2
WECS-DHM 1990	33.0	28.0	26.5	31.2	47.6	46.6	358.1	414.5	308.4	137.1	71.8	46.5	129.1
HEC-HMS	45.0	39.7	39.3	48.1	71.7	224.9	574.8	640.0	383.1	141.3	80.0	57.1	195.4

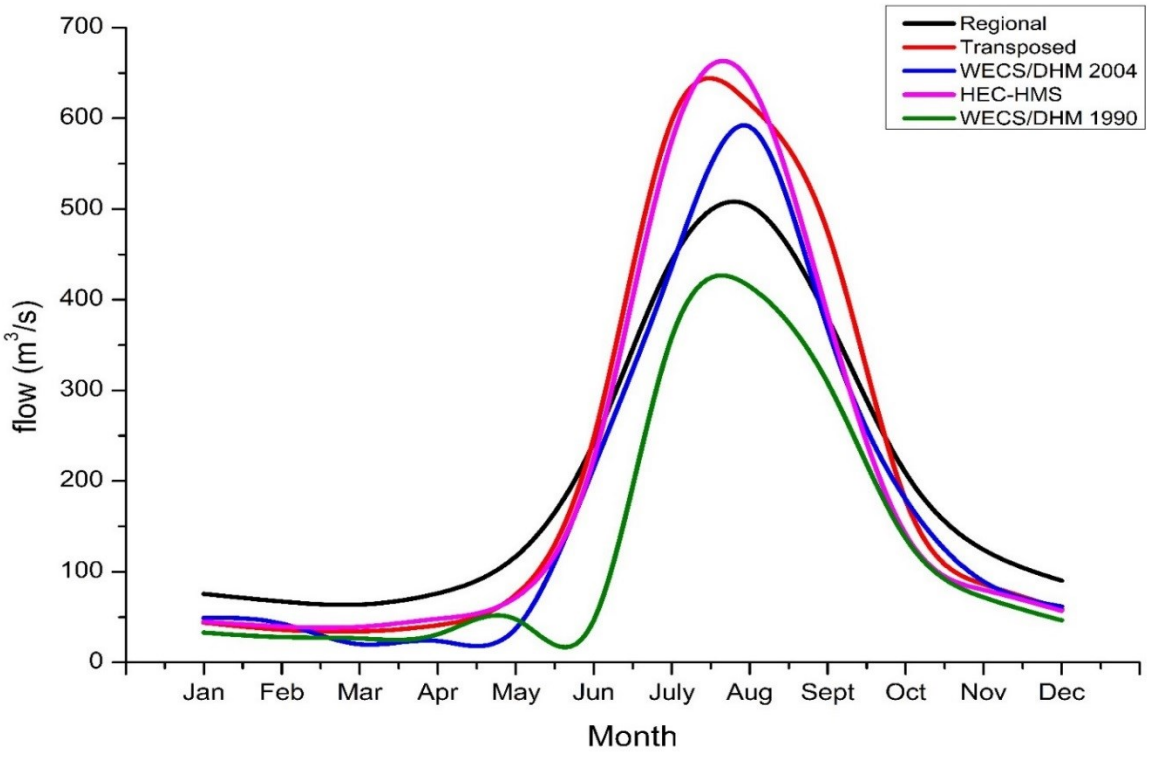

Fig. 4.12 Hydrographs of Dudhkoshi River at Dam Site by Different Methods

4.2.5 Flow Duration Curve

Flow duration curve (FDC) is an exceedence probability discharge curve which shows the percentage of time when a particular flow is equaled or exceeded. Flow duration curves are generally prepared using mean daily flow data or average of the daily flow data or mean monthly data. Flow duration curve, thus obtained are depicted in figure below and table shows the value of flow for a given probability of exceedence for the dam site.

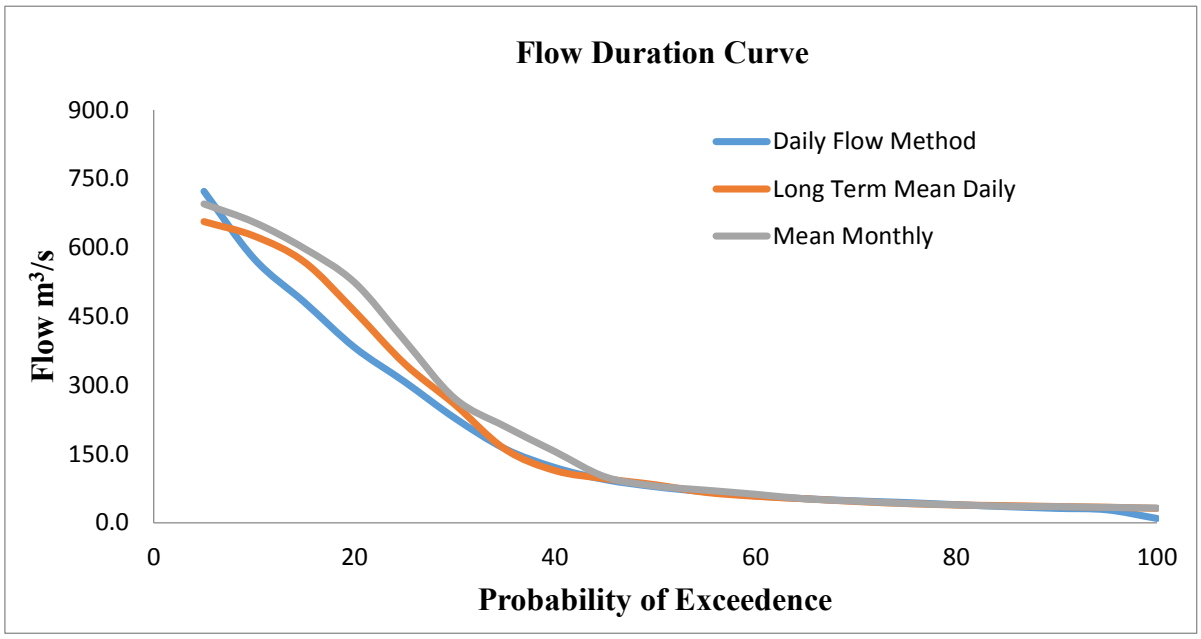

Figure 4.13 Flow Duration Curve at Dudhkoshi Damsite

Table 4.12 Flow Values of Different Probabilities of Exceedence at Damsite

Days	probability	Daily Flow Method	Long Term Mean Daily	Mean Monthly
18.3	5	722.4	656.4	695
36.5	10	575	625	655
54.8	15	481	569	598
73.0	20	382	461	524
91.3	25	307	347	398
109.5	30	228	258	271
127.8	35	161	161	210
146.0	40	120	114	155

164.3	45	94	96	100
182.5	50	78	83	80
200.8	55	67	66	71
219.0	60	59	58	62
237.3	65	52	52	52
255.5	70	48	46	47
273.8	75	44	42	42
292.0	80	39	39	39
310.3	85	35	37	36
328.5	90	31	35	35
346.8	95	28	34	33
365.0	100	9	31	32

This is the unregulated flow before construction of the reservoir which shows discharge in different probabilities.

4.2.6 Flood Frequency Analysis

The understanding of flood plays a key role in many hydrological studies, especially in the design of hydraulic structures. The estimation of floods is also important in the evaluation of flood risk, particularly in areas in close proximity of flood plains. Extreme hydrological events are not only important in the design of water resource projects but also in the design of the developmental structures such as dams, culverts, bridges and others.

This is a statistical method rather than usual design storm, unit hydrograph approach was used to derive the design flood for the dam site. The analysis of flood flow for Dudhkoshi River at Rabuwa had been carried out by taking yearly maximum discharge from DHM (1978 to 2008). The flood values were transposed to the Dam Site using equation 3.11. Gumbel, Log Normal and Log Pearson III distribution were, then, fitted to the observed annual maximum flow data. Of these 31 year floods peaks, the flood of 1985 is the devastating one. The outburst of the Dig-Tsho Lake on 4 August 1985 was catastrophic. Human casualties during the Dig-Tsho event were enormous, along with destruction of the Namche hydro power plant, 14 bridges, and cultivable land. The economic loss during this event was estimated to be more than $500 million. Similarly next devastating glof event of Tam Pokhari occurred in 3 sept 1998, in which many peoples were killed, six

bridges were destroyed, arable land washed away and economic losses estimated to $150 million. The flood peak discharge reached to about 9,800 m^3/s, the highest flood ever recorded.

Table 4.13 Annual Maximum Flood Series at Rabuwa Bazar Gauging Station and Dam Site

Year	Gauge Height Rabuwa	Date	Flow at Rabuwa	Flow at Dam Site
1978	4.9	9/14/1978	1410	1449
1979	4.64	7/24/1979	1060	1089
1980	4.1	7/19/1980	903	928
1981	4.5	8/2/1981	1080	1110
1982	5.45	7/19/1982	1670	1716
1983	6.15	7/15/1983	1550	1593
1984	4.48	7/21/1984	1110	1141
1985	4.94	7/23/1985	1460	1500
1986	4.65	7/31/1986	987	1014
1987	4.47	7/25/1987	1100	1130
1988	4.7	8/1/1988	1110	1141
1989	4.25	7/6/1989	786	808
1990	5.4	8/12/1990	1750	1798
1991	4.7	8/9/1991	1060	1089
1992	4.46	8/25/1992	1000	1028
1993	4.5	8/12/1993	1140	1172
1994	4	8/15/1994	766	787
1995	4.55	8/13/1995	1070	1100
1996	4.62	7/20/1996	1160	1192
1997	5.1	8/12/1997	1400	1439
1998	5.7	9/21/1998	1950	2004
1999	3.9	8/26/1999	755	776
2000	5	7/6/2000	867	891
2001	5.35	8/21/2001	1530	1572

2002	7	8/21/2002	2580	2651
2003	6.22	7/20/2003	2170	2230
2004	6.5	7/10/2004	2390	2456
2005	5.8	8/15/2005	2050	2107
2006	6.15	6/30/2006	1550	1593
2007	7.32	9/5/2007	2593	2665
2008	6	8/7/2008	1364	1402

i. Gumbel Distribution

The flow of different return periods are given in the table below

Table 4.14 (a): For Rabuwa Gauging Station

Tr	Yt	Kt	Qt
2	0.366513	-0.15287	1319
2.33	0.578588	0.037179	1419
5	1.49994	0.862837	1852
10	2.250367	1.535323	2205
20	2.970195	2.180388	2544
50	3.901939	3.015359	2982
100	4.600149	3.641051	3311
200	5.295812	4.264461	3638
500	6.213607	5.086932	4070
1000	6.907255	5.708536	4396
10000	9.21029	7.772372	5479

Table 4.14 (b): For Dam Site

Tr	Yt	Kt	Qt
2	0.366513	-0.15287	1356
2.33	0.578588	0.037179	1458
5	1.49994	0.862837	1903
10	2.250367	1.535323	2266
20	2.970195	2.180388	2613
50	3.901939	3.015359	3063
100	4.600149	3.641051	3401
200	5.295812	4.264461	3737
500	6.213607	5.086932	4180
1000	6.907255	5.708536	4515
10000	9.21029	7.772372	5627

For N = 31	Average	1399 (Rabuwa Bazar) & 1437.7 (Dam site)
Y_n = 0.5371	Standard Deviation	524.7 (Rabuwa Bazar) & 539.2 (Dam site)
S_n= 1.1159		

ii. Log Pearson Type III Distribution

The flow of different return periods are given in the table below.

Table 4.15 (a): For Rabuwa Gauging Station

Tr	Kt	Yt	Qt
2	-0.0745	3.107277	1280
2.33	0.023015	3.122247	1325
5	0.812	3.243374	1751
10	1.32	3.321363	2096
20	1.5615	3.358439	2283
50	2.286	3.469665	2949
100	2.6505	3.525624	3354
200	2.995	3.578512	3789
500	3.275313	3.621547	4184
1000	3.7425	3.69327	4935

Table 4.15 (b): For Dam Site

Tr	Kt	Yt	Qt
2	-0.0745	3.119121	1316
2.33	0.023015	3.134091	1362
5	0.812	3.255218	1800
10	1.32	3.333207	2154
20	1.5615	3.370283	2346
50	2.286	3.48151	3030
100	2.6505	3.537468	3447
200	2.995	3.590357	3894
500	3.275313	3.633391	4299
1000	3.7425	3.705114	5071

Average	3.119 (Rabuwa) & 3.131 (Dam Site)
Standard Deviation	0.1535 (Rabuwa) & 0.1535 (Dam Site)
Skewness Coefficient	0.381 (Rabuwa) & 0.381 (Dam Site)

iii. Log Normal Distribution

The flow of different return periods are given in the table below.

Table 4.16 (a): For Rabuwa Gauging Station

Tr	Kt	Yt	Qt
2	0	3.118714	1314
2.33	0.09262	3.132933	1358
5	0.842	3.24798	1770
10	1.282	3.315529	2068
20	1.475	3.345159	2214
50	2.054	3.434048	2717
100	2.326	3.475806	2991
200	2.576	3.514187	3267
500	2.76875	3.543778	3498
1000	3.09	3.593097	3918

Table 4.16 (b): For Dam Site

Tr	Kt	Yt	Qt
2	0	3.130558	1351
2.33	0.09262	3.144777	1396
5	0.842	3.259824	1819
10	1.282	3.327373	2125
20	1.475	3.357003	2275
50	2.054	3.445892	2792
100	2.326	3.48765	3074
200	2.576	3.526031	3358
500	2.76875	3.555622	3594
1000	3.09	3.604941	4027

Average	3.119 (Rabuwa) & 3.131 (Dam Site)
Standard Deviation	0.1535 (Rabuwa) & 0.1535 (Dam Site)
Skewness Coefficient	0.381 (Rabuwa) & 0.381 (Dam Site)

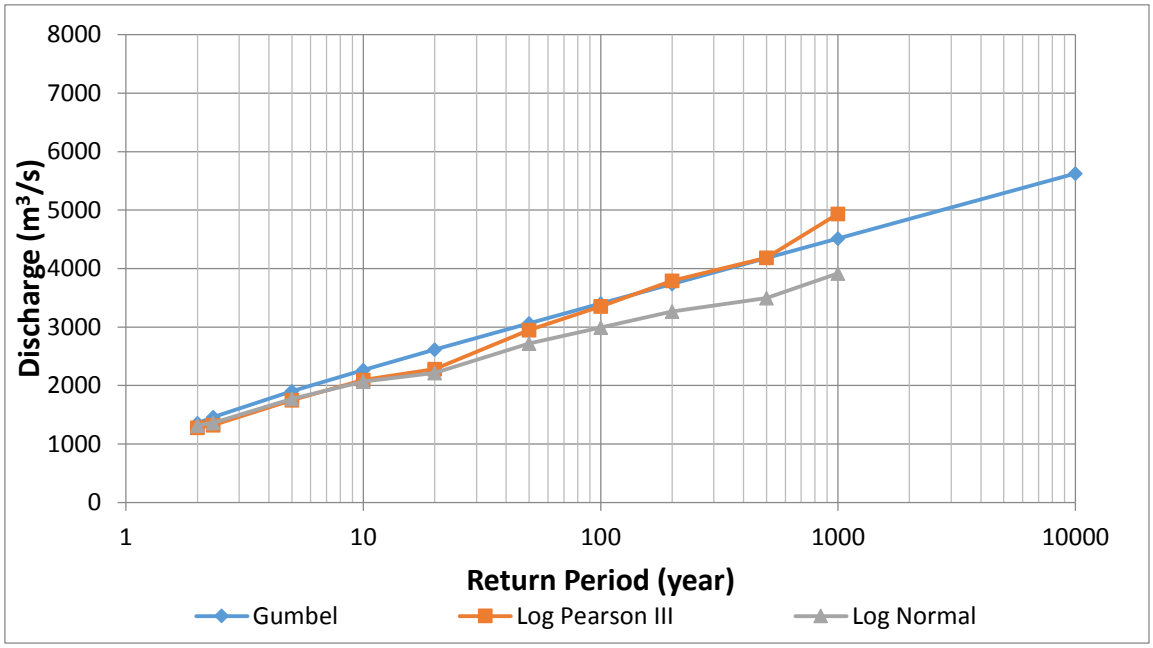

Figure 4.14 Flood Frequency for Dudhkoshi River at Rabuwa Station

Figure 4.15: Flood Frequency for Dudhkoshi River at Damsite

From the above figures, Gumbel distribution fitted the best distribution on both site, so the flow obtained from it is recommended.

4.2.7 Probable Maximum Flood (PMF)

Since the 10,000 year flood is 5,627 m^3/s, the PMF thus, comes to be 11,254 m^3/s.

From Hershfield's Technique the PMF is estimated as

$$PMF = \bar{Q} + K * \sigma$$

Where $\bar{Q}$ = mean of the maximum

σ= standard deviation

K = coefficient (6 to 30)

K value is taken as 19.

By this method PMF came to be 11,254 m^3/s

To be in safe side, PMF for this project is considered to be 11,300 m^3/s.

4.3 Continuous Simulation

The average rainfall obtained from the four precipitation station i.e. 1202, 1203, 1204 and 1219; and the discharge obtained from Rabuwa Bazar Station No. 670 after transposed to the damsite using CAR Method, HEC-HMS Model was used to calibrate the data of 10 years from 1989-1998. Not all year data was calibrated instead it was validated from 1999-2008; since validation tests the model ability to simulate the observed data not used during the calibration with acceptable accuracy and during validation process the model parameters obtained on calibration were not changed except those describing the initial conditions of the basin.

The results of calibration and validation of continuous model are given below.

4.3.1 Calibration

Figure below is the hydrograph comparison graph of continuous model calibrated for the period 1989 – 1998.

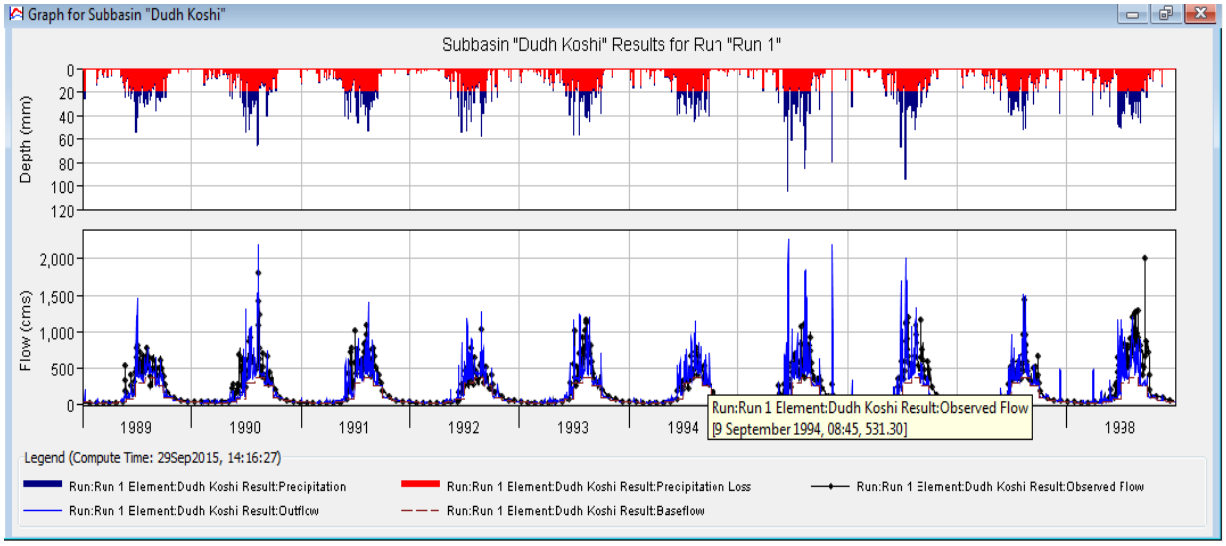

Figure 4.16 Hydrographs comparison results of Continuous model calibration

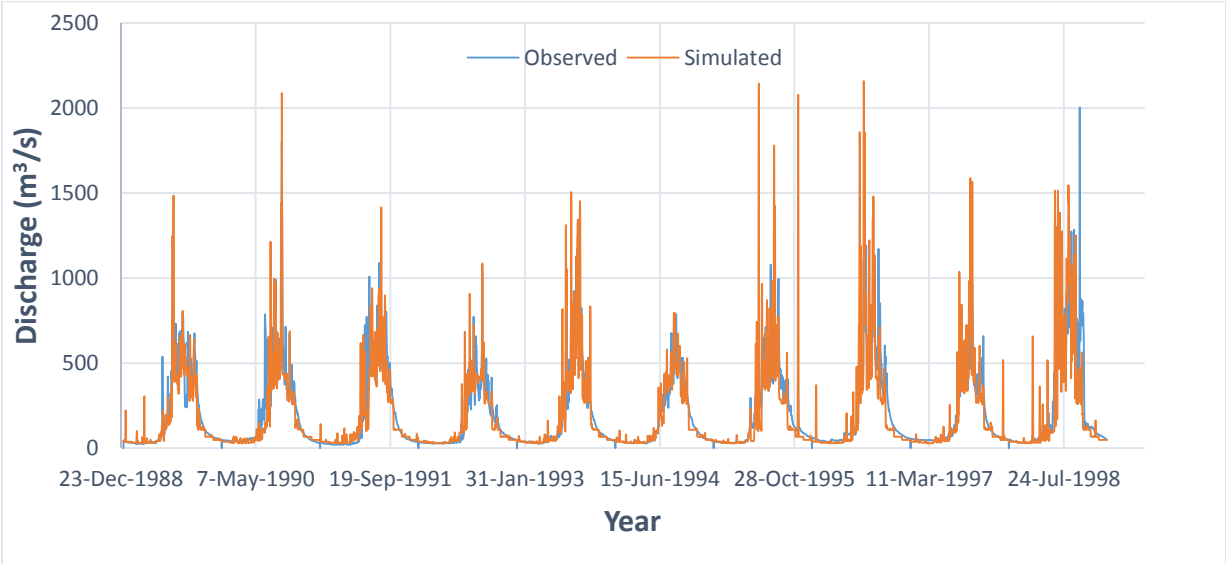

Figure 4.17 Hydrographs comparison results of Continuous model calibration

The hydrograph comparision of calibration figure 4.16 shows very good performance of the model. The model captures most of the peaks well while few of them are overestimated or underestimated. The graph also shows a very good simulation of the recession limbs and dry portions of the hydrograph and also for pre-monsoon seasons. The magnified and detailed figures with baseflow component are given in Annexes.

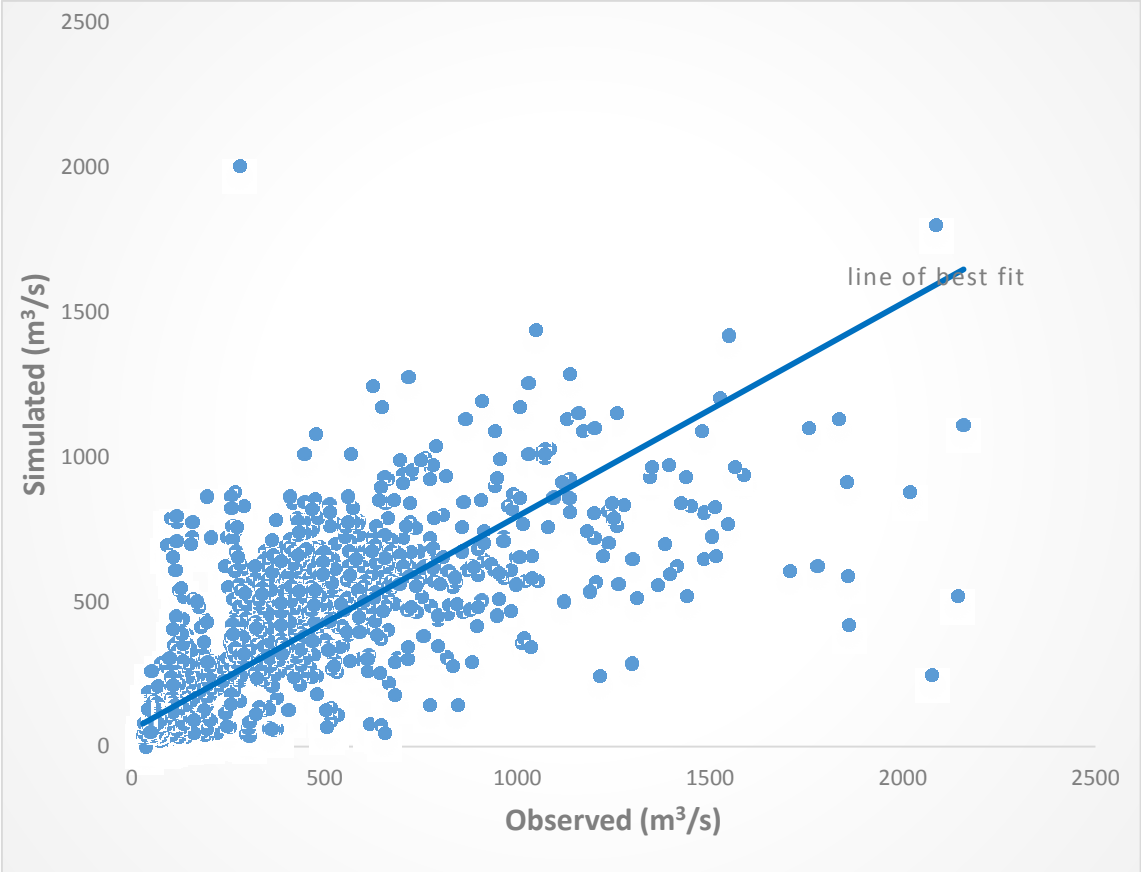

Figure 4.18 Scattered plot diagram of continuous model calibration

In the scattered plot diagram the proximity of the points with the line of best fit shows a good agreement between observed and simulated data except for some few peak events. The statistical performance values and calibrated values parameter are given in the table 4.3.2.

4.3.2 Calibrated Parameters

	Dudh Koshi						Thotne Khola			
Year	Initial Deficit (mm)	Maximum Deficit (mm)	Constant Rate (mm/hr)	Impervious (%)	Time of Concentration (hr)	Storage Coefficient (hr)	SCS Curve Number	Impervious (%)	Time of Concentration (hr)	Storage Coefficient (hr)
1989	6	9	0.9	14	4.46	10.15	61	8	1.5	3.75
1990	6	10	1	11	4.46	10.15	61	9	1.5	3.75
1991	5	7	1	21	4.46	10.15	61	6	1.5	3.75
1992	4	7	1.2	7	4.46	10.15	61	8	1.5	3.75
1993	6	8	0.6	9	4.46	10.16	61	8	1.5	3.75
1994	4	7	1.3	12	4.46	10.15	61	8	1.5	3.75
1995	7	9	1	9	4.46	10.15	61	7	1.5	3.75
1996	6	9	0.7	8	4.46	10.15	61	5	1.5	3.75
1997	4	7	0.8	9	4.46	10.15	61	7	1.5	3.75
1998	5	9	0.5	9	4.46	10.15	61	7	1.5	3.75
Mean	5.3	8.2	0.9	10.9	4.46	10.15	61	7.3	1.5	3.75

4.3.3 Validation

After calibration of model it is utmost to validate to know whether the model outputs are correct or not. For this purpose the model is validated with 10 years data from 1999 – 2008 with the average rainfall and discharge data of the basin using the average calibrated parameter values.

The hydrograph comparison figure 4.19 shows good performance of the model during validation. Here too most of the important peaks are captured and the dry period discharge is simulated very well. A magnified portion is given in Annexes.

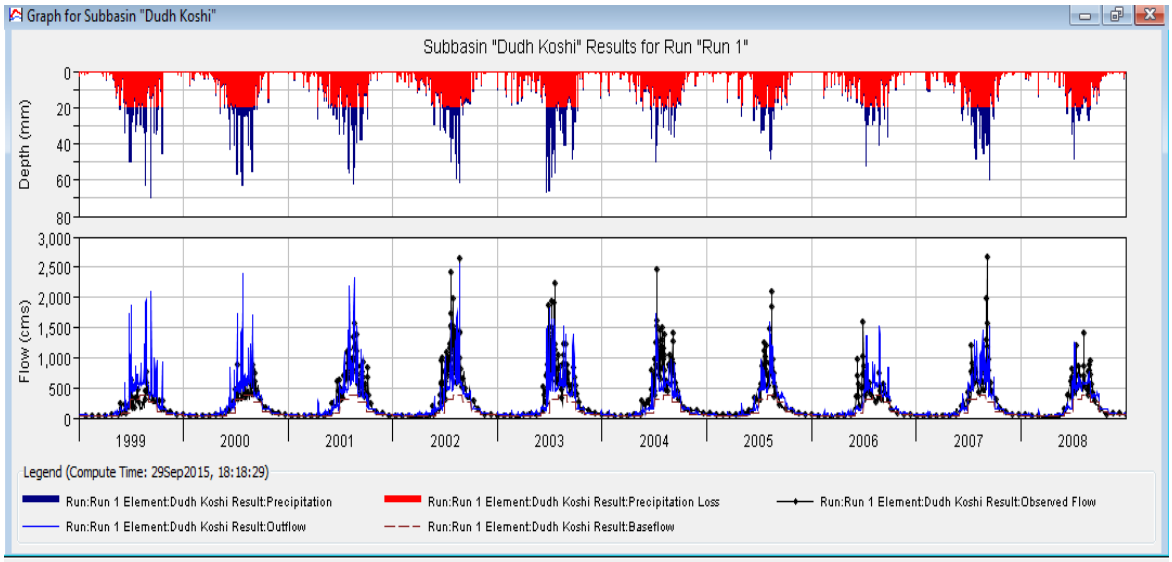

Figure 4.19 Hydrographs comparison results of Continuous model validation

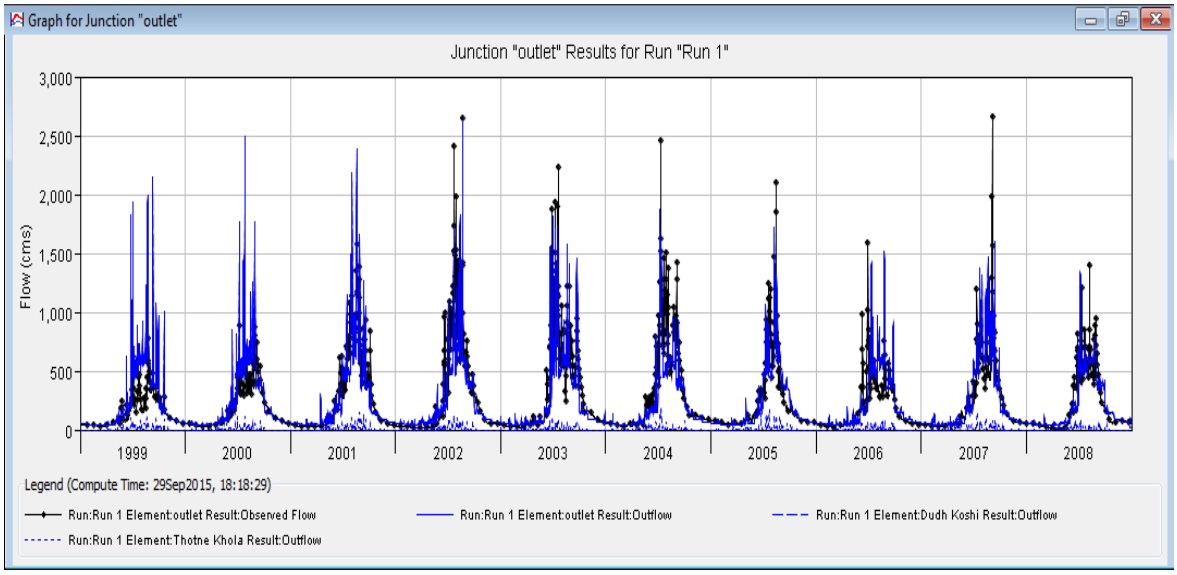

Figure 4.20 Hydrographs comparison results of Continuous model validation in outlet

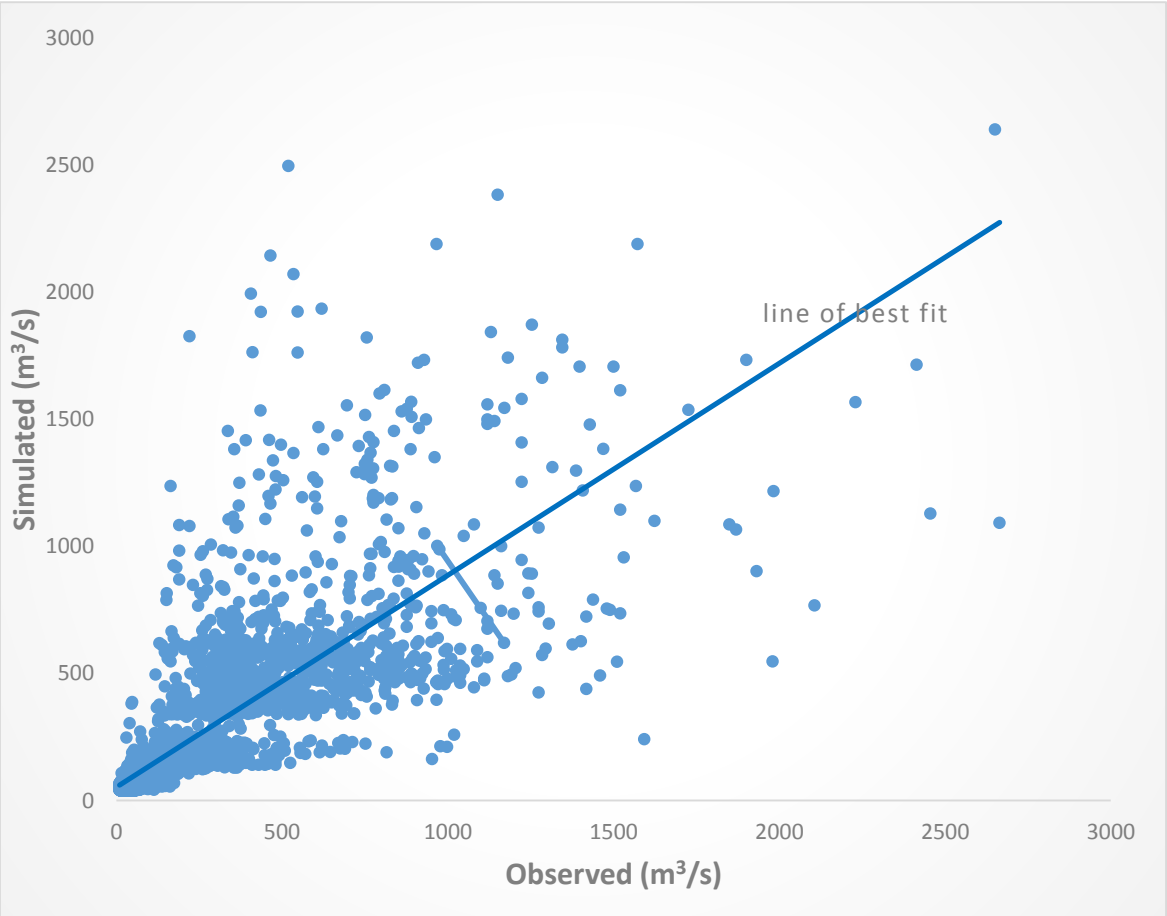

Figure 4.21 Scattered plot diagram of continuous model validation

4.3.4 Flood Frequency Analysis (HEC-HMS)

The model shows the good performance in the validation of the discharge data. So the discharge data of 31 years was validated from the calibrated parameter values. The peak discharges of those years were taken into account and gumbel distribution was fitted, which showed quite similarity with the observed data and proved to have a good performance. The fitted table is below.

Table 4.17 Flow obtained of different return period using HEC-HMS model

Tr	Yt	Kt	Qt
2	0.366513	-0.15287	1544
2.33	0.578588	0.037179	1624
5	1.49994	0.862837	1970
10	2.250367	1.535323	2253
20	2.970195	2.180388	2524
50	3.901939	3.015359	2874

100	4.600149	3.641051	3137
200	5.295812	4.264461	3399
500	6.213607	5.086932	3745
1000	6.907255	5.708536	4006
10000	9.21029	7.772372	4872

The flow obtained from the observed and model data are very much validated. The maximum values obtained doesn't have error greater than 15%, which is under consideration. This method is quite similar to Log Pearson Type-III Distribution.

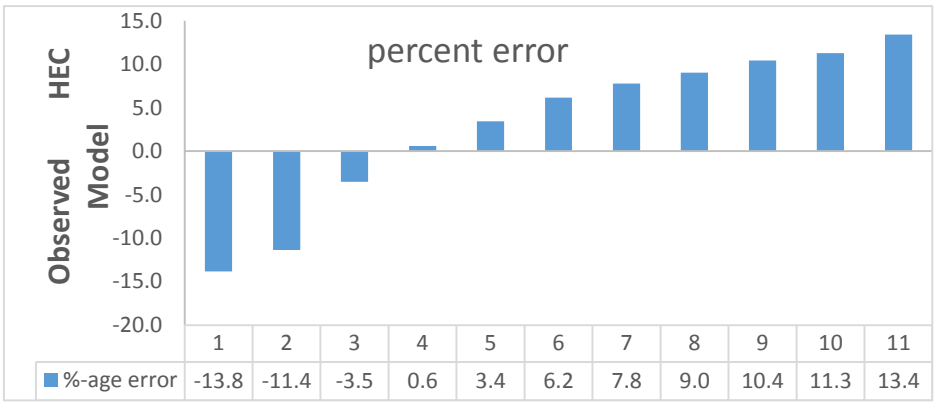

Figure 4.22 Percent of error of Observed and Model Maximum Values

4.3.5 RCM Data Projection

The Dudhkoshi Basin is topographically steep, hard with posing a risk of high flood. The gridded RCM (PRECIS) data of the basin were taken from DHM webportal. The validated parameter values of the basin were taken into account. RCM data i.e. precipitation were used to project 30 years (2030 – 2060) daily discharge of the basin. The gridded latitude and longitude of the basin is given in the Annexes.

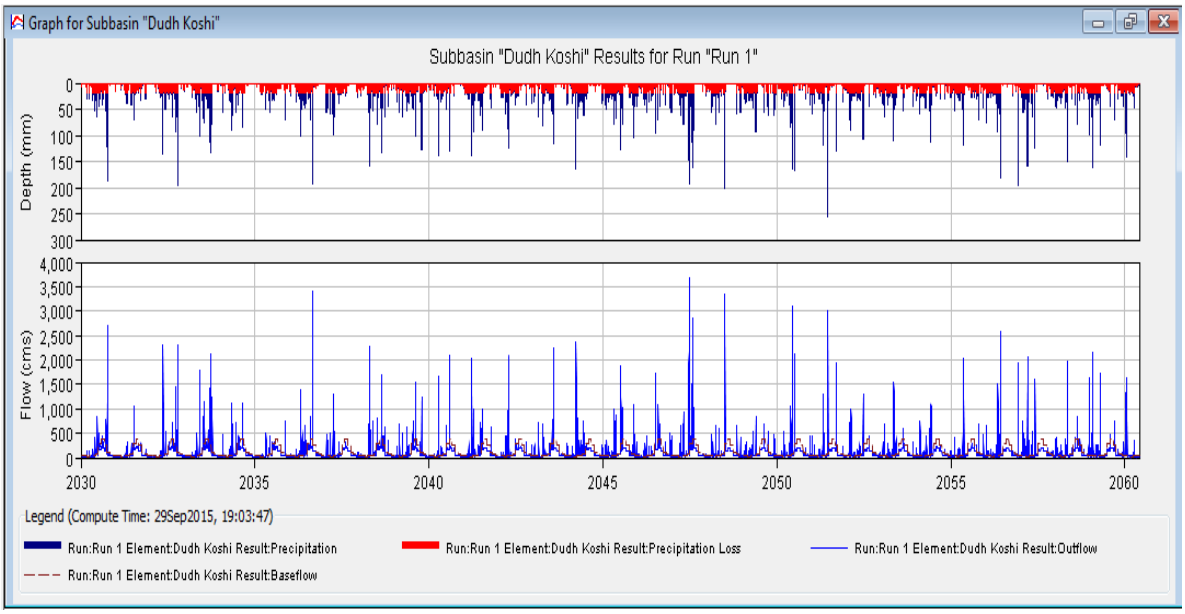

Figure 4.23 Hydrograph induced from RCM Precipitation Data

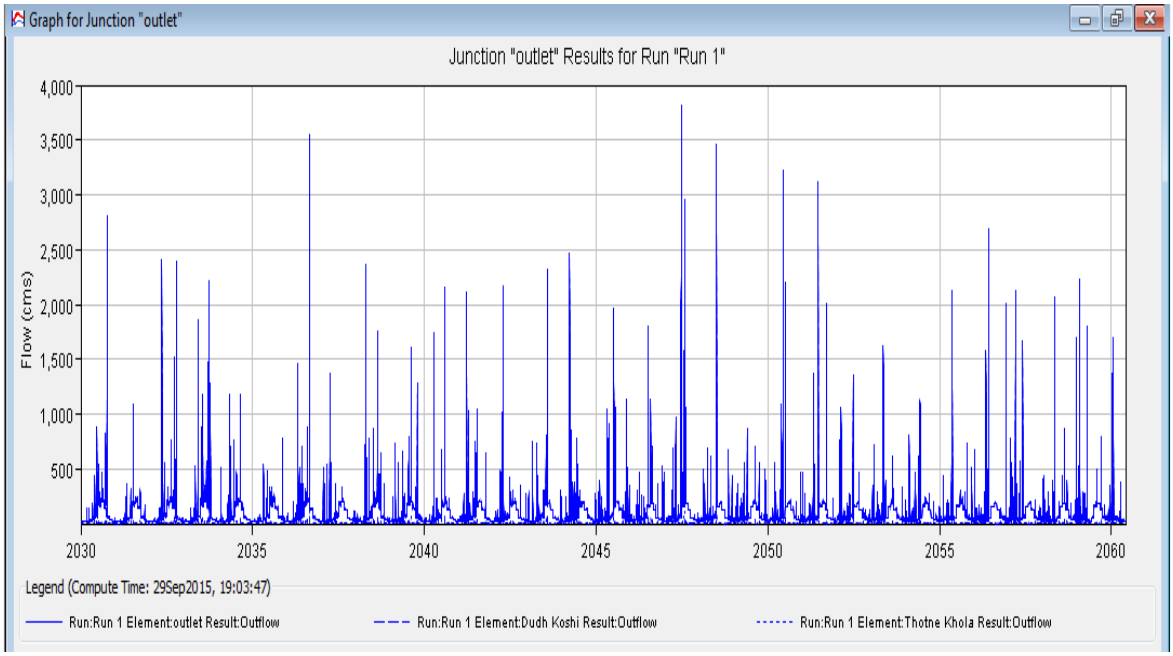

Figure 4.24 Hydrograph induced from RCM Precipitation Data

4.3.6 Frequency Analysis using RCM Data

i. Gumbel Distribution

Gumbel distribution was fitted to the discharge induced from RCM Data. The flow of different return periods are given in the table below.

Table 4.18: Projected discharge using Gumbel for DudhKoshi Dam Site

Tr	Yt	Kt	Qt
2	0.366513	-0.15287	2005
2.33	0.578588	0.037179	2154
5	1.49994	0.862837	2800
10	2.250367	1.535323	3326
20	2.970195	2.180388	3830
50	3.901939	3.015359	4483
100	4.600149	3.641051	4972
200	5.295812	4.264461	5460
500	6.213607	5.086932	6103
1000	6.907255	5.708536	6589
10000	9.21029	7.772372	8203

For N = 31	Average	2125 (Dam Site)
Y_n = 0.5371	Standard Deviation	782 (Dam site)
S_n= 1.1159		

ii. Log Pearson Type III Distribution

The flow of different return periods are given in the table below.

Table 4.19: Projected discharge using LPT-III for DudhKoshi Dam Site

Tr	Kt	Yt	Qt
2	-0.0745	3.282936	1918
2.33	0.023015	3.299949	1995
5	0.812	3.437601	2739
10	1.32	3.526231	3359
20	1.5615	3.568365	3701
50	2.286	3.694767	4952
100	2.6505	3.75836	5733
200	2.995	3.818464	6584
500	3.275313	3.86737	7368
1000	3.7425	3.948879	8890

Average	3.296 (Dam Site)
Standard Deviation	0.1745 (Dam Site)
Skewness Coefficient	0.5721 m Site)

iii. Log Normal Distribution

The flow of different return periods are given in the table below.

Table 4.20: Projected discharge using Log Normal for DudhKoshi Dam

Tr	Kt	Yt	Qt
2	0	3.295934	1977
2.33	0.09262	3.312093	2052
5	0.842	3.442836	2772
10	1.282	3.519601	3308
20	1.475	3.553274	3575
50	2.054	3.65429	4511
100	2.326	3.701746	5032
200	2.576	3.745362	5564
500	2.76875	3.778991	6012
1000	3.09	3.835039	6840

Average	3.296 (Dam Site)
Standard Deviation	0.1745 (Dam Site)
Skewness Coefficient	0.5721 (Dam Site)

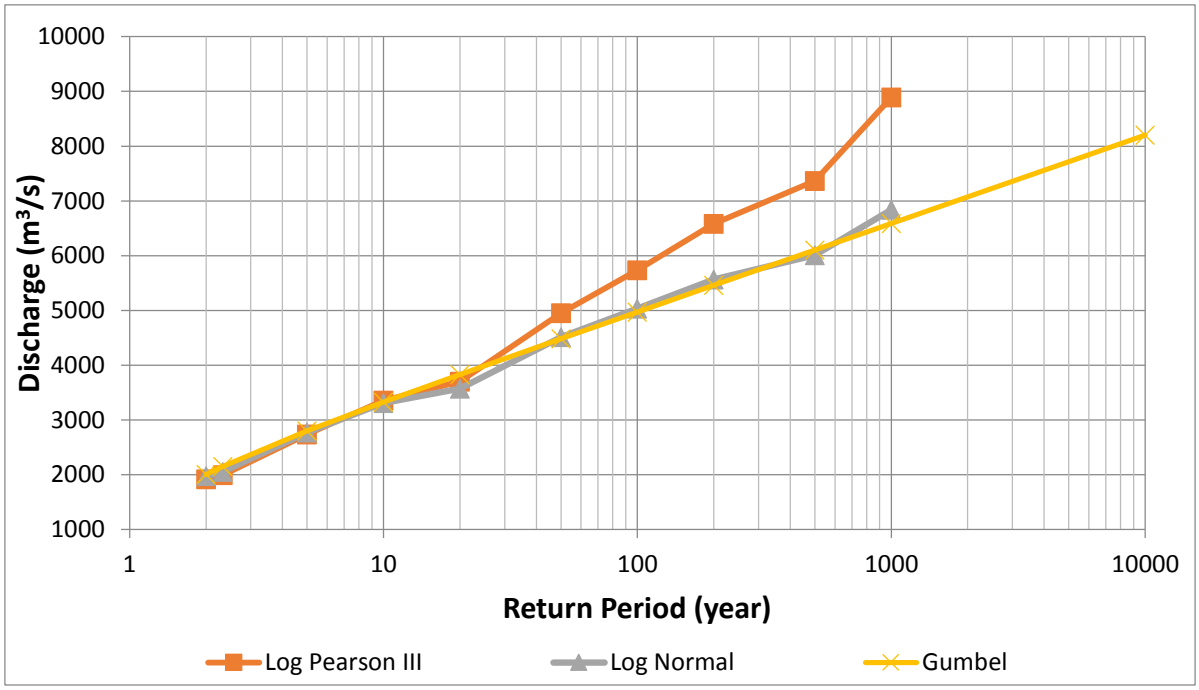

Figure 4.25: Flood Frequency for Dudhkoshi River at Dam Site

The figure clearly shows that the projected maximum discharge of DudhKoshi River Basin has increased. The above figure states that there is high risk of flood during the period of 2030 – 2060 s period.

4.3.7 Model Evaluation and Flood Scenario

The Hydrological HEC-HMS model used in this study is found to capture almost all of the events. Some hydrological events are not captured in most cases the high peak floods of some years. The most important thing in this might have been due to station swept away by the floods or the rainfall pattern not consistent in each year.

In this research, flood frequency analysis obtained from the station data and from the HEC-HMS model, the modeled data gave little high discharge than the station level discharge, which can be considered to the station level discharge and might have been due to human error or deposition or scuring in the river.

This basin is highly susceptible to the flood events. The frequency analysis from different methods showed that it has a high threat to the flooding event as depicted in the table above. The frequency analysis obtained from the future PRECIS data showed that it possesses a threat of flood event in the basin in the middle of twenty first century.

Due to Nepal's geographical and other climatological conditions, rugged and steep topography, extreme weather events and fragile geological conditions, the country is

regarded as a disaster hotspot and in eighth position for flood related deaths in global standards. In this case the study and technique used in this research can be applied to other basins in order to predict the flood events and ensure the safety.

Conclusion

This study was carried out to estimate the maximum flow in Dudh Koshi River basin using statistical method and hydrological model. The catchment area upstream from the dam site was found to 3849 km^2; meanwhile upstream of Rabuwa gauging station was 3722 km^2. Average annual flow of Rabuwa and Dam site was 203 m^3/s and 207 m^3/s. Similarly in meteorological analysis, the average basin precipitation is found to 1442.2 mm using the isohyetal method. And for PMP calculation, it is found to be 596 mm in 24 hr and 265 mm is the 100 year return period precipitation. In this study, PMF is found to be 11,254 m^3/s. Similarly, the results of calibration and validation of continuous lumped model in the Dudhkoshi River basin imply that this model is valid for the rainfall-runoff simulation in the basin with the calibrated parameters. The performance of the model was reasonable within the differences of error not exceeding 15 percent with the observed flow which is considerable. The projected discharge obtained signifies that the flow during the mid-twenty first centuries will be increased by certain extent.

As shown in the results above, the model predicted peak discharge accurately based on the available historical data. This shows that HEC-HMS is suitable for the studied basin. From the results, we can conclude that the complexity of the model structure does not determine its suitability and efficiency. Though the structure of HEC-HMS is simple, it is a powerful tool for flood forecasting. A further application of HEC-HMS should be encouraged to confirm its suitability for the Nepal basins for sustainable water resource planning, development and management and for data quality controlling purposes.

The calibrated model parameters should be checked with future water year data, and model should be further verified, if necessary. Model parameters should be updated for better performance.

Recommendations

The study was based on the available data and relevant assumptions. The study was purely academic fulfillment for the thesis. Following suggestions are made for further improvement of the study.

- It is recommended to study other meteorological, geological and socio-economical parameter of the basin to get more reliable information that can be the important gear for further study.
- Hydro-meteorological stations should be increased in the catchment to have sufficient and accurate data on climate variables.
- The developed continuous HEC-HMS model is suggested to use for basin long term water management and planning.
- From the study it is seen that bias correction should be done.
- A distributed HEC-HMS model can give better results than lumped one. So study of a comparative distributed model is suggested.
- The uncertainty in modelling, especially the uncertainty in the observed data should be estimated as the observed data seems to be a good source of error for reduced model performance.
- A large set of data extreme discharge should be used for the flood frequency analysis to estimate the large return period-floods with high confidence levels.

REFERENCES

Anshul Agarwal, Mukand S. Babel, Shreedhar Maskey: Analysis of future precipitation in the Koshi river basin, Nepal, Journal of Hydrology, 513 (2014) 422–434.

Bajracharya, S. R., Mool, P. K., Shrestha, B. R. (2007). Impact of climate change on Himalayan glaciers and glacial lakes: case studies on GLOF and associated hazards in Nepal and Bhutan. International Centre for Integrated Mountain Development (ICIMOD)

Bartlett, R.; Bharati, L.; Pant, D.; Hosterman, H.; McCornick, P. 2010. *Climate change impacts and adaptation in Nepal*. Colombo, Sri Lanka: International Water Management Institute. 35p. (IWMI Working Paper 139). doi:10.5337/2010.227

Dhakal S, 2013, Flood Hazard in Nepal and New Approach of Risk Reduction

Feldman, AD., 2000. Hydrologic Modeling System HEC-HMS: Technical Reference Manual, US Army Corps of Engineers

G. Silwal, 2014, Modelling Snow and Icemelt Runoff in the Context of Climate Change: A Case Study of Dudhkoshi River Basin, Nepal

Glacier Lakes and Glacier Lake Outburst Floods in Nepal, ICIMOD, 2011

Glacier Status in Nepal and Decadal Change from 1980 to 2010 Based on Landsat Data, ICIMOD, 2014

http://www.ajdesigner.com/phptimeconcentration/bransby_williams_equation_time_concentration.php

http://www.rrcap.ait.asia/glofnepal/Nepal/Report/chap11/chap11main.htm

Hunukumbura, P.B., Tachikawa, Y, and Shiba, M., 2011. Distributed Hydrological ModelTransferability across Basins with Different Hydro-climatic Characteristics, Hydrol. Process. 26(6):739-808

ICIMOD, (2011). *The Status of Glaciers in the Hindu Kush- Himalayan Region*. Sewa Printing Press, Kathmandu, Nepal

IPCC, (2008). *Observed and projected changes in climate as they relate to water*. Assessment Report of the Inter-governmental panel on climate change, Cambridge University Press

Juerg Merz*, Pradeep M. Dangol, Madhav P. Dhakal, Bhawani S. Dongol, Gopal Nakarmi,

Rolf Weingartner: Rainfall-run off events in a middle mountain catchment of Nepal, Journal of Hydrology (2006) 331 , 446 – 458

K. J. Beven, *Rainfall-Runoff Modelling: The Primer*: John Wiley & Sons, 2012

Kafle, T.P., Hazarika, M.K. & Samarakoon, L., 2007. Development of flood forecasting models for the Bagmati Basin in Nepal

Lochan Devkota, Alessandra Crosato, Sanjay Giri: Effect of the barrage and embankments on flooding and channel avulsion case study Koshi River, Nepal

Mujere, N., 2011. Flood Frequency Analysis Using the Gumbel Distribution. International Journal on Computer Science and Engineering, 3(7), pp.2774-2778

NCVST (Nepal Climate Vulnerability Study Team). 2009. *Vulnerability through the eyes of the vulnerable: Climate change induced uncertainties and Nepal's development predicaments*. Institute for Social and Environmental Transition (ISET), Nepal. Kathmandu, Nepal: Nepal Climate Vulnerability Study Team (NCVST)

Nepal: Strengthening Capacity for Managing Climate Change and the Environment - Climate Data Digitization and Downscaling of Climate Change Projections in Nepal

Nepal Disaster Report: The Hazardscape and Vulnerability Ministry of Home Affairs (MoHA) and Nepal Disaster Preparedness NetworkNepal. (DPNet), 2009

Nepal's Mahakali floods Darchula, red flag placed, emergency declared. Recent Natural Disasters [Internet]. 2013 Jun 17 [Cited 2013 Nov 5]; Available from http://www.disaster-report.com/2013/06/nepalsmahakali-floods-darchula-red.html

Nepal S, 2012; Evaluating Upstream-Downstream Linkages of Hydrological Dynamics in the Himalayan Region

Practical Action, 2009: Temporal and Spatial Variation of Climate Change Over Nepal (1976-2005)

Preparing for flood disaster: Mapping and Assessing Hazard in the Ratu Watershed, Nepal, ICIMOD, 2007

Problems of Disaster Management in Nepal and Measures to Solve them (1998), A Report prepared by a Task Force, His Majesty's Government of Nepal, Ministry of Home Affairs, Kathmandu, Nepal.

Reddy, P.J. 2008. A Text Book of Hydrology.

S. L. Dingman, *Physical Hydrology*: Waveland Press, 2008

Shital DHAKAL, Nepal and Dennis M. FOX, France, Hydrological Modeling of the Potential Impact of a Forest Fire on Runoff in a Mediterranean Catchment

Shrestha, M.L. (1997). *Development of climate change scenarios with reference to Nepal, in conference on climate changes in Nepal*. US country study program, Department of Hydrology and Meteorology of Nepal

S.K. Garg, 2010, Hydrology and Water Resources Engineering; Water Resources Engineering (Vol. I)

WECS (Water and Energy Commission Secretariat). 1999. Basin wise water resources and water utilization study of the Koshi River Basin. Water and Energy Commission Secretariat (WECS), Government of Nepal.

WECS. (2011). Water resources of Nepal in the context of climate change. Government of Nepal, Water and Energy Commission Secretariat, Singha Durbar, Kathmandu, Nepal, 2011

Yogacharya K S, Bista R.B, Poudel S.N, Shrestha H.O, Regmi N and Pandey S, 2000: Water-based Integrated Development of the GBM Region, IIDS Publication

ANNEXES

A. Regression Coefficient

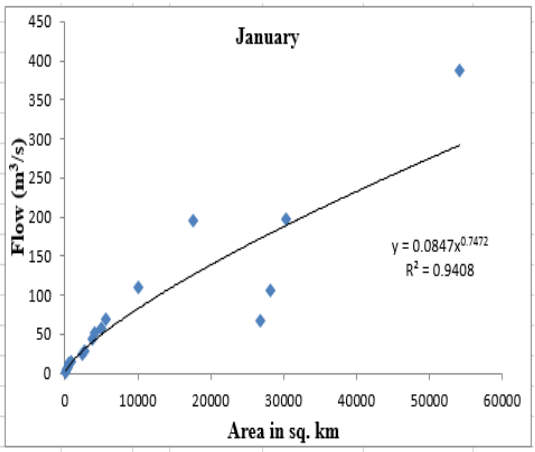

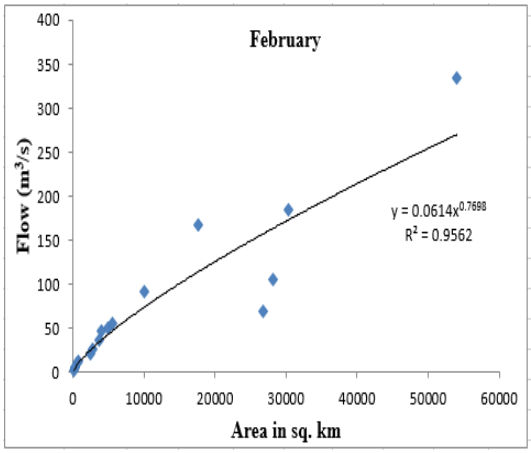

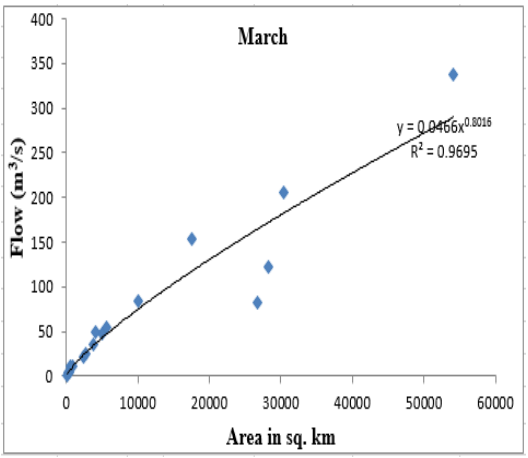

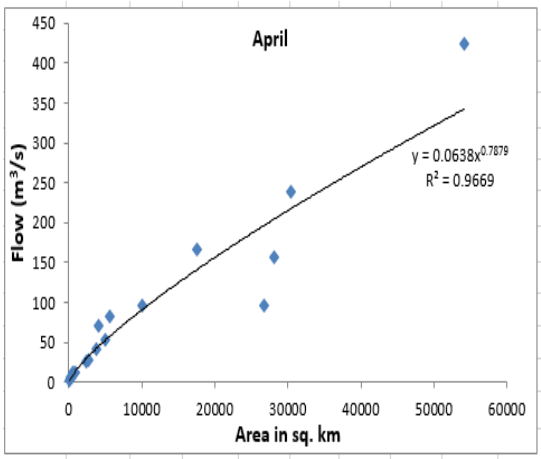

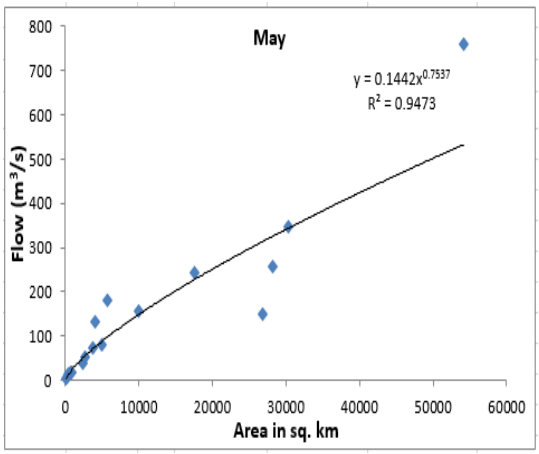

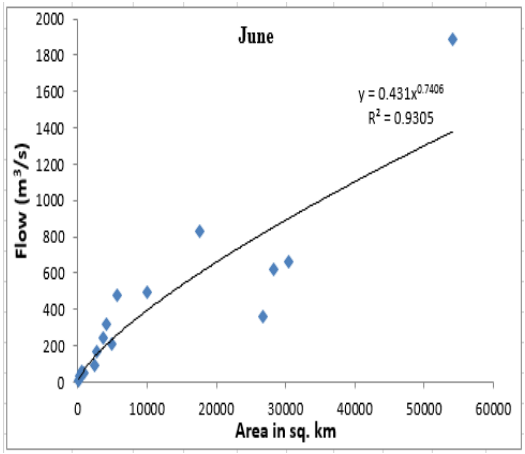

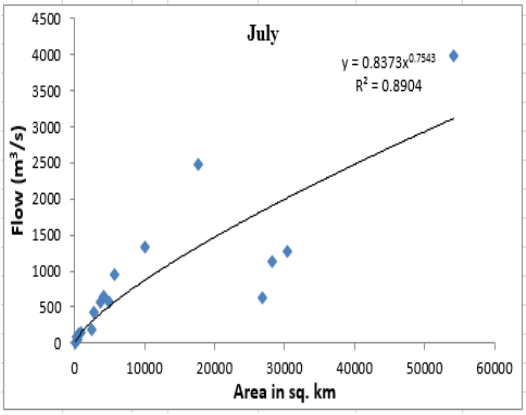
July
y = 0.8373x^0.7543
R² = 0.8904
Flow (m³/s)
Area in sq. km

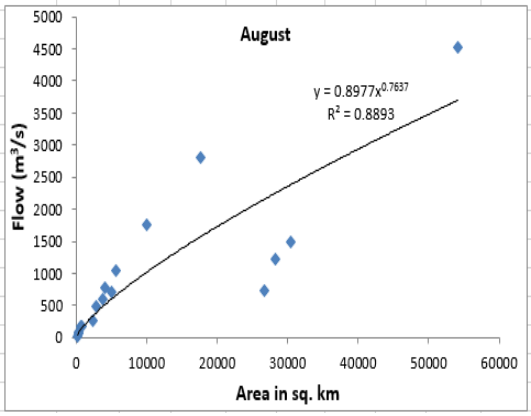
August
y = 0.8977x^0.7637
R² = 0.8893
Flow (m³/s)
Area in sq. km

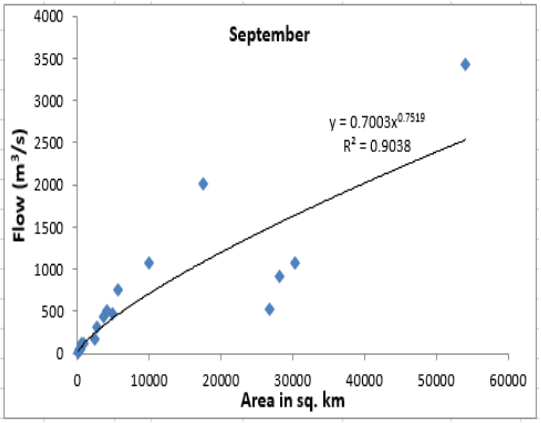
September
y = 0.7003x^0.7519
R² = 0.9038
Flow (m³/s)
Area in sq. km

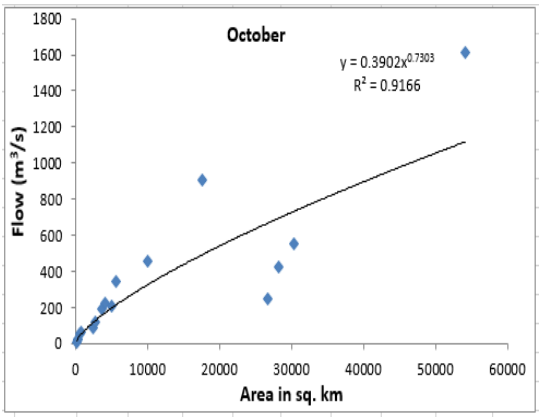
October
y = 0.3902x^0.7303
R² = 0.9166
Flow (m³/s)
Area in sq. km

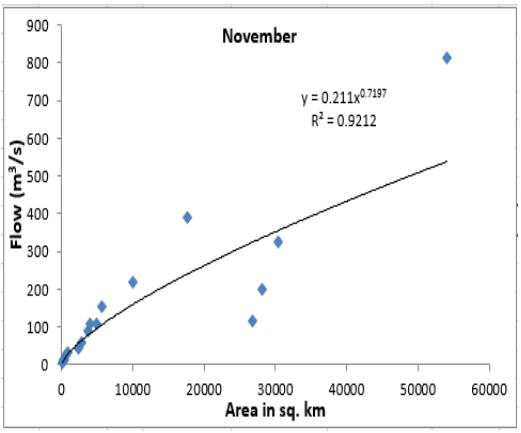
November
y = 0.211x^0.7197
R² = 0.9212
Flow (m³/s)
Area in sq. km

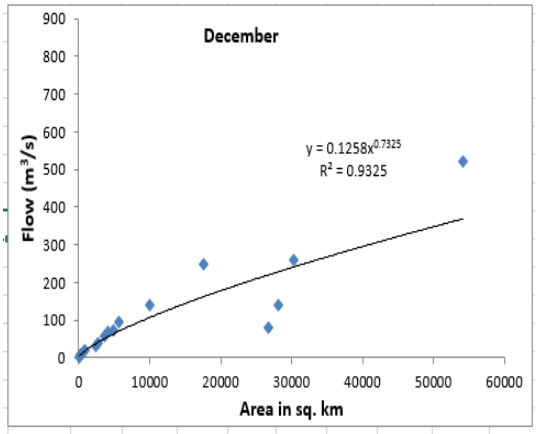
December
y = 0.1258x^0.7325
R² = 0.9325
Flow (m³/s)
Area in sq. km

B. Calibration parameter constraints of the models used:

Parameter limits for calibration in HEC-HMS

Model	**Parameter**	**Minimum**	**Maximum**
	Initial deficit	0 mm	500 mm
Deficit and constant loss	Maximum deficit	0 mm	500 mm
	Deficit recovery factor	0.1	5
	Initial abstraction	0 mm	500 mm
SCS Curve Number	Curve Number	1	100
	Time of concentration	0.1 hr	500 hr
Clark's Unit Hydrograph	Storage Coefficient	0 hr	150 hr
Baseflow	Initial baseflow	0 m^3/s	100000 m^3/s

Categorization of the HEC-HMS models

Runoff-volume models.

Model	Categorization
Initial and constant-rate	event, lumped, empirical, fitted parameter
SCS curve number (CN)	event, lumped, empirical, fitted parameter
Gridded SCS CN	event, distributed, empirical, fitted parameter
Green and Ampt	event, distributed, empirical, fitted parameter
Deficit and constant rate	continuous, lumped, empirical, fitted parameter
Soil moisture accounting (SMA)	continuous, lumped, empirical, fitted parameter
Gridded SMA	continuous, distributed, empirical, fitted parameter

Direct-runoff models.

Model	Categorization
User-specified unit hydrograph (UH)	event, lumped, empirical, fitted parameter
Clark's UH	event, lumped, empirical, fitted parameter
Snyder's UH	event, lumped, empirical, fitted parameter
SCS UH	event, lumped, empirical, fitted parameter
ModClark	event, distributed, empirical, fitted parameter
Kinematic wave	event, lumped, conceptual, measured parameter
User-specified unit hydrograph (UH)	event, lumped, empirical, fitted parameter

Baseflow models.

Model	Categorization
Constant monthly	event, lumped, empirical, fitted parameter
Exponential recession	event, lumped, empirical, fitted parameter
Linear reservoir	event, lumped, empirical, fitted parameter

Value of Base flow Used in the Model

Month	Jan	Feb	Mar	Apr	May	Jun	Jul	Aug	Sep	Oct	Nov	Dec
Baseflow	37.8	31.9	29.0	31.9	41.6	90.1	303.9	380.2	257.3	108.3	67.2	48.6

Maximum Value from Hec-Hms Model

Year	1978	1979	1980	1981	1982	1983	1984	1985	1986	1987	1988	1989	1990	1991	1992	1993	1994	1995	1996	1997	1998	1999	2000	2001	2002	2003	2004	2005	2006	2007	2008
max hec dis	1721	1425	1227	1277	1437	1864	1130	1337	898	1568	1473	1461	2184	1408	1279	1246	1150	2260	2000	1516	1193	2085	2397	2329	2553	1809	1725	1601	1517	1528	1246

Projected Maximum Yearly Discharge Obtained from RCM Data

Year	2030	2031	2032	2033	2034	2035	2036	2037	2038	2039	2040	2041	2042	2043	2044	2045	2046	2047	2048	2049	2050	2051	2052	2053	2054	2055	2056	2057	2058	2059	2060
Projected 2030-2060	2801	1087	2403	2216	1174	775	3543	1370	2370	1611	2158	2110	2163	2320	2474	1963	1797	3821	3459	874	3229	3118	1353	1622	1126	2126	2696	2132	2064	2229	1694

C. Hydrographs with baseflow and rainfall

i. Calibration:

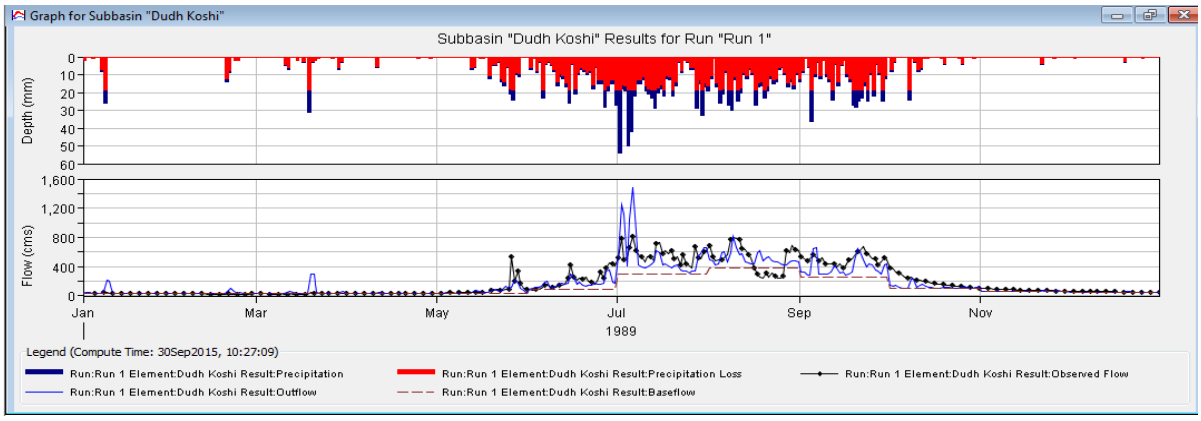

Detailed hydrograph of the 1989 period

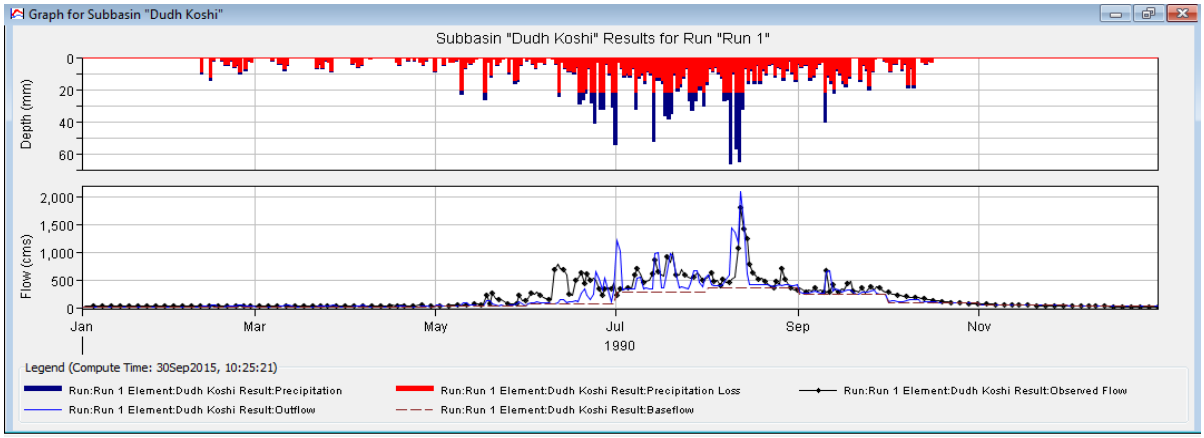

Detailed hydrograph of the 1990 period

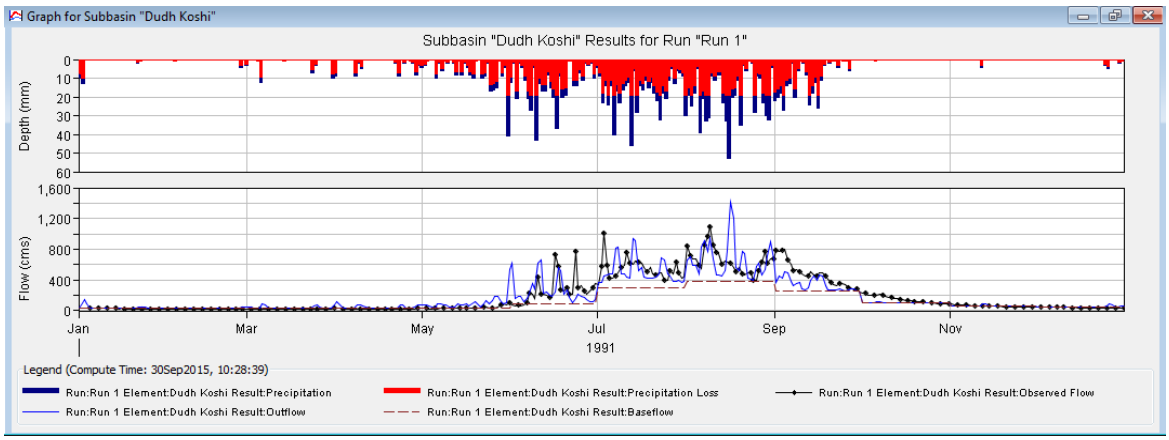

Detailed hydrograph of the 1991 period

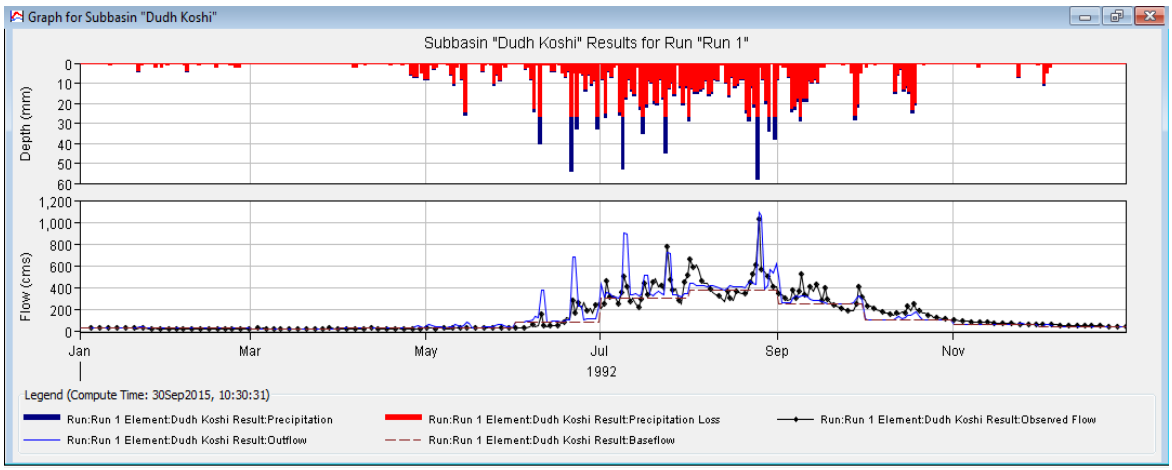

Detailed hydrograph of the 1992 period

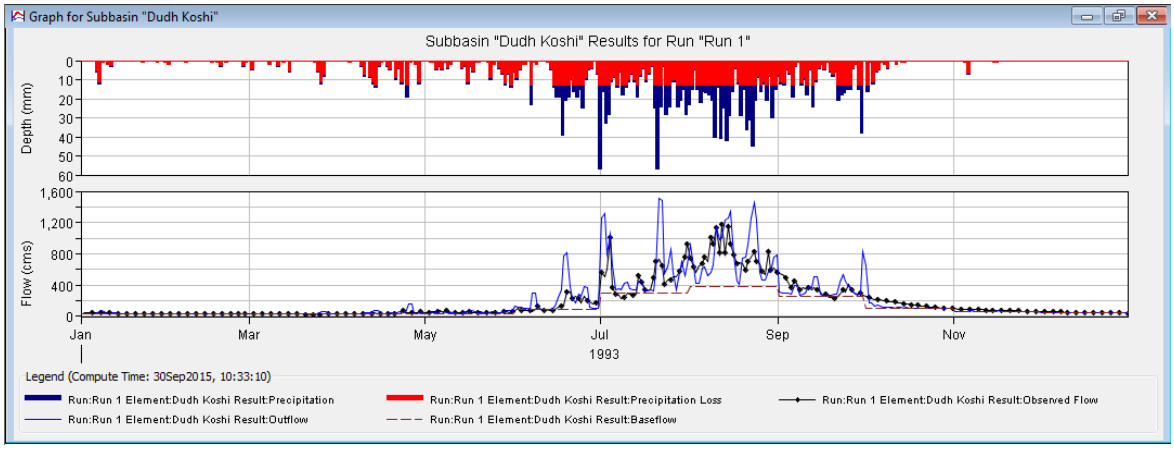

Detailed hydrograph of the 1993 period

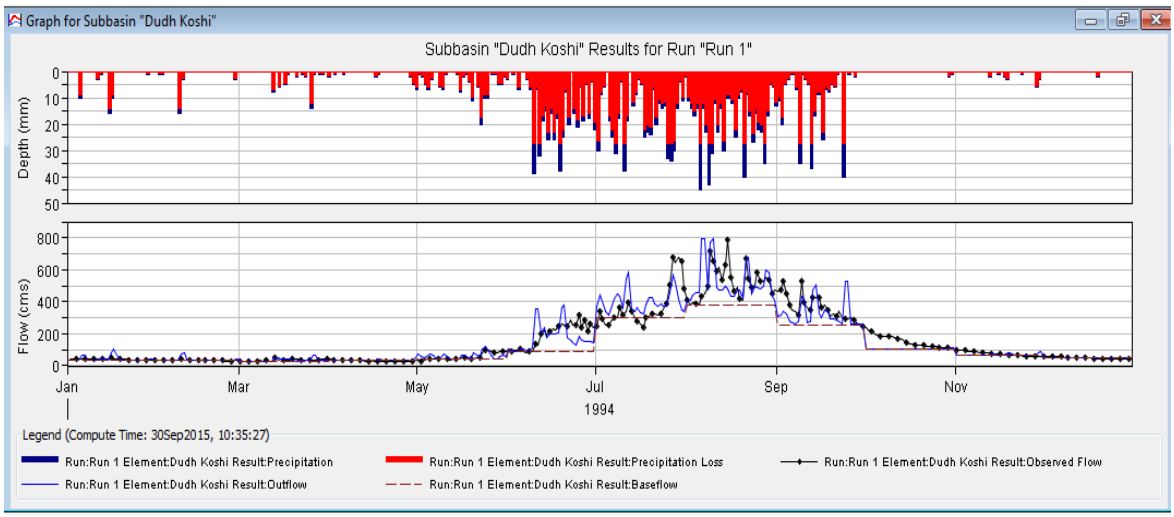

Detailed hydrograph of the 1994 period

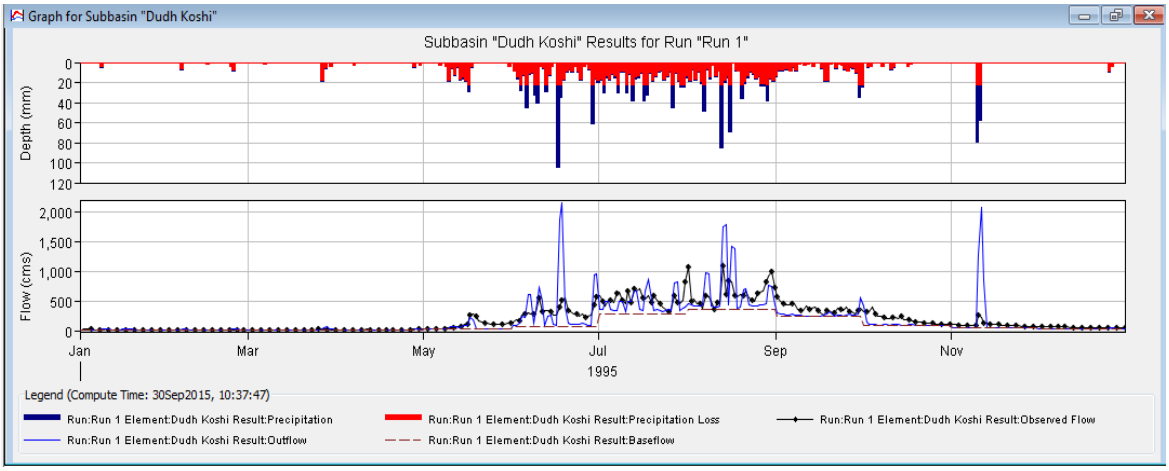

Detailed hydrograph of the 1995 period

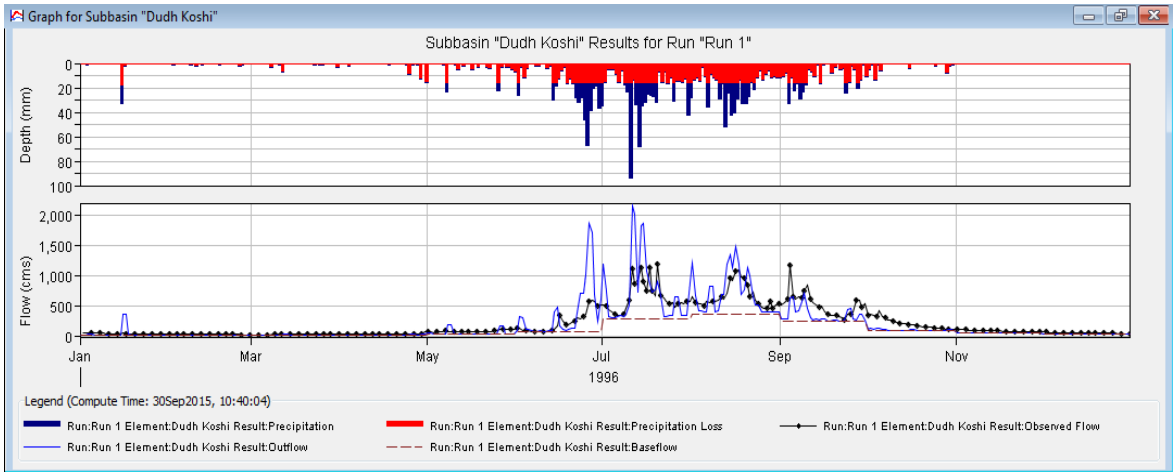

Detailed hydrograph of the 1996 period

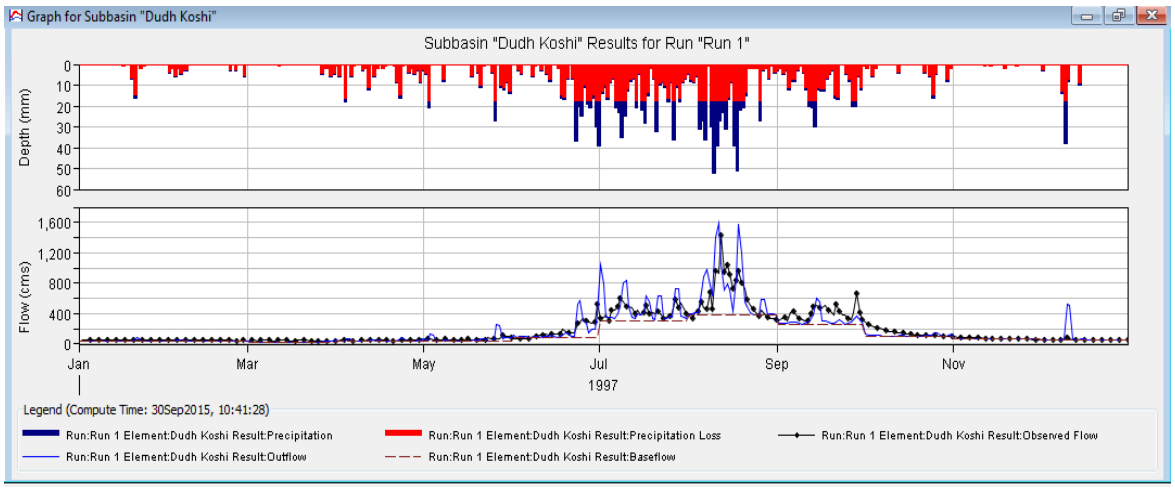

Detailed hydrograph of the 1997 period

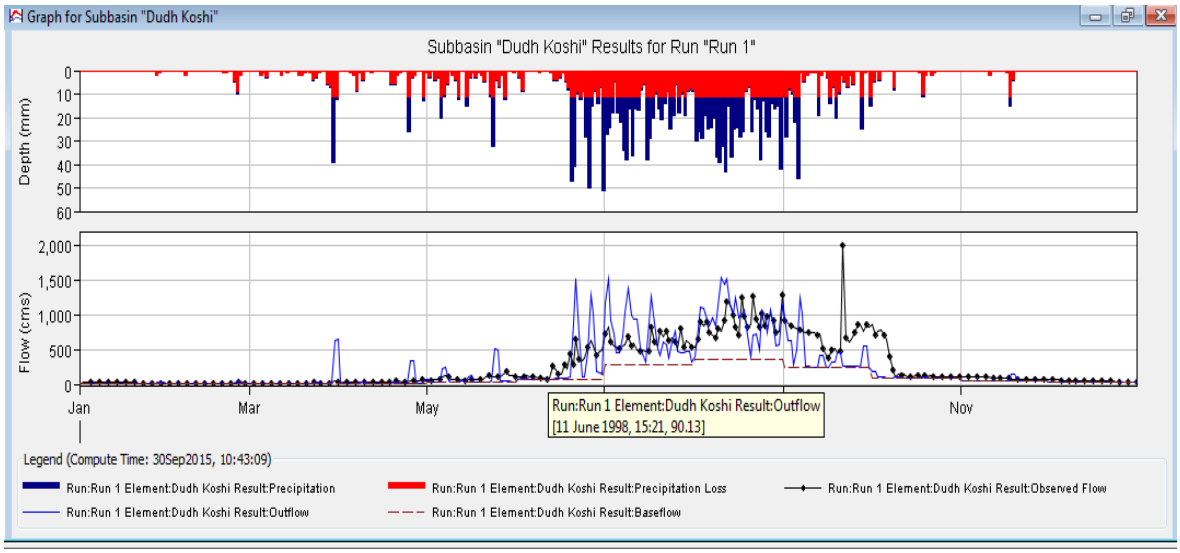

Detailed hydrograph of the 1998 period

ii. Validation

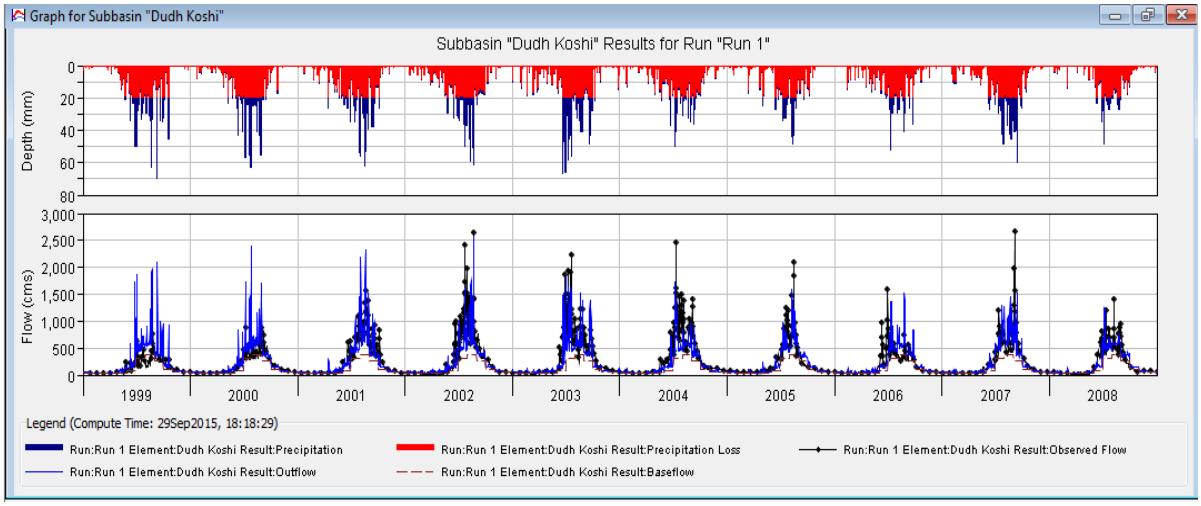

Detailed hydrograph of the 1999 – 2008 period